Deep-Sea Research Part I 145 (2019) 31–58

Contents lists available at ScienceDirect

Deep-Sea Research Part I

journal homepage: www.elsevier.com/locate/dsri

Deep-sea mining on the Rio Grande Rise (Southwestern Atlantic): A review on environmental baseline, ecosystem services and potential impacts

Francesc Montserrat[a,*], Maila Guilhon[a], Paulo Vinicius Ferraz Corrêa[a], Natascha Menezes Bergo[a], Camila Negrão Signori[a], Pedro Marone Tura[a], Mascimiliano de los Santos Maly[b], Denise Moura[b], Luigi Jovane[b], Vivian Pellizari[a], Paulo Yukio Gomes Sumida[a], Frederico Pereira Brandini[a], Alexander Turra[a]

[a] Department of Biological Oceanography, Institute for Oceanography – University of São Paulo, Praça do Oceanográfico 191, 05508-120 São Paulo, SP, Brazil
[b] Department of Physical, Chemical and Geological Oceanography, Institute for Oceanography – University of São Paulo, Praça do Oceanográfico 191, 05508-120 São Paulo, SP, Brazil

ARTICLE INFO

Keywords:
Cobalt crust
Ferromanganese
South Atlantic
Brazil
Anthropogenic pressure
Cumulative impacts
Environmental management plan
Oceanographic data

ABSTRACT

The Rio Grande Rise is an extensive seamount region in the South-western Atlantic, with potential for deep-sea mining activities in the future. Such activities pose significant long-term disturbances and potentially severe impacts to both ecosystem structure and functioning, as well as associated ecosystem services. The Rio Grande Rise presents a severely understudied area, with very little knowledge on either local and regional scales. Most detailed knowledge available is centered on highly localised geological information and interpolated and/or modelled environmental data, while high-resolution data on biogeography, ecosystem processes and functioning are lacking. The Rio Grande Rise is most likely a remnant of the Paraná-Etendeka igneous province, and formed when the African and South-American plates separated to form the Southern Atlantic basin, about 75 million years ago. More recent cruises have generated very local and high-resolution acoustic impedance data on the substrate, showing extremely dense layers, likely to be cobalt-rich crusts and underlying bedrock, interspersed with thick sediment layers. Literature studies revealed that nowadays the Rise appears to be located within a relatively low-productivity oceanic region. Open-database mining yielded large-scale, extrapolated environmental data rasters, which show the Rise to be an oceanic region relatively free of pollution and anthropogenic disturbances, with high geomorphological heterogeneity and potential for high biodiversity. This image was confirmed in a small number of scientific submarine cruises, where a diverse range of seascapes was observed, from soft sediment to carbonate pavement and cobalt crust outcrops. Especially the latter substrata were found to be inhabited by diverse benthic communities, dominated by sessile organisms, presenting three-dimensional structural heterogeneity and with associated vertebrate and invertebrate animals. Cobalt-rich crusts appear to

Abbreviations: AABW, Antarctic Bottom Water; BEF, Biodiversity and Ecosystem Functioning; BTA, Biological Traits Analysis; CCD, Carbonate Compensation Depth; CCZ, Clarion-Clipperton Zone; CICES, Common International Classification of Ecosystem Services; CL, Correlation Length; CPRM, Companhia de Pesquisa de Recursos Minerais, the Brazilian geological service and state-owned mining and exploration company; CRC(s), Cobalt-Rich Crust(s); DCML, Deep Chlorophyll Maximum Layer; DNA, Deoxyribonucleic acid; DS(M), Deep Sea (Mining); DSDP, Deep Sea Drilling Project; DSTP, Deep-Sea Tailing Placement; EBM, Ecosystem-Based Management; EBSA, Ecologically or Biologically Significant Area; EF, Ecosystem Functions; EIA, Environmental Impact Assessment; ES, Ecosystem Services; GEBCO, General Bathymetric Chart of the Oceans; GHG, Greenhouse gases; GLODAP, Global Ocean Data Analysis Project; GMED, Global Marine Environment Datasets; GOODS, Global Open Ocean and Deep Sea; ICCAT, International Commission for the Conservation of Atlantic Tuna; IDW, Inverse Distance Weighting; IPCC, International Panel on Climate Change; ISA, International Seabed Authority; MAR, Mid-Atlantic Ridge; MEA, Millennium Ecosystem Assessment; Mya, Million years ago; MT, Metallo-thionein; NADW, North-Atlantic Deep Water; NGS, Next-Generation Sequencing; NOAA, National Oceanic and Atmospheric Administration; NW, North-West; OBIS, Ocean Biogeographic Information System; OM, Organic Matter; OMZ, Oxygen-Minimum Zone; OTU, Operational Taxonomic Unit; POC, Particulate Organic Carbonate; PMN, Poly-metallic nodules; PMP, Paraná-Etendeka Magmatic Province; PRA(s), Preservation Reference Area(s); qPCR, quantitative Polymerase Chain Reaction; REE(s), Rare Earth Element(s); RGR, Rio Grande Rise; RNA, Ribonucleic acid; SD, standard deviation; SE, South-East; SEM, Scanning Electron Microscope; (S)EMP, (Strategic) Environmental Management Plan; SM, seamounts; SMS, Seafloor Massive Sulfides; SNR, Signal-to-Noise Ratio; SPM, Suspended Particulate Matter; TA, Total Alkalinity; TEM, Transmission Electron Microscope; TTP, Typical Tropical Profile; TWT, Two-Way Time; UCDW, Upper Circumpolar Deep Water; VGPM, Vertically Generalised Production Model; VME, Vulnerable Marine Ecosystem; WOD, World Ocean Database; WoRMS, World Register of Marine Species; WR, Walvis Ridge

* Corresponding author.
E-mail address: montserrat@usp.br (F. Montserrat).

https://doi.org/10.1016/j.dsr.2018.12.007
Received 22 January 2018; Received in revised form 24 December 2018; Accepted 24 December 2018
Available online 09 January 2019
0967-0637/ © 2019 Elsevier Ltd. All rights reserved.

grow at an extremely slow rate of several mm per million years, in the deep ocean where biological and ecological processes such as reproduction, growth and recolonisation are characterised by slow dynamics. The main disturbances posed by deep-sea mining of cobalt-rich crusts on the Rio Grande Rise consist of (1) complete removal of substrate with its particular benthic communities, (2) strong localised increases in suspended particulate matter, causing smothering of breathing apparatus and dilution of food particles, (3) crushing by tailings and overburden and (4) toxicity effects by released metals and other toxic substances, likely to be increased under high pressure. These impacts will likely change the deep-sea ecosystem at the Rio Grande Rise and its functioning for time scales in the order of decades to centuries. State-of-the-art geological, environmental and ecological modelling, complemented with high-quality, fine-resolution data are needed to provide a detailed evaluation of the impacts of cobalt-rich ferromanganese crust mining in the Rio Grande Rise, with the goal to formulate strategic environmental management plans.

1. Introduction

Deep-sea mining is a potential multi-billion dollar industry, expected to become operational in all the world's oceans within the next 25 years (Wedding et al., 2013, 2015). Areas previously inaccessible in the deep seas are currently within reach, due to the development of new technologies (Ramirez-Llodra et al., 2010, 2011). Resources targeted by deep-sea mining activities are ores with high contents of both base metals and rare earth elements (REEs; (Hein, 2004; Hein et al., 2013; Hein and Koschinsky, 2014b)). Currently, the best-known exploration schemes are those targeting polymetallic nodules (PMN) in the Clarion-Clipperton Fracture Zone (central Pacific; ISA, 2011a, 2011b; Lodge et al., 2014) and seafloor massive sulfides (SMS) found at both active and inactive hydrothermal vent sites along the Mid-Atlantic Ridge (MAR) spreading zone (Morato et al., 2015; Dunn et al., 2018).

Considerably less attention has been given to mining activities targeting cobalt-rich ferro-manganese crusts (CRCs). Like PMNs, CRCs contain high concentrations of base metals like iron and manganese, and are relatively rich in cobalt (Co), nickel (Ni) and REEs (Halbach et al., 1982; Hein et al., 1997, 2013; Hein and Koschinsky, 2014a). Cobalt-rich ferro-manganese crusts form under very specific conditions, and grow with an extremely slow rate, in the order of several millimeters per million years (Hein et al., 1997; Hein and Petersen, 2013; Hein and Koschinsky, 2014a; Conrad et al., 2017). Among the potential mineral-rich areas with CRCs, the Rio Grande Rise (RGR), a prominent topographic feature in the deep south-west Atlantic Ocean, has been targeted for prospection. In 2015, the International Seabed Authority (ISA) and the state-owned Companhia de Pesquisa de Recursos Minerais (CPRM) of Brazil have signed a 15-year contract for CRC exploration in the RGR.[1] CPRM is targeting CRCs that have formed mainly along the summit of the western bulge of the RGR. As the CRCs constitute hard substrate (Hein, 2004; Morgan et al., 2015), any associated epibenthos is expected to be severely impacted by mining activities (Sharma, 2015). Surrounding ecosystems are expected to experience impacts as well, most notably crushing and smothering by mine tailings and chronic increases in suspended particulate matter and (toxic) dissolved metals (Sharma, 2015).

The southern Atlantic is a severely under-studied ocean basin and knowledge about benthic biodiversity and ecosystem functioning on the RGR in particular is scarce (Perez et al., 2012). However, in light of the proposed deep-sea mining activities and mandatory associated impact assessments (ISA, 2011b), a proper baseline needs to be established, in order to formulate a Strategic Environmental Management Plan (SEMP) for the region. By using information and data from both the literature and public databases, complemented by new data from recent expeditions, this review aims to provide an environmental baseline, as well as an identification of ecosystem services and potential (in)direct impacts caused by CRC mining in the Rio Grande Rise.

The first part of this paper consists of a literature review on different aspects (geology and oceanography, pelagic geochemistry and primary production, benthic biodiversity, formation and function of cobalt crusts as benthic habitat) of the RGR. Secondly, formulating a SEMP creates the need for spatially explicit data. Because of the paucity of environmental (field) data from the literature, and the need for the spatially explicit data, the second part of this review consists of a data-mining exercise, in which modelled and extrapolated environmental data from public, global and quality-controlled databases are presented in the shape of time-averaged maps. It is therefore conceivable, and even logical that there is some degree of overlap and redundancy between the literature review and the data-mining parts. The third part of this review attempts to valuate the RGR ecosystem, by determining the ecosystem services that derive from it. Finally, the fourth part of this paper discusses the spectrum of environmental impacts on the RGR as a consequence of proposed CRC mining activities.

2. Geography and geophysics of the Rio Grande Rise

2.1. Geography and -morphology

The Rio Grande Rise (RGR) is situated ca. 1200 km off the SE Brazilian coast and about 2000 km west of the Mid-Atlantic Ridge (MAR), between the Argentine (AB in Fig. 11) and Brazilian (BB in Fig. 11) oceanic basins. The RGR is divided into four subregions (Fig. 11): The Alpha subregion (A, Fig. 11) is located in the western part of the RGR and encompasses an elliptical bulge of 500 km × 300 km. The bulge is marked by a graben that runs roughly NW-SE, starting as a depression in the NW corner, while deepening to the abyssal plain depth in the SE corner of the Alpha subregion.

The Bravo subregion (B, Fig. 11) of the RGR is a guyot, or flat-topped seamount, located just east from the eastern entrance of the Alpha subregion graben. The Charlie subregion (C, Fig. 11) lies in the SE section of the greater RGR area, and consists of two ridges running NW-SE, separated by another, deeper graben. The SE part of the Charlie graben terminates in a deep, sill-like blind end. According to Mohriak et al. (2010), both the grabens of the Alpha bulge and the Charlie subregion are evidence of a regional NW–SE lineament that extends from the oceanic crust towards the continental crust. The Delta subregion (D, Fig. 11) consists of a seamount arc, located towards the NE and E of Alpha subregion, separated by a narrow and constrained abyssal plain (Gamboa and Rabinowitz, 1984).

The RGR is bounded to the north by the Florianópolis/Rio Grande Fracture Zone (FFZ in Fig. 11) and to the south by an unnamed 35°S latitude fracture zone (UFZ in Fig. 11). In the east, the RGR is bordered by the Hunter Channel (Perez et al., 2012) and fracture zones extending westwards from the MAR (Fig. 11). The Vema Channel (VC in Fig. 1; Johnson, 1984; Johnson et al., 1984) within the Rio Grande Gap (Gamboa et al., 1983) is the western limit of RGR, and constitutes a structural boundary between the RGR and the continental São Paulo Plateau (SPP in Fig. 1; Mohriak et al., 2010; Evain et al., 2015).

[1] https://www.isa.org.jm/news/isa-and-companhia-de-pesquisa-de-recursos-minerais-brazil-sign-exploration-contract.

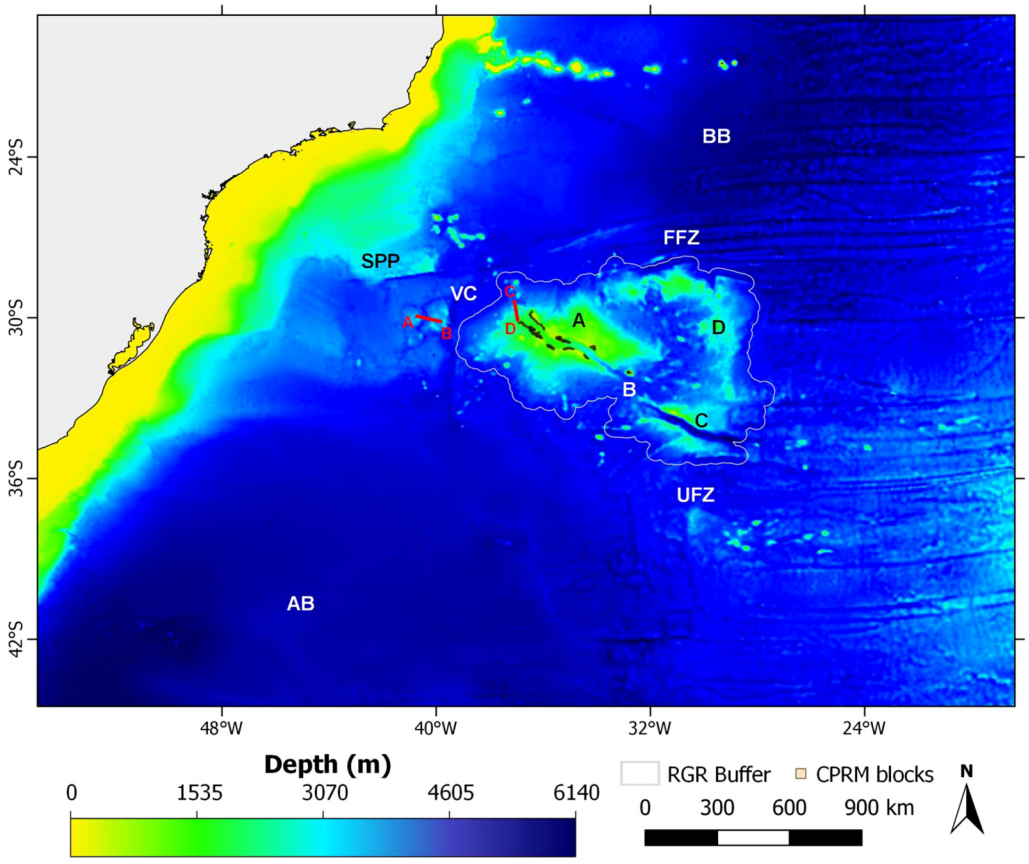

Fig. 1. The location and bathymetry of the Rio Grande Rise (RGR) in the SW Atlantic, relative to the Brazilian continental shelf. The subregions (see text) are denoted by letters: (A) The Alpha subregion is the main geological feature, and comprises the elliptical bulge in the western part of the RGR (WRGR). (B) The conspicuous Bravo flat-topped seamount, or guyot, is located just east of the eastern entrance of the central graben in the Alpha bulge. (C) The Charlie subregion is located south-east from the Alpha bulge, and characterised by two extensive ridges, separated by another central graben. (D) The Delta arc is located due east from the Alpha bulge and directly north of the Charlie subregion, and consists of seamounts, knolls and ridges. AB: Argentine Basin; BB: Brazil Basin; VC: Vema Channel; SPP: São Paulo Plateau; FFZ: Florianópolis Fracture Zone; UFZ: Unnamed Fracture Zone. The red transects AB and CD are approximate locations of the seismic imaging transects discussed below in Section 2.3 and Figs. 3, 4 and 5. (For interpretation of the references to color in this figure legend, the reader is referred to the web version of this article.)

2.2. Geology

Despite episodic sampling campaigns in the region, the precise formation of the RGR remains unresolved (Fodor and Thiede, 1977; Fodor et al., 1977; Barker et al., 1983b; Barker and Carlson, 1983; O'Connor and Duncan, 1990; Mohriak et al., 2010; Ussami et al., 2012). The classic interpretation for its origin is that the RGR and the Walvis Ridge (WR) formed by ocean spreading along a section of the South Atlantic spreading-axis, as the African and South American plates migrated apart (Fig. 2, from: O'Connor and Duncan, 1990). The RGR is

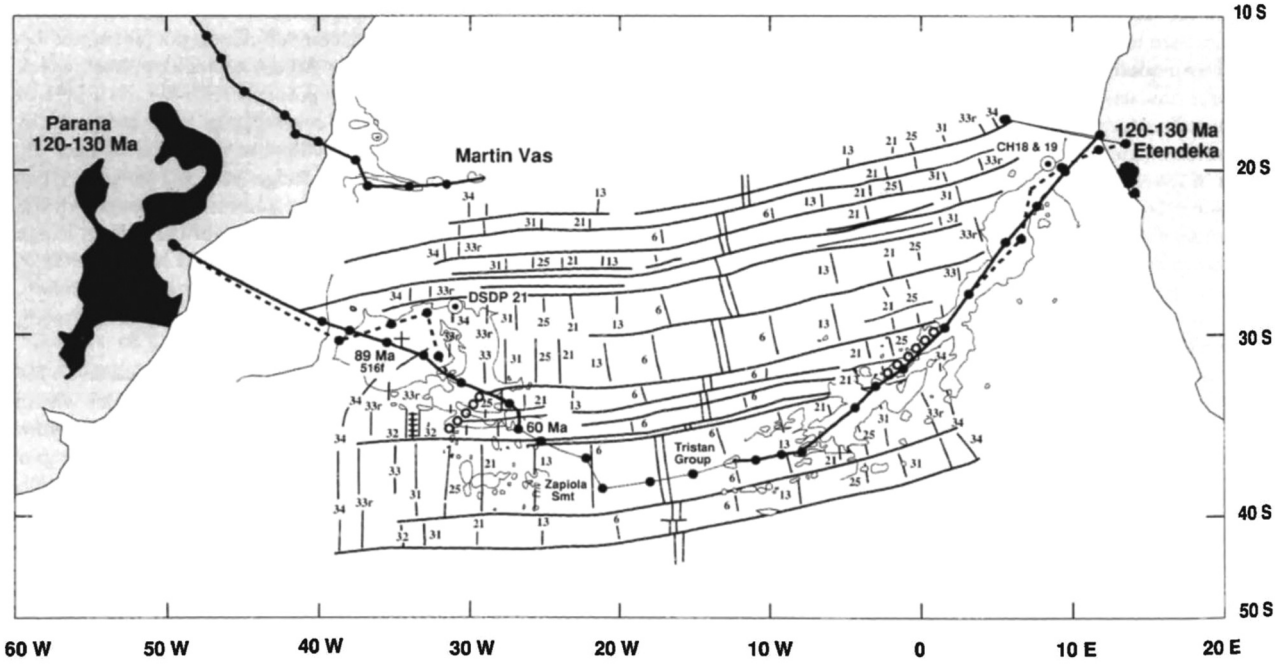

Fig. 2. Reconstruction of the ocean spreading in the South Atlantic Ocean (from: O'Connor and Duncan, 1990). Thick black lines with solid black circles indicate the predicted trail of both the African and South American plates over the Tristan hot spot and the Martin Vas plume.

thought to have formed as a "volcanic pile" resulting from the formation of the conjugate continental flood basalts of Etendeka (Namibia) and Paraná (Brazil; Fig. 2; Gamboa and Rabinowitz, 1981, 1984; O'Connor and Duncan, 1990; Gallagher and Hawkesworth, 1994; Mohriak et al., 2010) ca. 85 million years ago (Hoernle et al, 2015; Constantino et al., 2017), and has subsequently been moving westwards as the South-American and African plates separated (Fig. 2). Although its origin is volcanic, the RGR itself is distinctly aseismic (Gamboa and Rabinowitz, 1984).

The Mid-Atlantic spreading axis underwent a westward migration during the Late Cretaceous, ca. 70 million years ago (Mya), isolating the RGR from the Tristan da Cunha hotspot source and separating it from the conjugate margin of the Walvis Ridge (O'Connor and Duncan, 1990; Rohde et al., 2013). However, Mohriak et al. (2010) pointed out that there are several alternative interpretations for the origin of the Rio Grande Rise, such as the one considering the RGR as an isolated remnant of continental crust left outboard of the Brazilian continental margin during the westward drifting process. This hypothesis is supported by paleobathymetry data of Detrick et al. (1977), suggesting that the RGR was initially very shallow, with parts of it above sea level during the Santonian to Campanian (72.1 – 86.3 Mya).

Initial studies from the Deep-Sea Drilling Project Leg 72 (DSDP 72) provided the first evidence supporting the hypotheses of volcanic origin of the RGR. Seismic refraction studies (Leyden et al., 1971) showed that the RGR is separated from the continent by a region of typical oceanic crust, and the rise has no structural connection with the mainland. Further dredging and drilling recovered alkaline basalts and volcanic breccia, reinforcing the interpretation of the RGR as an aseismic ridge of volcanic origin connected to the Walvis Ridge (Fodor and Thiede, 1977; Fodor et al., 1977; Detrick et al., 1977; Kumar, 1979).

Data from Drilling Hole 516 showed two volcanic episodes of Coniacian-Santonian and Middle-Eocene ages (Barker et al., 1983a; Barker and Carlson, 1983). Subsequent work from DSDP 72 (Drilling Hole 516; north flank of Alpha subregion) recovered tholeiitic basalt samples at the bottom of the hole, dated to 84.5 Mya (Barker et al., 1983a; b). Site 516 was characterised by a thick section that comprises all stratigraphic units of the Upper Cretaceous, beginning in the Coniacian, and covered by Cenozoic deposits (Mutter et al., 1982; Mohriak et al., 2002, 2008; Paton et al., 2017). From the same drilling hole, the deepest nanofossil was dated to the Santonian-Coniacian (83.6–89.8 Mya). Interpretation of seismic reflection data located the basement ca. 3000 m above present depth and directly overlaying sediments indicate a paleodepth of less than 20 m (Barker et al., 1983a, 1983b), while Coniacian–Maastrichtian (66–83.6 Mya) limestone and a 276 m thick clay layer compose the basal sedimentary sequences.

Recent expeditions and new data analysis gave rise to a different interpretation for the origin of the RGR being a remaining continental crust fragment, which was left behind during the Gondwana breakup (Pushcharovsky, 2013), although sources of information are not always mentioned (Stica et al., 2014). Crustal models obtained by different techniques confirm a thicker crust under the RGR than under the surrounding abyssal plain. Ussami et al. (2012) showed that flexural modelling, constrained by gravity data, predicts a total crustal thickness up to 30 km. Inverse gravity modelling carried out by Constantino et al. (2017) determined the Mohorovičić Discontinuity (boundary between Earth's crust and mantle) depth at 25 km below the western (Alpha) bulge of the RGR.

2.3. Seismic imaging

A recent acquisition survey by SeaSeep (Rio de Janeiro, Brazil) and SeaBird Exploration (Cyprus) with the seismic vessel "Northern Explorer" in the Rio Grande Rise region, yielded seismic profiles of the basement structure along two transects AB and CD (Fig. 11), of which two examples are presented here. The seismic profiling was performed with a 5100 cubic inch (= 83,574 cm^3) Airgun and streamer with 12,000 m length of 960 channels and 3–5–90 and 120 Hz frequency. The resulting data have been processed by Invision Geophysics (Rio das Ostras, Brazil) and are here presented in two-way time (TWT) seconds. Here, we describe two unpublished seismic images provided by SeaSeep for this study (Figs. 3, 4 and 5).

A high-resolution seismic image of the seabed to the west of the Vema Channel (transect A-B; Fig. 3), shows a depression at ca. 1000 m water depth (~1500 s in sea water) and a valley of ca. 15 km wide. Within this valley, thick packages of 0.8 s (~1230 m assuming a mean speed of 1600 m/s) of what are probably hemipelagic sediments are observed (Richardson and Briggs, 1993; Kim et al., 2004). The sedimentary packages are characterised by parallel reflectors in the outer

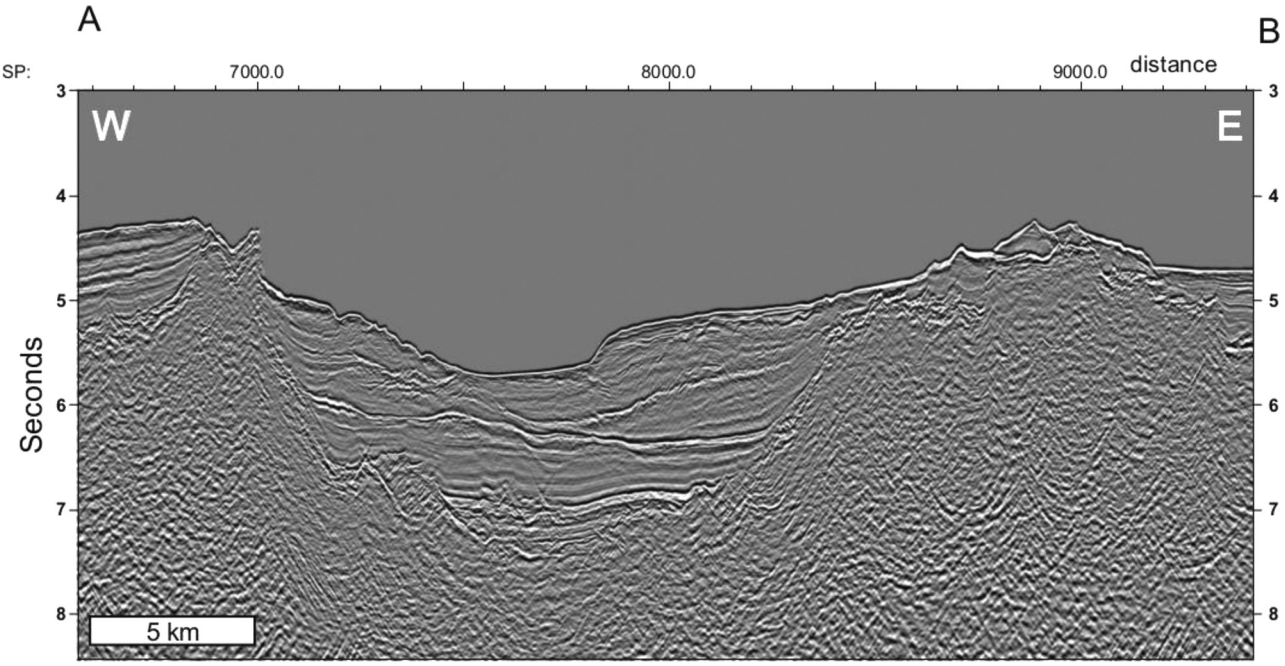

Fig. 3. Seismic imaging profile of the AB transect (Fig. 1), over a depression located west of the Vema Channel (see text).

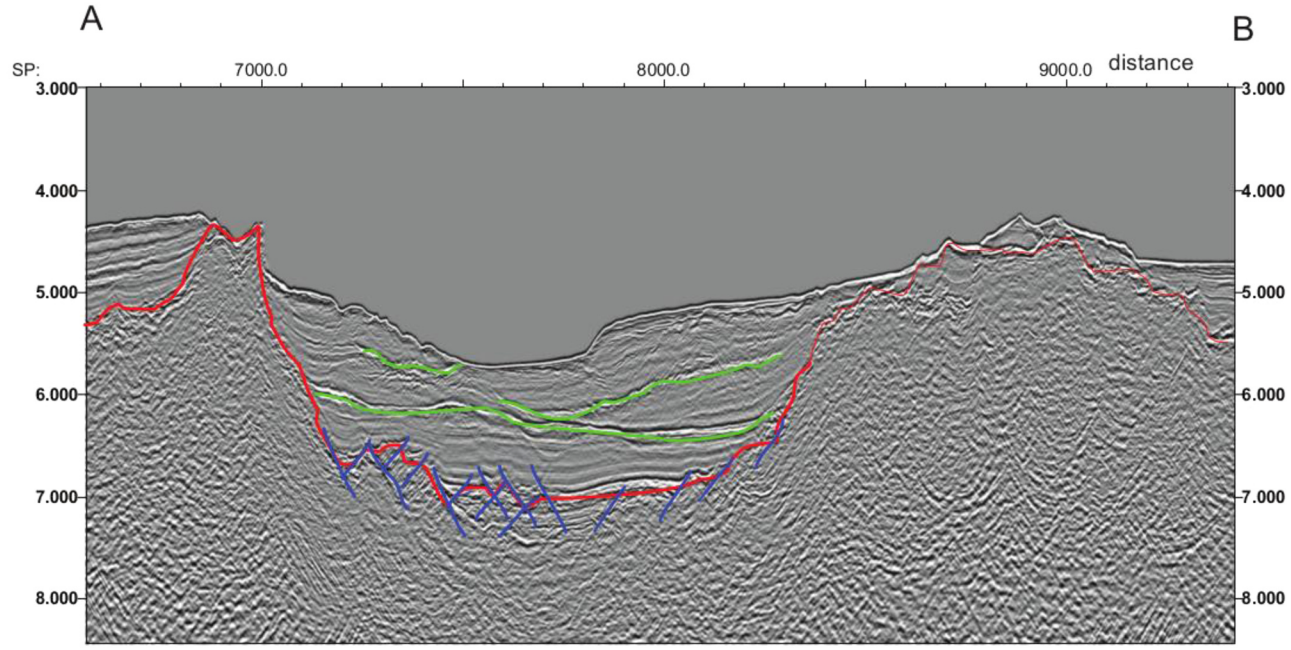

Fig. 4. Interpretation of the seismic imaging profile of the AB transect, over a depression located west of the Vema Channel. The red line denotes the basement material, intersected by parallel uplifts in purple. The light green lines denote layers of (hemi)pelagic sediments (see text). (For interpretation of the references to color in this figure legend, the reader is referred to the web version of this article.)

sectors of the valley (Fig. 4). The apparent western tilt of these reflectors on the western margin, demonstrate uplift of the valley edge relative to the side basin, after the deposition of the sediments (Fig. 4). The eastern margins of the valley show outcropping acoustic basement material, with strong amplitudes in the first layer (Fig. 4). The contrast in acoustic impedance between two different units in the top layers signifies that these rocks are covered by (much) denser material (Figs. 3, 4).

A second seismic profile acquisition was performed over the north-western section of the RGR (Fig. 11, transect C-D; Fig. 5). The seismic profile shows a massive and complex structure of the acoustic basement developing from the 0.7 s (~1100 m) thick (pelagic) sediment at the NW end of the transect. The acoustic basement likely represents a massive magmatic body, as can be observed from the geometries of fluids surge (Fig. 5). The profile shows a north-western structure at ~2.5 s water depth (~3700 m water depth), of which the top is

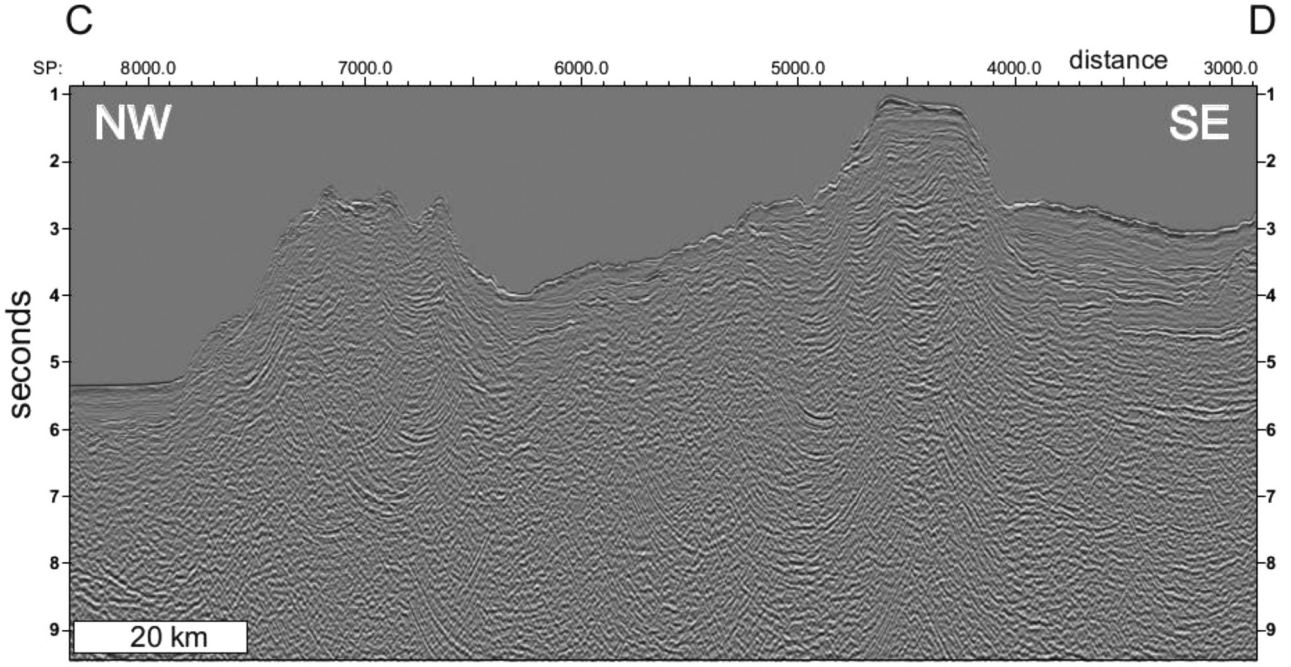

Fig. 5. A seismic profile from the north-western section of the western RGR bulge (transect C-D; Fig. 1). The profile shows a north-western structure at ~2.5 s water depth (~3700 m water depth), of which the top is characterised by strong amplitudes (high-density material) and no evidence of accumulated sediments. The seismic profile shows a massive structure of the acoustic basement developing from the (pelagic) sediment at the NW end. The structure towards the south-eastern end of the transect is located at much shallower depth (~1 s = ~650 m). In addition, it is covered by ~0.5 s (~800 m) of sediments.

characterised by strong amplitudes (i.e. high-density material) and no evidence of accumulated sediments (Fig. 5). The structure towards the south-eastern end of the transect is located at much shallower depth (~1 s = ~650 m). In addition, it is covered by ~0.5 s (~800 m) of sediments. Between the two structures there are several packages of sediments, encompassing a series of small basins at different depths, with parallel deposition inside each one. Those basins (visibly three) do not appear inter-connected, and are separated by moats, mainly towards SE (Fig. 5). The sediment packages' internal structures of the small basins consist of contourite deposits of the Flemish drift type. The south-eastern structure is characterised towards SE by a steep slope, which terminates abruptly into a basinal sector consisting of (sub-)parallel and locally faulted sediments of ~2 s (~3200 m) thick (Fig. 5).

Information on paleo-oceanography, diagenesis and past metabolic processes is essential in studying the formation of polymetallic deposits, representing a major economic interest in the RGR. Both the great depth of penetration and high resolution of the data will enable producing a novel and refined structural model for the region in future works. In addition, these high-resolution seismo-stratigraphic data will shed light on paleo-oceanographic settings, including paleocurrents, diagenetic conditions and metabolic processes in the sediments and rocks on the ocean floor.

3. Pelagic and benthic biological oceanography

3.1. Pelagic biogeochemistry

At the surface, the southern Atlantic Ocean is dominated by the relatively oligotrophic water water mass of the Subtropical South Atlantic Gyre (Schmid et al., 2000; Perez et al., 2012). The flow patterns of deeper water however, are affected by the position of the RGR in the South Atlantic, separating the Argentine basin abyssal province to the south, from the Brazilian basin abyssal province to the north (Perez et al., 2012). Antarctic Bottom Water (AABW) flowing north is forced west through the Vema Channel, and eastwards through the Hunter Channel (Speer et al., 1992), east of the RGR. The upwelling portion of AABW over the southern flanks of the Alpha sub-region, collides with North-Atlantic Deep Water (NADW) flowing from the north, between 1500 and 3500 m depth (Florindo et al., 2015, and references therein).

Oceanographic surveys carried out in areas surrounding the RGR showed no comparative differences in nutrient concentrations or net primary production over the rise (Reid et al., 1977; Johnson, 1983; Rijkenberg et al., 2014). For the southwest Atlantic along the 30°S latitude, typical primary production rates range between 155 and 210 mg C m^{-2} day^{-1} (Longhurst et al., 1995; Froneman et al., 2001; Marañón et al., 2003). Gardner et al. (1997) reported vertical fluxes, ranging between 1.1 and 3.1 mg C m^{-2} day^{-1} over the Vema Channel. However, the low spatial and temporal resolution in the abovementioned works could not identify the effect of recurrent physical process over seamounts and rises such as Taylor columns, internal waves, tidal amplification and eddy trapping (Roden, 1987). This finding stands in contrast to a high-resolution study, which showed the isotherm uplift and high chlorophyll concentration over the Minami-Kasuga Seamount summit (Tropical Western Pacific), due to Taylor column effects (Genin and Boehlert, 1985). Such processes can fertilise the euphotic zone (Boehlert and Genin, 1987a, 1987b) enhancing net primary production, hence increasing rates of biogenic sedimentation (e.g. Vilas et al., 2009).

Particulate matter from the Brazilian margin is not exported significantly further than the lower continental slope (de Mahiques et al., 2017). It is therefore highly unlikely that terrestrial organic matter (OM) contributes to the RGR food web. Recirculation cells and eddies originating from the Brazil-Malvinas Confluence Zone transport cold, nutrient-rich waters to the South Atlantic basin (Gordon, 1989; Garcia et al., 2004). At mid-depths (approx. 2500–3500 m), high contents of lithogenic elements (K, Li, and Rb) and kaolinites in sediments suggest a lateral flux of material driven by nepheloid layers, most likely coming from the São Paulo Plateau (Jones, 1984). Sediments from the São Paulo Plateau (SPP in Fig. 11) are generally resuspended by bottom turbulence and benthic activity, being horizontally advected through isopycnals (Emelyanov et al., 1983; Jones, 1984). Above 1400 m, the suspended sediment is mainly biogenic, with high calcareous content (foraminifers, pteropods, nanofossils and shell fragments), and no obvious terrigenous influence (Johnson, 1983). The dominance of terrigenous components increases below 3200 m, as carbonates start to dissolve, until carbonate dissolution is complete at 4250 m (Johnson, 1983). Although the generalities of such transport have been studied, both the influence on the RGR and its variability in time and space are still unknown.

Other sources of horizontal export of OM, which might fuel the pelagic foodweb over the RGR, are the active hydrothermal vents along the MAR spreading ridge and cold seeps along the equatorial African margin (Morato et al., 2015; Levin et al., 2016a). Plumes of hydrothermal vents and/or methane seeps are capable of travelling over large distances (Lupton and Craig, 1981; Baker et al., 1995; cited in Levin et al., 2016a), and have been postulated as an organic carbon source for pelagic bacterial production in larger ocean basins (Levin et al., 2016a). The distance from the RGR to the nearest recorded chemosynthetic systems -the active hydrothermal vents along the MAR spreading ridge- is ca. 2000 km in a straight line (Table 3). However, surface water masses following the South-Atlantic Gyre tend north-west after the MAR, before bending southwards and entering the region of the RGR (Peterson and Stramma, 1991; Stramma, 2001). The total distance travelled by potential organic carbon from the MAR is therefore considered too great, effectively excluding lateral trophic contribution to the RGR.

3.2. Pelagic primary production

The location of the RGR in oligotrophic waters with relatively low phytoplankton biomass in surface waters, suggests that both primary and secondary productivity originates locally (Perez et al., 2012). Seamounts and other submarine topographic features that rise > 1000 m from the seafloor tend to modify water masses (Roden, 1987; Vilas et al., 2009; van Haren et al., 2017). Recurrent physical processes over seamounts and rises such as Taylor columns, internal (trapped) waves, upwelling of deep, nutrient-rich water masses, tidal amplification and eddy trapping may concentrate (micro)nutrients (Roden, 1987), and so fertilise the euphotic zone (Genin and Boehlert, 1985; Boehlert and Genin, 1987b). This can lead to higher primary production (PP) in the photic zone above such features, which in turn may both fuel higher trophic levels regionally, and increase sedimentation rates of particulate organic carbon (e.g. Vilas et al., 2009). Surface primary production is thus an important driver of benthic (deep-sea) production and diversity (Smith et al., 2008b). Despite low primary productivity over the RGR, abovementioned processes, as well as upwelling of deep Antarctic Bottom Water (AABW) and bentho-pelagic coupling in the shallower parts may enhance biological production (Le et al., 2017). This regionally increased primary production would then lead to increased organic matter deposition and thus fuel the benthic foodweb in the RGR. The apex of the Alpha subregion is indeed modelled to receive a higher POC flux (Morato et al., 2015) compared to surrounding abyssal basins.

As the Rio Grande Rise is located below the highly stable and permanently stratified oligotrophic waters of the Subtropical South Atlantic Gyre, the main reservoir of new nutrients (*sensu* Dugdale and Goering, 1967) is the South Atlantic Central Water mass, far below the permanent pycnocline. Photoadaptation at low-light conditions and minor inputs of new nutrients from molecular diffusion have been suggested as contributors to the development of deep chlorophyll maximum layers (DCML), a common feature in all stratified oceans

(Cullen, 2015). The only macronutrients and trace elements available for phytoplankton growth are those recycled within the upper mixed euphotic layers or brought in by atmospheric inputs (Fung et al., 2000).

Phytoplankton over the RGR is mostly dominated by the pico-prokaryotes *Prochlorococcus* and, to a lesser extent, *Synechococcus* (the other ubiquitous phototrophic cyanobacteria) and pico-eukaryotes (Zubkov et al., 1998, 2000; Doolittle et al., 2008). Such vertical physical and chemical gradients impart a biogeochemical structure known as "typical tropical profile" (TTP, *sensu* Herbland and Voituriez, 1979), with the superposition of three main layers: (i) The "high light-low nutrient" (HLLN) well-mixed layer down to ca. 80–100 m, with very low inorganic nitrogen and chlorophyll concentrations ($< 0.05\ \mu M$ and $< 1\ \mu g\ L^{-1}$, resp.). Within the HLLN, phytoplankton density and chlorophyll concentration are homogeneously distributed down to the permanent pycnocline/nutricline. (ii) The "low light-high nutrient" (LLHN) intermediate layers, with the phytoplankton carbon biomass remaining unchanged, but its intracellular chlorophyll content increasing manifold allowing the efficient use of prevailing very low light intensities (usually 1–5% of surface irradiances). (iii) The deepest, "no light–nutrient rich" (NLNR), layer in the aphotic zone below the pycnocline (Partensky et al., 1999). Here, phytoplankton is unable to grow due to lack of irradiation, although residues of the plankton photosynthetic machinery may be detected in the form of detrital particulate matter and degraded chlorophyll compounds.

In this vertically wide ecotone, minor contributions of carbon fixation at the first trophic level may happen through chemosynthesis, which seems to increase downwards (Signori et al., unpublished), but overall heterotrophic processes tend to dominate the water column (Duarte et al., 2013). There is scarce knowledge on the export and remineralisation of organic matter production in the water column over the RGR. Micro-elements, either complexed in organic forms or adsorbed to suspended particles, are ultimately exported to the deep ocean (Hansell et al., 2009). Downward export of micro-elements occurs either directly, or indirectly via microbial aggregates originating from primary and secondary production (Honeyman et al., 1988).

3.3. Chemosynthetic primary production

Chemosynthesis is defined as the autotrophic production using the energy generated by redox reactions of inorganic or C-1 organic molecules (Enrich-Prast et al., 2014 and references therein). Also referred to as dark carbon fixation, dissolved inorganic carbon (DIC) fixation, or non-phototrophic CO_2 fixation, it was initially investigated at vents and seeps, oxic-anoxic interfaces and oxygen minimum zones (Tuttle and Jannasch, 1979; Jørgensen et al., 1991; Casamayor et al., 2001; Glaubitz et al., 2009; Canfield et al., 2010; Hügler and Sievert, 2011; Wright et al., 2012; Ulloa et al., 2012). More recent studies concluded that microbial dark carbon fixation may constitute a considerable contribution to the carbon cycle of coastal sediments and shallow-water hydrothermal environments (Boschker et al., 2014; Dyksma et al., 2016; Gomez-Saez et al., 2017).

By using a wide range of energy sources, Bacteria and Archaea are important contributors of newly synthesized organic matter for the deep-sea habitat (Herndl and Reinthaler, 2013). In marine sediments, oxygen is regarded to be the preferred terminal electron acceptor, followed by nitrate, Mn(IV) and Fe(III) compounds, sulfate and finally carbon dioxide (Claypool and Kaplan, 1974; Froelich et al., 1979). Electron sources in the dark ocean come from the oxidation of organic matter, hydrogen, methane, sulfur compounds, iron, manganese, and ammonium (Orcutt et al., 2011). Rate estimates of these redox reactions derived from microbial metabolism are the fundamental stepping stones for understanding dark carbon cycling in the deep ocean (Boschker et al., 2014). Recent discoveries have revealed a variety of reduced inorganic compounds (e.g., hydrogen, sulfide and ammonia) used as energy source by pelagic microbes in the oxygenated water column of the dark ocean (Gasol et al., 2008; Swan et al., 2011; Anantharaman et al., 2013; Herndl and Reinthaler, 2013; Baltar et al., 2016). The associated chemosynthetic production rates were found to be of the same order of magnitude as the dark ocean's heterotrophic production (Manganelli et al., 2009; Reinthaler et al., 2010; Signori, 2014).

Oceanic crusts present an enormous potential for chemosynthetic carbon fixation. Orcutt et al. (2015) provide evidence of a potential 10^9–10^{12} g carbon per year (g C y^{-1}) of carbon fixation by basalt-hosted microbial communities. It is suggested that the communities in these deep habitats use the Calvin cycle as the primary biochemical mechanism for chemoautotrophy (Orcutt et al., 2015). Global rates of dark carbon fixation have been estimated at 0.29, 0.11 and 0.37 Pg ($=10^{15}$ g) C y^{-1} for the euphotic zone, the dark ocean and sediments, respectively (Middelburg 2011). These estimates reveal the potential contribution of chemoautotrophy to the marine carbon cycle.

Measurements of in-situ dark carbon fixation rates using radioactive (^{14}C) or stable isotope (^{13}C) labelling have been rarely performed in deep ecosystems, especially in such highly under-studied areas of the global ocean as the (deep) South Atlantic oceanic basin. To the best of our knowledge, there is no chemosynthesis data on the RGR and adjacent areas, emphasizing the need of more efforts in quantifying its contribution to the marine biogeochemical cycles in deep areas of the South Atlantic Ocean.

3.4. Presence of megafauna and seabirds

Regional fishing effort and landing and bycatch numbers can be used as a proxy for pelagic secondary production. The in-depth data report of Morato et al. (2016) on the environmental settings in the central Atlantic shows presence of demersal fishing, mainly in the Alpha subregion, and some in the Delta and Charlie subregions, but overall the fishing pressure is classified as "low" (Morato et al., 2015). In the 1980s, the RGR area was fished by former USSR vessels, targeting mainly Alfonsino (*Beryx* spp.; Perez et al., 2012). Bycatch data of marine turtles in the RGR reveal the presence of mostly Leatherback (*Dermochelys coriacea*, Vandelli 1761) and Loggerhead turtles (*Caretta caretta*, Rafinesque 1814), concentrated over the apex of the Alpha subregion and the Charlie sub-region, respectively (Marcovaldi et al., 2006).

The RGR is considered an area where pelagic longline fishing is associated with bycatch of mainly white-chinned petrel (*Daption capense,* Stephens 1826), black-browed albatross (*Thalassarche melanophris,* Temminck 1828) and yellow-nosed albatross (*T. chlororhynchos,* Gmelin 1789; Bugoni et al., 2008; Jiménez et al., 2010; ICMBio 2011), of which the latter is classified as Endangered (International Union for the Conservation of Nature; http://www.iucnredlist.org/). Habitat suitability models suggest the area as a hotspot (high occurrence probability) for both albatrosses and petrels, especially in warm periods (Bugoni et al., 2008). Additionally, non-breeding individuals of the spectacled petrel (*Procellaria conspicillata*, Gould 1844) mostly visit the warmer, oligotrophic waters of the RGR on foraging trips away from their nesting sites on the Tristan da Cunha islands (Reid et al., 2014). The hypothesis here is that the breeding individuals satisfy their high energy demand by fishing in higher-yield waters, located closer to the breeding grounds, thus spending less energy (Reid et al., 2014). The non-breeding individuals, which conceivably have a lower energy demand, were thus displaced further away from the islands, to waters with notably less prey fish, such as the RGR.

SIMMAM (http://simmam.acad.univali.br/site/), a monitoring system for marine mammals managed by the University of the Itajaí Valley (UNIVALI, SE Brazil), reports three sighting records for unidentified marine mammals over the Rio Grande Rise. There are no records of marine mammal bycatch in the area.

Even though most landing and bycatch numbers do not originate from properly and continuously executed census data, they do provide -albeit indirect- a qualitative estimate of the (macro-)ecological

importance of the RGR. They sketch an image of the RGR being located in an extended low-productivity region in the South Atlantic. This is corroborated by the relatively low fishing effort in the Brazil and Argentine basins (Jiménez et al., 2010; Anticamara et al., 2011; Morato et al., 2015), being largely correlated with the chlorophyll minima of the south Atlantic gyre biogeographic province (Longhurst, 2007; Secretariat of the Pacific Community, 2013). Notwithstanding, the region seems to fulfill a role as feeding grounds for (migrating) seabirds (Bugoni et al., 2008; Jiménez et al., 2010; Reid et al., 2014). It is clear however, that a large knowledge gap exists on pelagic secondary production over the RGR, which prevents robust inferences to be made about relevant derivative ecosystem services, such as fisheries (see below).

3.5. Benthic biodiversity

The RGR represents habitat heterogeneity on both a large, ocean basin-scale and on a smaller spatial scale (Gamboa and Rabinowitz, 1984; Cavalcanti et al., 2016). Rising about 3500 m from the surrounding ocean floor, the western RGR bulge (Alpha subregion) represents a giant seamount-like structure, while small-scale or local topographic heterogeneity is represented by the slopes, summits, ridges and canyons of the RGR (Mohriak et al., 2010). Structural heterogeneity of the seafloor is linked to gradients in environmental conditions due to differences in depth, hydrodynamics, sediment and substrate composition, and is potentially responsible for strong variations in abundance, biomass and diversity of benthic communities (Wilson and Kaufmann, 1987a; Costello and Chaudhary, 2017).

Due to habitat diversity and its isolation from other oceanic bottom features, the RGR may offer high degrees of endemism and unique assemblages in terms of abundance or frequency of species, as traditionally reported for several seamounts (Wilson and Kaufmann, 1987b; Richer de Forges et al., 2000; Lundsten et al., 2009). However, recent studies and reviews have suggested seamounts are generally not ecologically isolated and indicated problems with estimates of endemism (Schlacher et al., 2010; Rowden et al., 2010; Clark et al., 2012). Thus, a large remaining question is whether and how much difference there is between RGR benthic communities and those on the neighbouring features and abyssal plains.

In a joint Brazilian-Japanese expedition, the manned submersible *Shinkai 6500* made two dives on the Alpha western bulge of the RGR in 2013, as part of the Japanese "QUELLE" project and the Brazilian "Iata-Piuna" expedition. Both the dives lasted for about 4.5 h, and took place in similar depths (Perez et al., 2018). The first transect briefly explored the bottom of the graben in the NW part, ascending the graben wall to the summit and surveyed several substrate types, amongst which crusts and carbonate rocks, while following the summit. The second transect was situated ca. 200 km towards the SE from the first transect, and surveyed only the summit (Perez et al., 2018). Although the two locations comprised notably distinct seascapes, there was a clear overlap in habitat types.

The habitat type along the graben bottom was a uniform soft-sediment substrate, with regular ripple marks, while that along the graben wall consisted of hard substrate formed by outcrops, alternately covered with CRCs and sediment pockets (Hajdu et al., 2017; Perez et al., 2018). The abrupt relief of the outcrops provided habitat for obvious hard-substrate organisms, such as Hexactinellid sponges and other associated fauna, which occurred in abundance (Hajdu et al., 2017). The crusts along the summit surveyed during the first dive consisted mainly of a gentle relief of alternating soft-sediment pockets and hard substrate, covered by plate-like CRCs (Perez et al., 2018). The hard substrate was covered by both Hexactinellid sponges and scleractinian (stony) corals, both in moderate abundances. The carbonate rock pavement observed along the summit during the first dive also presented hard substrate habitat for Hexactinellid sponges and smaller suspension feeders (Hajdu et al., 2017; Perez et al., 2018). The fact that the carbonate pavement was subject to strong currents, caused a virtual absence of soft sediment (Hajdu et al., 2017; Perez et al., 2018).

The second dive along the summit, in a sector towards the SE of the first dive, described a plain benthic terrain of which the first half was covered with soft sediment with both regular and irregular ripple marks (Perez et al., 2018). Benthic organisms were rarely observed on this soft sediment. The second half of the second dive consisted of interspersed soft sediment pools and plate-like CRCs, on which stony corals and Hexactinellid sponges were sparsely present (Perez et al., 2018)

Both the records mean and variability were higher during the first dive, in which the highest variation in seascape and habitat type were observed as well. In total, an assumed 30 fish species ("morphotypes") belonging to 17 families were found, along with recordings of 7 decapods, including some shrimp-like species (Perez et al., 2018). Although the graben wall was excluded from quantitative analysis, records of large, mobile benthic and bentho-pelagic organisms (fish and crustaceans) showed a significant higher abundance in the first dive (Perez et al., 2018). Between habitat types, the highest overall abundance was observed in the "carbonate rock pavement" habitat type along the summits of both locations. This higher abundance was ascribed to the dominant presence of two fish genera (*Chaunax* sp. and *Lepidon* sp.), so that the carbonate rock pavement habitat type was at the same time also the least diverse (Perez et al., 2018).

3.6. Crust formation and microbial mediation

Cobalt-rich ferro-manganese crusts (CRCs) are formed when Fe- and Mn-oxyhydroxides precipitate out of seawater, at depths between 800 and 2500 m, often associated with the presence of an OMZ (Hein, 2004). Other metals that absorb onto the mineral precipitate structure are cobalt, nickel, platinum, thallium and tellurium, to form the metal-rich CRCs at very slow rates in the order of mm per million years (Hein, 2004; Hein and Koschinsky, 2014b). An important condition for CRCs to form is the absence of sediment settling on the hard substrate (Hein, 2004; Secretariat of the Pacific Community, 2013; Hein and Koschinsky, 2014b). Currents and current patterns (e.g. eddies, upwelling, trapped waves), are often modified and/or amplified by seamount structures and are strongest in force near the summits (Roden, 1987). There they winnow away sediments or prevent them from settling, allowing the crusts to grow thickest.

Although the formation of Fe-Mn deposits is generally assumed to occur through abiotic geochemical processes, such as the hydrogenetic and/or diagenetic precipitation of Fe-oxyhydroxide and Mn-oxide (Konhauser, 2009), it has been suggested that the formation of polymetallic deposits is mediated by biochemical activity (biomineralisation). Until a few years ago, the formation mechanisms of CRCs were still not well understood (Hein et al., 2000), whereas currently there has been an improvement in understanding Fe-Mn deposit formation and the role of microbial mediation in the process (Wang and Müller, 2009; Wang et al., 2009, 2011; Jiang et al., 2017). In the biomineralisation process, several cycles of oxidation and reduction are alternated by Bacteria, Archaea (Ehrlich, 2002; Wang et al., 2009) and Fungi (Miyata et al., 2006). Because very little is known about the RGR, the available knowledge on biomineralisation processes elsewhere has been compiled below.

The first evidence of bacterial and archaeal cells in Fe-Mn nodules was published by Ehrlich et al. (1972). Since then, several studies have investigated the role of Bacteria, Archaea, Protozoa, Foraminifera and even microalgae in the formation of Fe-Mn deposits (Ehrlich, 2002; Konhauser, 2009; Wang and Müller, 2009; Hein and Koschinsky, 2013; Wu et al., 2013). Burnett and Nealson (1981) identified filamentous structures and coccoid bacteria, associated with a biofilm on the surface of a Fe-Mn nodule, and quantified about 10^7 bacterial cells m^{-3}. Ehrlich (2001, 2002) described the presence of three types of bacteria in Fe-Mn nodules: (i) Mn(II) oxidants, (ii) Mn(IV) reducing agents and (iii) a group that can neither oxidize Mn(II) nor reduce Mn(IV). Furthermore,

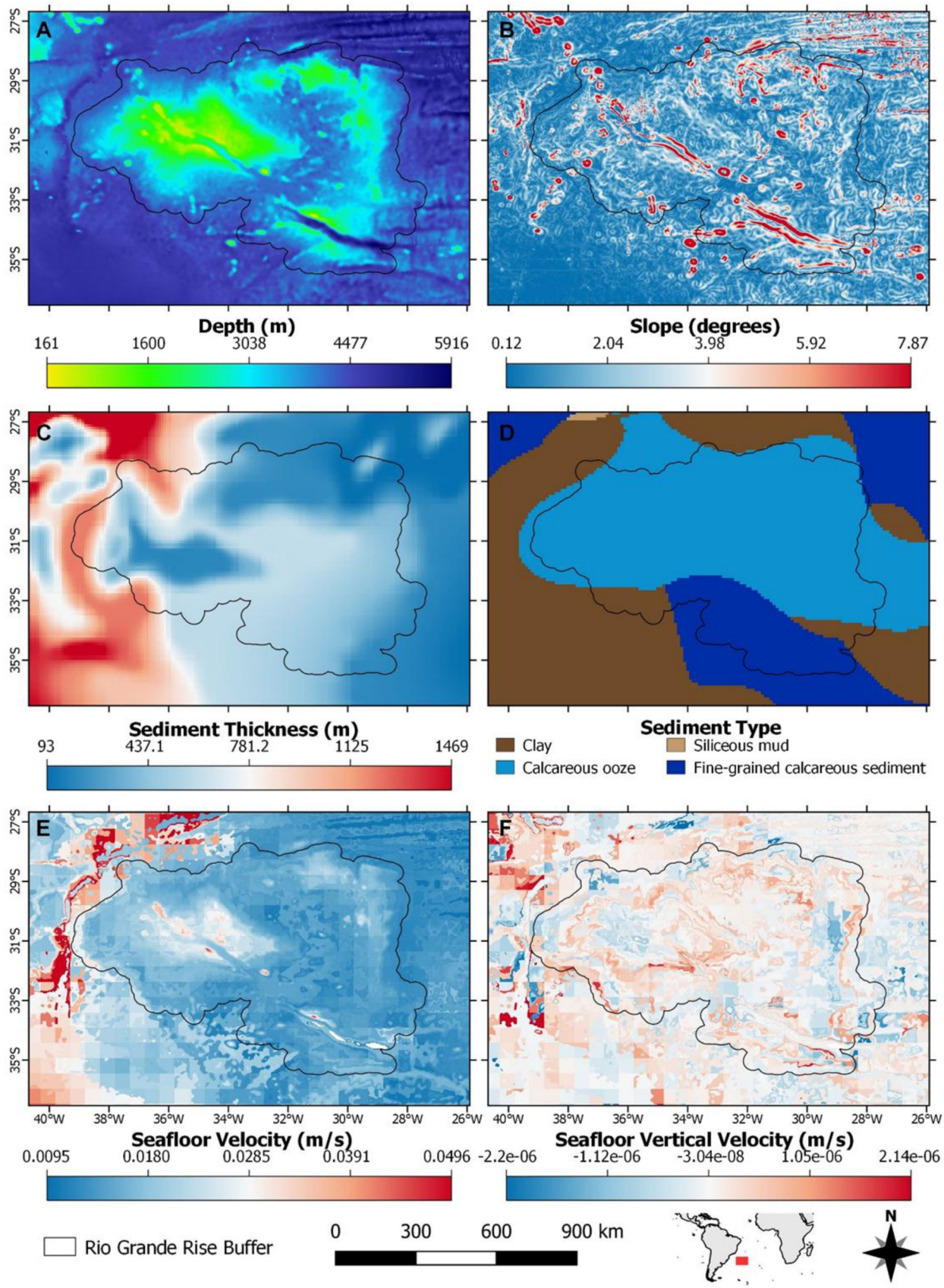

Fig. 6. Maps showing time-averaged environmental data for the RGR buffer area and surroundings. Top-left to bottom-right (A): Bathymetry [m below sea level], (B): Slope [degrees], (C) Sediment thickness [m], (D) Sediment type, (E) Horizontal current velocity along seafloor [m/s], (F) Vertical current velocity [m/s].

Wang and Müller (2009) proposed that the phylum Proteobacteria would be abundant in Fe-Mn oxides, including some bacteria that are metabolically active in the manganese and iron cycles.

More recently, culture-independent techniques, such as quantitative PCR (qPCR) and the sequencing of the 16S rRNA gene (clone libraries) have been used to study the relationship of microorganisms with Fe-Mn nodules and crusts of the Pacific Ocean (Liao et al., 2011; Hein and Koschinsky, 2013; Wu et al., 2013; Blöthe et al., 2015; Huo et al., 2015; Zhang et al., 2015; Nitahara et al., 2017). The main source of energy supporting the microbial ecosystem of the Fe-Mn crusts on the Takuyo-Daigo Seamount (NW Pacific) was proposed to be ammonia (Nitahara et al., 2011). Based on the detection of phylotypes related to *Nitrosospira* (class Betaproteobacteria) and *Nitrosopumilus* (phylum Crenarchaeota), these ammonia-oxidizing chemolithoautotrophs were suggested to play a key role as primary producers in the microbial ecosystem of hydrogenetic Fe-Mn crusts (Nitahara et al., 2011, 2017). Moreover, the ammonia monooxygenase structural gene *amoA* was detected in crusts, sediment and seawater in the northwest Pacific, although ammonia-oxidizing Archaea (*Nitrosopumulaceae*) and Bacteria (order *Nitrosomonadales* and phylum *Nitrospinae* and *Nitrospirae*) in crusts and sediments were phylogenetically different from the seawater (Nitahara et al., 2017). Nitahara et al. (2017) propose that the nitrite produced by ammonia oxidizers can be sequentially oxidized to nitrate, by nitrite oxidizers of the taxa *Nitrospirae* and *Nitrospinae* detected in the crusts and sediments.

In a crust originating from the Magellan and Marshall seamounts in the East Mariana (Western Pacific), a combination of techniques such as scanning electron microscope (SEM), transmission electron microscope (TEM) and clone library (16S rRNA) sequencing, has revealed abundant spherical aggregates of Mn-oxide filaments, which are closely associated with filamentous cells within the biofilm (biofilm mineralisation; Jiang et al., 2017). These biofilms were dominated by Mn-oxidizing bacterial families (Bacillus, Arthrobacter and Pseudomonas; Jiang et al., 2017).

Analogously, high abundances of *Shewanella* and *Colwellia* (phylum Proteobacteria), which are Mn^{4+} reducers and Mn^{2+} oxidizers, respectively, were detected in Fe-Mn nodules originating from the CCZ (Blöthe et al., 2015). The oxidation of cations from the Fe-Mn nodules can provide energy to microorganisms living on the nodules as a specific habitat (Tebo et al., 2004; Tully and Heidelberg, 2013; Wu et al., 2013; Blöthe et al., 2015). The archaeal sequences belonged to the Marine Group I (phylum Thaumarchaeota), which are normally associated with ammonia oxidation in the deep-sea and to providing primary carbon for the food chain (Walker et al., 2010; Nitahara et al., 2011), thus playing an important role in the nitrogen and carbon cycles. Cell densities on the surface of a seafloor nodule were estimated at $\sim 10^8$ cells cm^{-3}, in contrast to the lower cell densities ($\sim 10^6$ cells cm^{-3}) in the surrounding sediments of the ultra-oligotrophic South Pacific Gyre (Shiraishi et al., 2016). Possible explanations for the high cell density on the nodule surface is the organic matter degradation by manganese oxidizers, or the primary production by chemolithoautotrophs (Tully and Heidelberg, 2013; Blöthe et al., 2015).

Sediments and nodules are considered large reservoirs of microbial diversity, distinct from the deep waters (Shulse et al., 2017). It was recently discovered that microbial composition and diversity vary with the habitat (nodules, water and sediment), depth and location in the CCZ (Shulse et al., 2017). By using next-generation DNA sequencing (NGS), the phylum Thaumarchaeota was found to be predominant in the sediments and nodules, in comparison with the water column, whereas the class Gammaproteobacteria was abundant in the nodules. The relative abundance of 16S rRNA gene sequences in nodules was dominated by members of Gammaproteobacteria (23%, *Piscirickettsiaceae*), Alphaproteobacteria (12%, family *Rhodospirillaceae*) and Thaumarchaeota (21%, genus *Nitrosopumilus*), which was consistent with previous studies examining microbes associated with nodules (Tully and Heidelberg, 2013; Wu et al., 2013). The chemolithoautotrophic *Nitrosopumilus*-related operational taxonomical units (OTUs) in the sediments and nodules were different from those found in the surrounding waters and in the bathypelagic zone, inferring niche specialization between the nodule, sediment and the water column (Konneke et al., 2005).

Despite the increasing efforts using the 16S rRNA gene sequencing and qPCR, mainly on samples from the Pacific Ocean, molecular studies of phylogenetic and functional microbial diversity in deep-sea mineral deposits using high-throughput DNA and RNA sequencing are still scarce (Nitahara et al., 2017). Thus, studying the Rio Grande Rise crusts by using a combination of complementary high-throughput techniques, like metagenomics and metatranscriptomics, is fundamental to determine its microbial diversity and community structure. More importantly, implementing a combined approach is needed to effectively explore the role of lithotrophic microbes in the formation of deep-sea Fe-Mn deposits in the South Atlantic Ocean.

3.7. Cobalt crusts as benthic macrofaunal habitat

Once formed, crusts provide hard substrate for benthic organisms, most notably macrofauna (Schlacher et al., 2013; Morgan et al., 2015). Because crusts strictly form in the absence of sediment (Hein, 2004; Hein and Koschinsky, 2014b), the dominant macrofauna found on CRCs will be typical hard-substrate sessile groups like sponges and corals. Among the most recorded taxa on Pacific seamounts with CRCs are Crinoidea, followed by Anthozoa, Ascidia, Ophiuroidea, Holothuroidea, Crustacea and sponges (Schlacher et al., 2013; Morgan et al., 2015). There is growing evidence that cobalt-rich ferromanganese crusts harbour a high diversity of benthic organisms (Schlacher et al., 2013; Morgan et al., 2015). However, there seems to be a tendency for lower abundance inside CRC areas, compared to reference locations outside of CRC areas (Grigg et al., 1987), cited in Schlacher et al. (2013). This likelihood of lower abundance also implies a higher potential for (local) extinction in the case of strong disturbance events, like deep-sea mining. Therefore, special attention is required when assigning both mining areas and special preservation areas, to ensure both the species richness and species diversity as well as the ecological integrity of the region.

4. Environmental baseline from databases

The deep South Atlantic is one of the least-studied ocean basins (Perez et al., 2012). Moreover, there are very few data on benthic fauna, implying a severe lack of knowledge on benthic biodiversity and ecosystem functioning (BEF) in the RGR region. For example, Morato et al. (2016) report only one data point in the lower half of the water column, located in (the margins of) the Vema Channel to the west of the Alpha region. In order to construct an overview of the environmental baseline conditions at the RGR, publicly accessible global databases were used.

In order to evaluate the baseline conditions of the seafloor around the RGR, as well as making the obtained information spatially explicit, maps were generated of environmental variables using both cruise and modelled data, which are publicly available in different sources. The reader is referred to the Supplementary material for further details.

4.1. Geomorphology, sediment and bottom water movement

While the bathymetric map of the RGR shows a depth range of 5755 m, the mean ± standard deviation depth of the RGR "buffer area" (see above) is 3328 ± 935 m deep (Fig. 6A). The minimum depth in the RGR buffer area is 161 m at the apex of the Alpha western bulge, while the deepest point is located in the deep trough in the Charlie south-eastern subregion, at 5916 m below sea level (Figs. 11, 6A). Most of the RGR is situated in the bathyal depth zone (200–4000 m depth), which offers a wider range of ecological opportunities for larger

organisms, and thus supports a higher macro- and megafaunal species diversity than the abyss (Rex et al., 2006). Slope displays a rather narrow range of less than 8 degrees (Fig. 6B), although these are mean values of the grid cells. The actual range in the RGR buffer area lies between 0 and 30.8 degrees, with a mean ± sd slope of 2.1 ± 2.1 degrees for the RGR buffer area. The steepest slopes are found along the graben wall, both in the Alpha and Charlie subregions, in the north-western section of the Alpha bulge and along the slopes of the various seamounts distributed throughout the RGR area (Fig. 6B). The flat top of the Bravo guyot (table seamount) can be readily discerned, as well as some other guyots south of the Alpha bulge and west of the Charlie subregion (Fig. 6B). The gentle relief of the RGR is illustrated by the fact that more than 75% of the entire RGR buffer area has a slope between 0 and 5 degrees (Fig. 6B; Table 1). Most of the surface of the Alpha bulge, which is the single largest feature of the entire RGR, has a very gentle relief with slope values between 0 and 4 degrees, illustrating the overall low relief of the RGR (Fig. 6B).

Sediment cover over the entire RGR varies by about two orders of magnitude (Fig. 6C) between ~95 and 1270 m (mean ± sd = 460 ± 238 m) thickness, although a higher level of variation can be expected at a smaller spatial scale. The lowest sediment cover was observed along the southern slopes of the Alpha bulge and the highest cover along its north-western slopes and on the plain separating the western bulge from the eastern arc (Fig. 6C). The sediment cover in the Vema Channel and the abyssal plains of the Argentine basin are higher than the highest cover within the RGR buffer area. Most of the RGR is modelled to be covered in calcareous sediments of varying grain size, which are biogenic in origin (Fig. 6D). A map of the sediment types in the area (Fig. 6D), revealed that most of the western bulge (Alpha) was covered in very fine-grained calcareous ooze, which is corroborated by observations made during the *Shinkai 6500* dives (Perez et al., 2018). Its origin being calcareous phyto- and zooplankton, the ooze was most likely formed over the RGR itself, and subsequently settled over the summit. The calcareous ooze sediment stretches eastward, covering the Delta subregion and tends to become coarser towards the Charlie subregion, which is modelled to be mainly fine-grained calcareous sediments (Fig. 6D).

The current velocity over the entire RGR is invariably low, with a mean ± sd of 0.016 ± 0.004 m/s, ranging between values as low as 0.008 m/s in the eastern section, and up to six times higher over the shallow peaks in the northwestern part of the Alpha bulge, modelled at 0.05 m/s (Fig. 6E). The highest current velocities can be found in the Vema Channel west of the Alpha bulge (Fig. 6E). The vertical current velocity (Fig. 6F) shows whether the residual current is either from the bottom upwards, toward the surface (positive values) or from the surface downward, towards the seafloor (negative values). Fig. 6F shows a general upwelling over the shallow parts of the Alpha bulge and the central part of the eastern Delta arc (Fig. 6F). Downwelling areas are located markedly along the western and north-western deeper slopes of the Alpha bulge, the Charlie subregion and the inner part of the eastern Delta arc (Fig. 6F). These up- and downwelling patterns are in general concordance with the large-scale hydrodynamic processes around seamounts described in e.g. Boehlert and Genin (1987a, 1987b) and White et al. (2007).

4.2. Temperature, salinity, oxygen and nutrients

Temperature distribution patterns show highest values over the summits, naturally explained by the limited depth, and decreasing more or less linearly with depth (Fig. 7A). The relatively narrow range of temperature along the features of both the western and eastern RGR, suggests that species living there may be spatially constrained, which may be especially relevant when designating protected areas.

Salinity showed a discontinuous pattern (Fig. 7B), with a range in values of 1.3 PSU and a mean ± sd of 34.8 ± 0.1 PSU. The highest values of ~35 were modelled over the summits of the higher features, likely a consequence of evaporation in the surface ocean, and at depths of 1500–3000 m. Although the differences are very small and likely not ecologically very relevant, the lower salinity values were modelled to be around 34 and found at depths ~200–800 m.

Bottom-water levels of dissolved oxygen reveals the lowest values again along intermediate-depth slopes, mainly along the western bulge (Fig. 7C). Florindo et al. (2015) and references therein (i.e. Koltermann et al., 2011) characterise the waters over the (western) RGR between 1200 and 1500 m depth as Upper Circumpolar Deep Water (UCDW) with the lowest O_2 concentration of all the overlying water masses. However, the UCDW dO_2 concentration (4–4.5 mL/L) is well above hypoxic levels (below 2 mL/L), and thus the waters over the RGR do not harbour an oxygen-minimum zone (OMZ). The highest dissolved O_2 values are along the deepest margins of mostly the northern slopes (Fig. 7C), and likely constitute oxygen-rich North Atlantic Deep Water (NADW; Florindo et al., 2015).

Nutrient availability, such as silicate, nitrate and phosphate (Fig. 7D-F) are lowest over the summits of the western bulge and the deeper slopes. Silicate is an important nutrient for diatoms, and for sponges below the photic zone (Egge and Aksnes, 1992; Maldonado et al., 2005). Silicate concentrations are modelled to be lowest over the summits, as a consequence of utilisation by diatoms and highest in the deepest abyssal plains and the deeper graben in the southeastern Charlie subregion (Fig. 7D). There appears a horizon on the Alpha subregion, at depths of ca. 750–1000 m, characterised by relatively higher dissolved silicate bottom water concentration. This could be caused by local downwelling of dissolved (dead) diatom frustules. The typically high-nutrient waters (order of magnitude higher) are found in the abyssal plains surrounding the RGR (Fig. 7E-F). These nutrient-rich waters are brought to the surface by upwelling (Boehlert and Genin, 1987a), where they are depleted by primary productivity in the euphotic waters over the summits. The high nutrient levels along the shallower slopes (Fig. 7E-F) may reflect a retention of nutrients caused by vertical circulation of (decomposing) organic matter from the euphotic zone downward (White et al., 2007).

Bottom water pH is markedly lower in the abyssal waters of the Brazil basin than in those of the Argentine basin (Fig. 8A). Situated in shallower water layers, the bottom waters of the features of the RGR are characterised by pH values of between 7.77 and 8.07, with the highest values along the summits and deeper slopes of the Alpha bulge (Fig. 8A). This discontinuity may be caused by mixing of different water masses and/or secondary downwelling (White et al., 2007). Total Alkalinity (TA), or the seawater's total proton (acid) buffer capacity, was lowest along the summits of the Alpha bulge (Fig. 8B) and decreased with depth. This modelled vertical alkalinity trend is largely in line with the general observed trends for the South Atlantic (Chung et al., 2003; Takahashi et al., 2006, 2014), which shows mean surface values of ~2300 μEq/kg seawater, increasing with depth, with an inflection between 400 m and 900 m (Takahashi et al., 2006).

Virtually all relief features of the RGR display an aragonite saturation state (Omega; Ω_{Arag}) of more than 0.75, and up to 1 in near-bottom water along the intermediate slopes and along the summits (Fig. 8C). The higher Ω_{Arag} values imply favourable seawater chemistry for calcifying organisms, like molluscs, foraminifera and cold-water corals. The calcite saturation state (Ω_{Cal}) displays a similar trend, with values

Table 1
The percentage of the total surface area of CPRM mining blocks at the RGR, occupying substrate with a particular slope angle interval.

slope angle interval	% surface area blocks
0–5	78.87
5–10	18.81
10–15	1.61
> 15	0.71
total	100

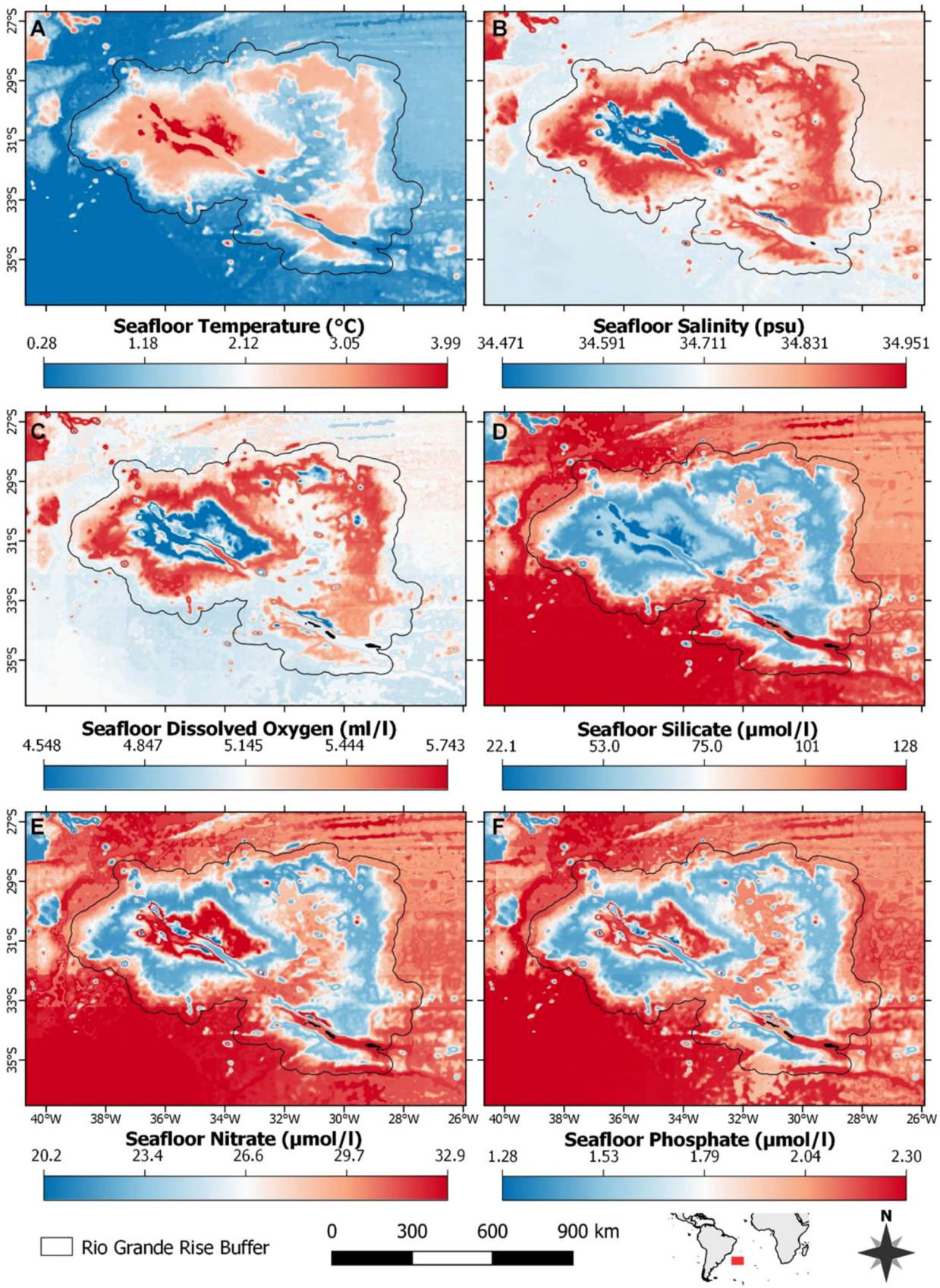

Fig. 7. Maps showing time-averaged environmental data for the RGR buffer area and surroundings. Top-left to bottom-right (A): Temperature [degrees Celsius], (B): Salinity [-], (C) Bottom water dissolved oxygen [mL/L], (D) Bottom water silicate concentration [µmol/L], (E) Bottom water nitrate concentration [µmol/L], (F) Bottom water phosphate concentration [µmol/L].

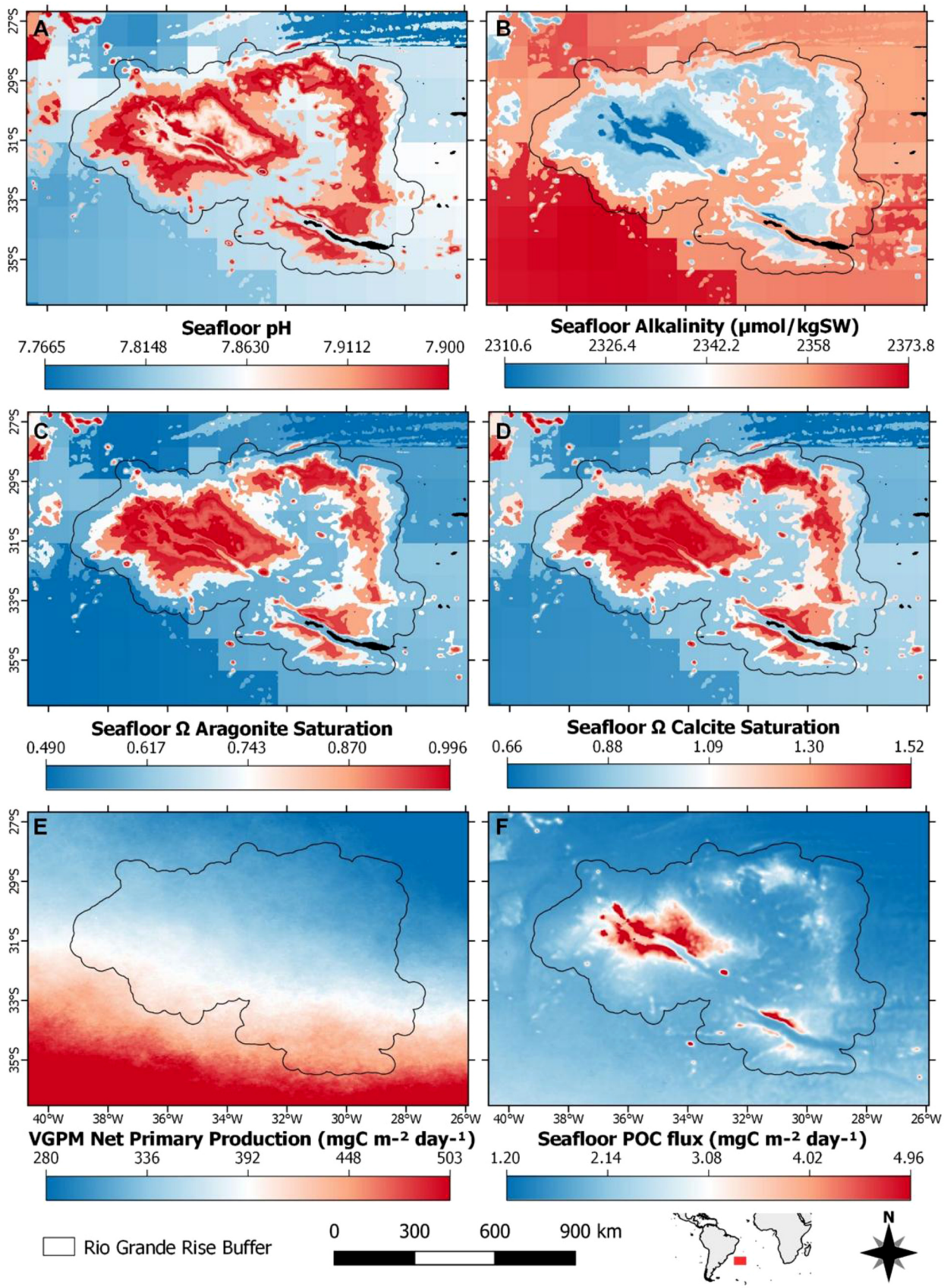

Fig. 8. Maps showing time-averaged environmental data for the RGR buffer area and surroundings. Top-left to bottom-right (A): Bottom water carbonate concentration [µmol/kg SW], (B): Bottom water alkalinity [µmol/kg SW], (C) Bottom water Aragonite saturation state [-], (D) Bottom water pH, (E) Surface water primary production [mg C/m^2/day], (F) downward flux of Particulate Organic Carbon [mg C/m^2/day].

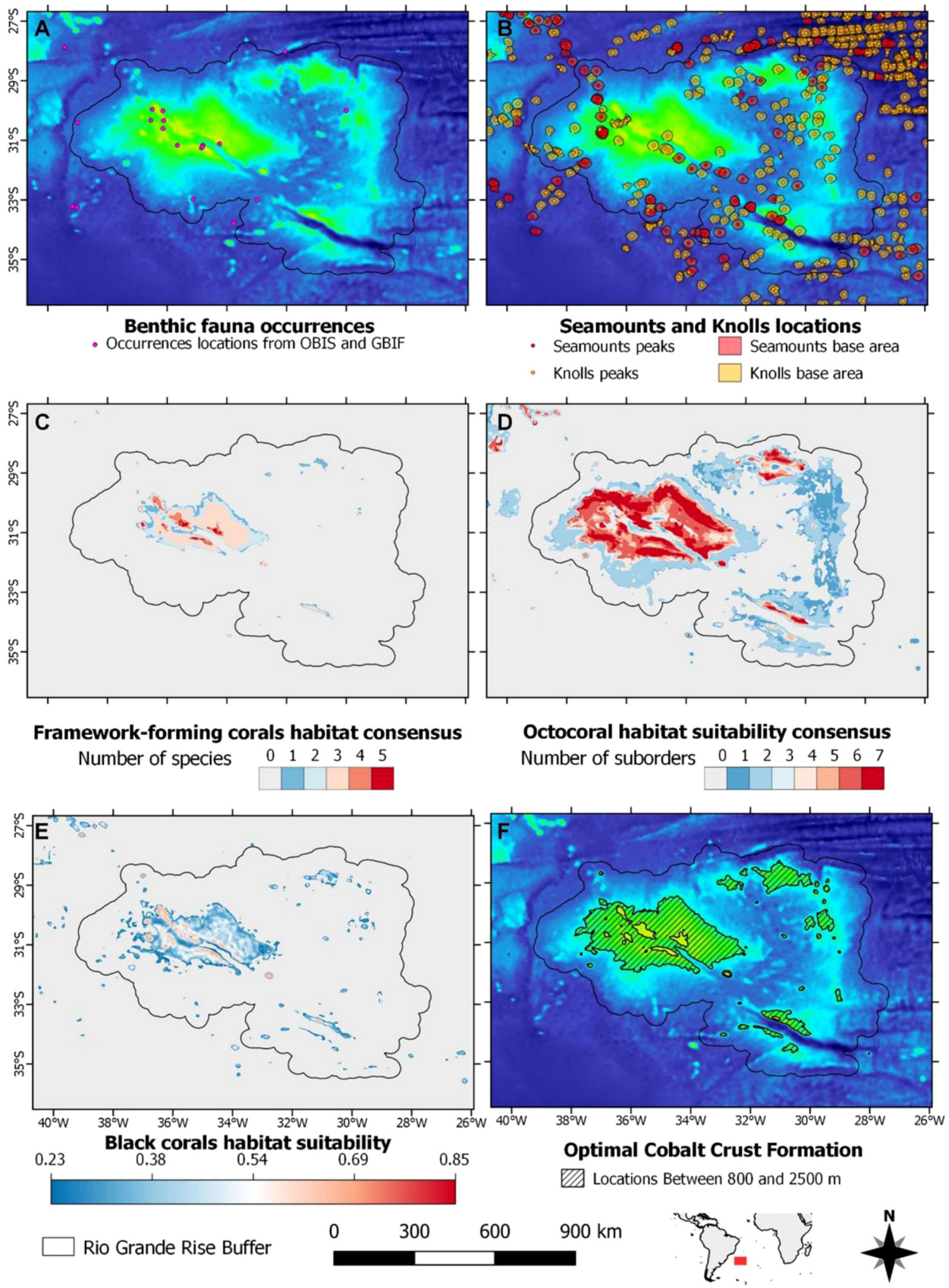

Fig. 9. Maps showing biogeographic data for the RGR buffer area and surroundings. Top-left to bottom-right (A): Benthic fauna occurrences (GBIF and OBIS databases), (B): Locations of seamounts (red) and knolls (yellow) with their respective estimated base area, (C) Habitat consensus for framework-forming (stony) corals, (D) Habitat suitability for Octocorals (Octocorallia), (E) Zonation for cobalt-rich crust (CRC) optimal formation conditions (hashed area) over the RGR. (For interpretation of the references to color in this figure legend, the reader is referred to the web version of this article.)

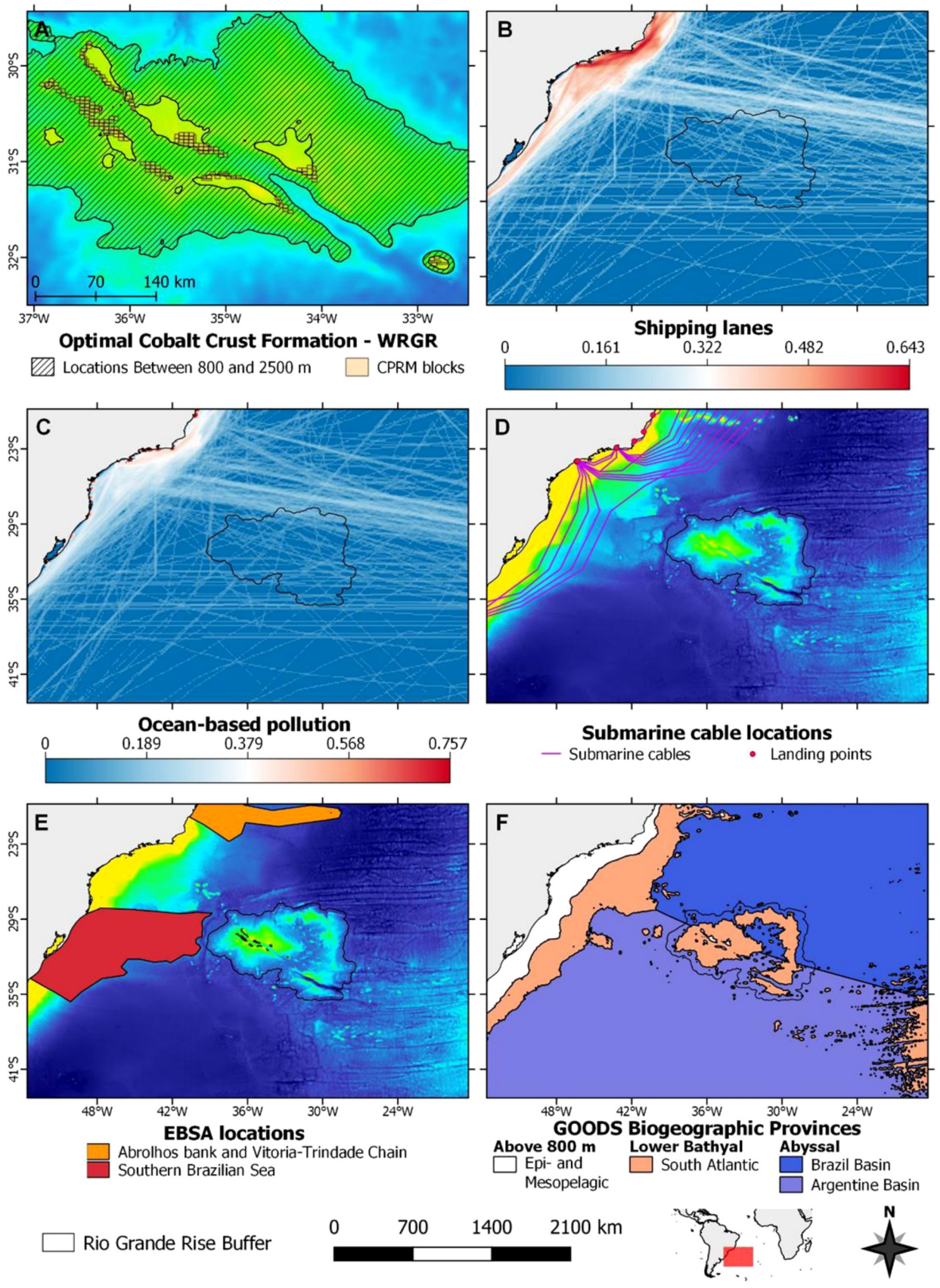

(caption on next page)

Fig. 10. Maps showing biogeographic data and human uses for the RGR buffer area and surroundings. Top-left to bottom-right (A): Zonation for cobalt-rich crust (CRC) optimal formation conditions (hashed area) over the western Alpha bulge region, with overlay of the location of the CPRM blocks (yellow rectangles) (B): Shipping routes with traffic intensity in and around RGR, (C) Ocean-based pollution with intensity in and around RGR, (D) Submarine (data traffic cables superimposed on bathymetric chart for RGR and SE Brazil coast, (E), Locations of Ecologically or Biologically Significant Areas (EBSA) superimposed on bathymetric chart of the RGR and SE Brazil coast, (F) Distribution of GOODS biogeographic provinces over the RGR and SE Brazil coast. (For interpretation of the references to color in this figure legend, the reader is referred to the web version of this article.)

between 1 and 1.5 (Fig. 8D). The carbonate compensation depth (CCD, depth at which $\Omega_{Carb} \approx 1$), below which calcium carbonate spontaneously dissolves, is located at ca. 4700 m in the Brazilian part of the Atlantic (Lisitzin, 1977; Emelyanov, 2005).

The location of the RGR in the subtropical oligotrophic waters of the South Atlantic, means that net primary production (NPP) is uniformly low over the area (Fig. 8E). NPP over the RGR displays a maximum variation of a factor 4 between the far north-northeastern and the far southeastern regions. The higher NPP in the latter region is likely influenced by the high-production Brazil-Malvinas confluence zone, located further south (Brandini et al., 2000). The relatively low NPP over the RGR results in a low downward POC flux (Fig. 8F). In the modelled POC map, the summits of the western Alpha bulge and those of the ridges at the Charlie subregion can be discerned, as they experience about three times higher POC fluxes, due to their much shallower depths (Fig. 8F).

4.3. Benthic biogeography and habitat suitability

After accessing the GBIF (http://doi.org/10.15468/dl.indh75) and OBIS databases (accessed 15 June 2017), a table with 11867 records was generated, where the great majority (76.3%) were Foraminifera. After further data processing (detailed information on data treatment in Supplementary material), only 22 Animalia records were classified as "Benthic" (18 species; see Suppl. Mat. for details), ranging from 185 to 4818 m in depth, spread over 21 locations within the RGR buffer (11 points in western RGR Alpha bulge; Fig. 9A and Table S2 in Suppl. Mat.). While Morato et al. (2016) show at least a few records of vulnerable marine ecosystems (VME) indicator taxa in the RGR, our search yielded no such records in the RGR, due to removal of records from the "Vulnerable Marine Ecosystems in the South Pacific Ocean region" dataset. (Table S2 Suppl. Mat.).

Apart from being pelagic biodiversity hotspots (Morato et al., 2010), deep seamounts and smaller knolls are important benthic habitats for deep-sea corals and VME indicator species, like octocorals, crinoids and sponges (Tittensor et al., 2009; Davies et al., 2015). A total of 47 seamounts and 122 knolls were recorded within the RGR buffer area (Fig. 9B), occupying a total base area of ca. 44,000 (7% of RGR buffer), and 99,400 km^2 (15% of RGR buffer), respectively.

As records from RGR are scarce, we also used three habitat suitability models available from the literature to define areas more likely to presence of corals. The consensus of species occurrence of hard (framework-forming) cold-water corals (Davies and Guinotte, 2011) ranges between 0 and 5 species, with the maximum number of species to be expected along the shallowest summits (Fig. 9C). Similarly, the number of octocoral (Alcyonaria) species (range 0–7; Yesson et al., 2012) is expected to be highest along the shallowest summits, and decreasing with depth, due to due to low current speeds, inconsistent food supply, and the reduced aragonite saturation state (Davies and Guinotte, 2011). However, a maximum is found along the deeper slopes (2000–2500 m) of both the Alpha bulge and the northern bulge of the Delta arc, with a large area of maximum consensus (7 species) along the northern deep slopes of the Alpha bulge (Fig. 9D). Habitat suitability of black corals (Yesson et al., 2017) is uniformly highest along the shallowest summits, decreasing more or less linearly with depth until ca. 2500 m (Fig. 9E).

4.4. Crusts and other human uses of the RGR region

Figs. 9F and 10A show the spatial overlap between the CPRM mining blocks and the optimal CRC locations in the western Alpha bulge of the RGR. The CPRM blocks are largely located within the 800–2500 m horizon, although in multiple cases, the blocks tend to be located either just on the 800 m isobath or above that, effectively placing them outside the optimal CRC location horizon (Fig. 10A). This apparent incongruence may be explained by local (past) environmental variability, and is a point of interest which may be investigated in a dedicated expedition.

Other human uses in the RGR area, that may either contribute to environmental impacts due to mining or pose a limitation to them, constitute marine traffic, pollution and submarine cables. The RGR is not located in a notoriously busy shipping area, such as the North Sea, Persian Gulf or the East China Sea. Although shipping is more intensive along the Brazilian coast, the ocean-crossing marine traffic is much lower, and associated shipping pressure on the RGR is low to moderate (Fig. 10B). There is an oceanic shipping lane passing through the northern part of the RGR. The busiest shipping lane is located north of that, and leads through deeper waters, not intersecting the RGR buffer area (Fig. 10B).

Due to its location, more than 1000 km offshore and in the deep ocean, direct human influence over the RGR is low. However, shipping traffic (see above) is invariably correlated with pollution of all types: oil spills, waste dumping (intentional or not), metal and/or plastic pollution. Pollution over the RGR can thus be attributed mostly to shipping activity, and although generally low, the highest pollution pressure is located in the same locations as the busiest shipping lanes to the north (Fig. 10C). The extracted data do not contain information on the nature and/or origin of the pollution. As the economic position of Brazil is expected to grow stronger and more important on the global commodities market (http://www.oecd.org/eco/outlook/brazil-economic-forecast-summary.htm), both shipping and associated pollution pressures on the RGR are expected to increase.

Submarine cables are large telecommunication cables that have been laid down on the seabed. Submarine cable circuits are very reliable, consisting of several redundant intercontinental cable circles and accounting for > 99% of international data traffic (the remainder travels via satellite links). Along the eastern seaboard of South America, the main hub and landing point for submarine cables from North America, Europe and Africa is Fortaleza (State of Ceará, NE Brazil). From there, a series of submarine cables run as far south as Montevideo (Uruguay) and Buenos Aires (Argentina), with the São Paulo/Santos coastal zone and Rio de Janeiro being the southern landing hubs in Brazil. Of this latter cluster, the nearest submarine cable is located > 300 km away from the Northwestern border of the RGR buffer area, and is therefore regarded to be of no significant consequence to the RGR (Fig. 10D).

The RGR is located less than 150 km east of a large Ecologically and Biologically Significant Area or EBSA (https://www.cbd.int/ebsa/), known as the South Brazilian Sea EBSA (Fig. 10E). About 850 km to the north, the Abrolhos Bank/Trinidade Seamount Chain EBSA is located. Fig. 10F shows the delineations of the GOODS biogeographic provinces over the RGR and the SE Brazil coast, as well as the depth zones in which different features are located. The RGR almost entirely in the bathyal depth zone (Fig. Error: Reference source not foundF), and separates the Brazil from the Argentine abyssal basins. Only the highest

summits of the Alpha bulge are located in the mesopelagic depth zones (Fig. 10F).

In the absence of information on regional biodiversity and/or ecosystem functioning, a seascape mapping was performed, based on the broad-scale environmental drivers shown above. We used an unsupervised classification method to look for patterns in the environmental data, which does not requires ground-truthing (Brown et al., 2011), as such data is still not available for the area. For detailed methodologies used here to construct the seascape map (Fig. Error: Reference source not found), similar to those outlined by Harris et al. (2008) and Harris and Whiteway (2009), the reader is referred to the Supplementary material. We would like to re-iterate here that the classification of these seascapes is a first step in characterising the virtually unknown benthic ecosystem in and around the RGR, and that more and high-fidelity data is needed to perform detailed habitat suitability modelling.

The first seascape (seascape 1; Fig. Error: Reference source not found) is located in the shallowest regions of RGR and it is the most distinguished from the others. It has the highest POC flux and temperature values (Fig. 12) and a high variation in slope, which could be a proxy for a higher abundance of specimens. It also features the lowest dissolved oxygen (dO_2), but with a high variation as well. The CPRM blocks are exclusively located in this seascape (Fig. Error: Reference source not found), which would constitute a disproportionately strong disturbance in this area once the exploitation phase begins. Seascapes 2, 3 and 4 (Fig. Error: Reference source not found) have similar values of low POC flux, low temperature, low slope and medium dO_2 (Fig. 12). They are located in deeper regions of RGR; seascape 2 covers the mid-south portion of RGR, seascape 3 covers the southwestern area and the Vema Channel and seascape 4 covers the mid-north portion. Seascape 5 is distinguished by a steep slope (Fig. 12) and it is mostly found around seamounts and in the graben walls (Fig. Error: Reference source not found). Seascapes 6 and 7 include the lower slope of the Alpha bulge and most area of the Delta and Charlie Subregions (Fig. Error: Reference source not found). They have medium temperature and high dO_2 values and they mainly differentiate by a higher dO_2 on seascape 7 (Fig. 12).

5. Ecosystem services from the RGR

Although the characterisation of ecosystem services (ES) is of great importance to manage impacts in mining areas, up till now ecosystem goods and services have not been properly accounted for in deep-sea resource management (Le et al., 2017). In a recent report for a deep-sea mining project in Papua New Guinea territorial waters, ES were identified for the area under investigation (Batker and Schmidt, 2015).

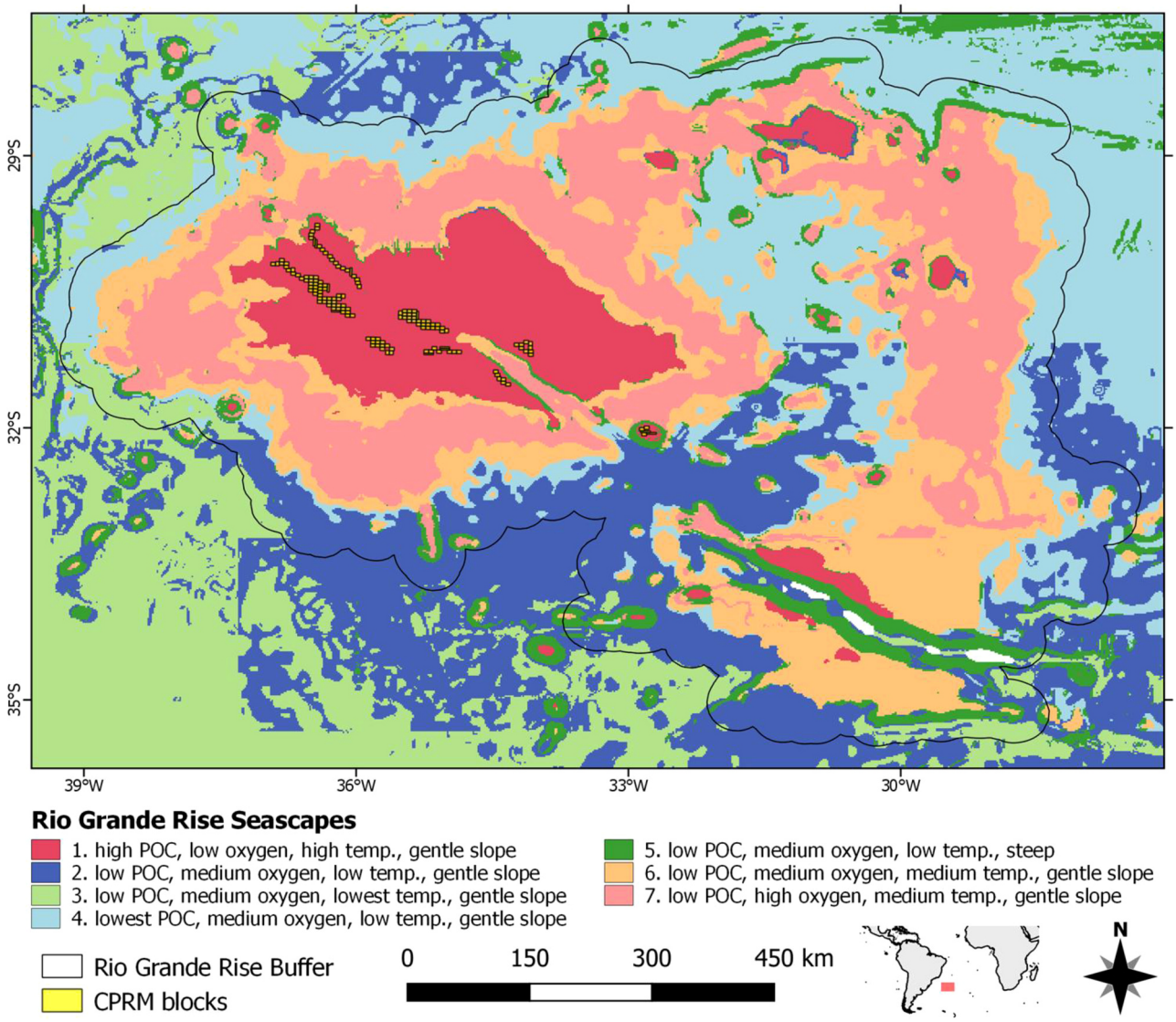

Fig. 11. Map showing seascape classification of the Rio Grande Rise, using ArcGIS ISO Cluster Unsupervised Classification tool (see Suppl. Mat. for more details).

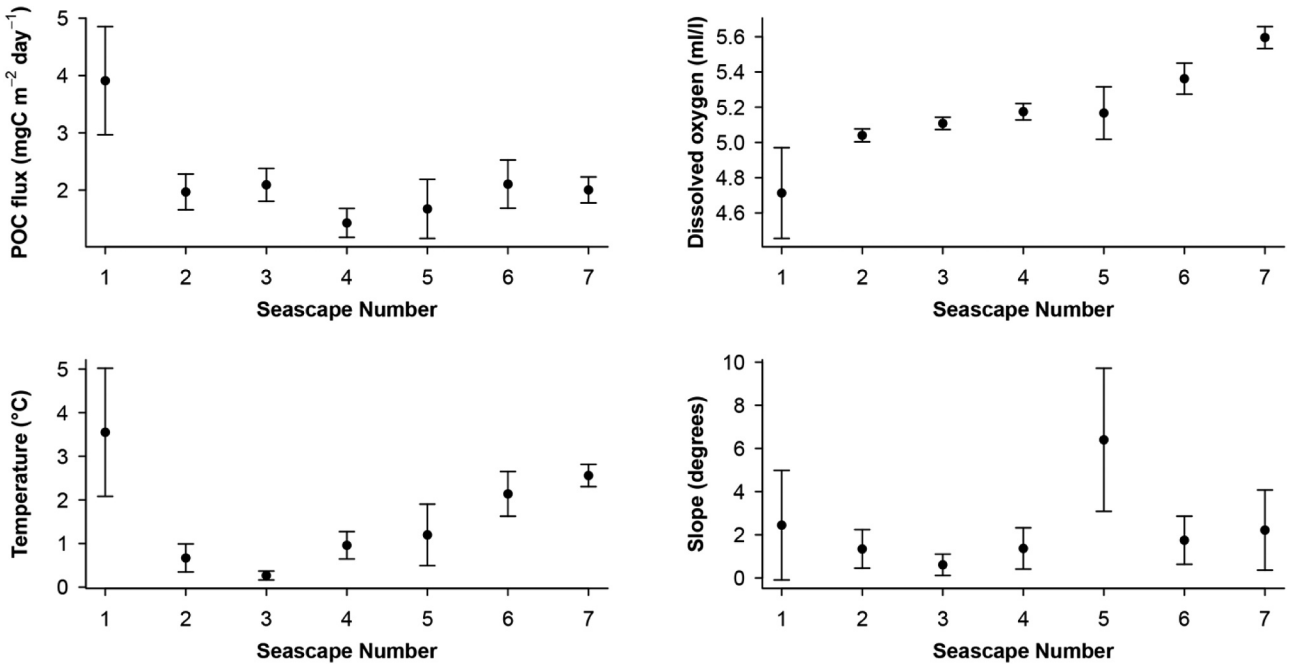

Fig. 12. Mean values of each variable used in the classification for each seascape in Rio Grande Rise. Error bars represent standard deviation (SD).

However, this report was considered controversial, since the authors considered ecosystem services that were applicable exclusively to terrestrial ecosystems, in a marine context (Rosenbaum Helen, 2015). In the two most recent and extensively worked-out environmental management plans (EMP), for large-scale PMN mining in the CCZ (Smith et al., 2008a; ISA, 2011a) and SMS mining along the MAR (Dunn et al., 2018), ecosystem services are not explicitly mentioned, and remain without further elaboration (Seascape, 2014). However, the CCZ EMP (ISA, 2011a) does mention guidelines to 1) incorporate ecosystem-based management (EBM) principles in mining strategies to safeguard biodiversity and ecosystem functioning in the region and 2) design Preservation Reference Areas (PRAs) to preserve ecosystem structure and function, consistent with EBM.

5.1. Definitions and challenges

There are still many knowledge gaps as to how ecosystem functions (EF) and services (ES) translate into actual benefits to society (Le et al., 2017). An ecosystem function (EF) represents a natural structure or process that may generate a service which provides human well-being and exists independent of humans (Armstrong et al., 2010). A global definition of ES is still under discussion (Böhnke-Henrichs et al., 2013), but Armstrong et al. (2010) define ES as "…the results of ecosystem functions that provide benefits to human well-being, and they only exist as a service by reference to human users of the service…".

The evaluation of both ecosystem functions and ecosystem services considers both the costs and benefits of resource exploitation (Thurber et al., 2014), and thus allows for more balanced management strategies and decision-making. Current baseline and monitoring requirements recommended by ISA (to contractors) do not explicitly include evaluation of ES, but do contain measurements to characterise habitats and biodiversity (Le et al., 2017).

The lack of information about deep-sea processes severely limits our understanding of its ecosystem services, and by extension, its economic value (Folkersen et al., 2018). However, the provision of ecosystem services is intrinsically related to the conservation status of natural habitats (Maes et al., 2012), and a decrease in species richness and biodiversity is generally associated with an exponential decline of ecosystem function, efficiency and resilience (Danovaro et al., 2008; Armstrong et al., 2014). Studies in deep-sea environments suggest that the maintenance of ecosystem functioning is related to the performance of biological and biogeochemical processes, which in turn are associated to higher biodiversity (Danovaro et al., 2008). Following that, a decline in ecosystem functioning has a potentially negative impact on the provisioning of goods and services (Worm et al., 2006; Danovaro et al., 2008; Loreau, 2008). A possible approach to linking biodiversity and ecosystem functioning, and therefore ecosystem services, is to integrate Biological Traits Analysis (BTA; Bremner et al., 2006; Frid et al., 2008; Bremner, 2008) in any planned benthic sampling campaign. By using BTA, taxa are described by series of biological traits, which may function as qualitative proxies of ecosystem functions, and can thus be used in the hierarchical structure linking ecosystem processes to ecosystem services, proposed in Böhnke-Henrichs et al. (2013). In this manner, spatial and/or temporal patterns in biological traits may be used to shed light on ecosystem functions and ultimately ecosystem services originating from the RGR.

The challenge of mapping ES in the deep sea arises from a lack in coverage and resolution on environmental and socio-economic data, ambiguity of maritime boundaries, the multidimensional structure of marine habitats and the difficulty of assessing connectivity between habitats (Liquete et al., 2013). This is in concordance with Le et al. (2017), stating that high-quality ecological baseline information (e.g. physiology and metabolism, dispersal and connectivity, nutrient and element cycling, life histories) is necessary to assess details about the structure and function(s) of the ecosystem, and consequently the ES provided. Additionally, establishing marine ES typologies is challenging due to difficulties in appropriate differentiation between ecosystem processes and the magnitude of benefits derived from services (Böhnke-Henrichs et al., 2013). Moreover, the current lack of information on the deep sea and indeed any derived ecosystem services may limit our understanding of the magnitude and distribution of the potential monetary value that is under threat by human activities, such as deep-sea mining (DSM; Folkersen et al., 2018)

Although the current ES classifications seem incompatible with deep-sea reality (Thurber et al., 2014), the adoption of an ES framework can aid in balancing conservation and natural resource exploitation in a context of DSM (Le et al., 2017). The integration of ecosystem services is of major importance in linking health and functioning of ecosystems

on one side, to human uses on the other. The inclusion of ecosystem services may thus be applied in approaches such as Ecosystem-Based Management (EBM) and Marine Spatial Planning (MSP; Böhnke-Henrichs et al., 2013).

5.2. Ecosystem services evaluation for the RGR

Currently, several ecosystem services (ES) frameworks are available (Millennium Ecosystem Assessment, 2005; Beaumont et al., 2007; de Groot et al., 2010; Böhnke-Henrichs et al., 2013; Haines-Young and Potschin, 2013). However, most of these frameworks were developed based on terrestrial environments and need to be adapted in order to be applied in a marine context (Thurber et al., 2014). Identification of ES represents an opportunity to better comprehend the importance of the deep sea to human well-being and acts as a first step toward recognition of potential impacts of deep-sea mining (Armstrong et al., 2010). The RGR presents an area with a stark paucity of data (Perez et al., 2012), which may hamper accurate definition of ES for the area. This highlights once more the importance of obtaining more high-quality data, especially when considering measures to guarantee the maintenance of ecosystem services and conservation of the area. The identification of ES for the RGR here (Table 3) represents the first qualitative classification of ecosystem services for an area under ISA exploration contract. Schlacher et al. (2013) discuss spatial variation of benthic communities and potential loss of benthic ecosystem functions in relation to deep-sea mining impacts on a central pacific seamount for the first time. Armstrong et al. (2012) and Le et al. (2017) have been the first to touch upon the importance of ES associated to seamounts, and make general mention of it. However, this study presents the first attempt to truly characterise ES derived from a (deep sea) seamount area.

In this study we have opted for the adoption of the Millennium Ecosystem Assessment (MEA; Millennium Ecosystem Assessment, 2005) as a framework (see Suppl. Mat. for procedural details), following Armstrong et al. (2010), stating that: (i) the supporting services facilitate the identification of deep-sea ecosystem services and (ii) there is a considerable distance (in space and time) between the supporting services and the benefit received to human well-being from the deep sea. According to the MEA (2005), four categories are used to categorise ecosystem services: (1) **Provisioning services** are products used by humans that are obtained directly from habitats and ecosystems; (2) **Regulating services** are the benefits obtained through the natural regulation of habitats and ecosystem processes; (3) **Cultural services** represent the non-material benefits people obtain from habitats and ecosystems; (4) Finally, **Supporting services** represent (ecosystem)

Table 2
Classification of ecosystem services for the RGR region. Scale of application: RGR = Rio Grande Rise; SM = Seamounts in general; DS = Deep Sea in general.

Type	Indicator	Scale of Application	References
Provisioning	Food - fish stocks	DS/SM/RGR	Armstrong et al. (2012); Batker and Schmidt (2015)/Thurber et al. (2014); Le et al. (2017)/Morato et al. (2016)
	Biological resources for pharmaceuticals	DS/SM	Armstrong et al., (2012, 2014); Thurber et al. (2014); Batker and Schmidt (2015); Le et al. (2017)/Secretariat of the Pacific Community (2016)
	Biomaterials	SM	Le et al. (2017)
	Oil and gas production	DS	Armstrong et al. (2012); Thurber et al. (2014); Batker and Schmidt (2015)
	Mining resources (CRCs, phosphorites)	DS/RGR	Armstrong et al. (2012); Thurber et al. (2014); Batker and Schmidt (2015)/Cavalcanti et al. (2016)
	Waste disposal	DS	Thurber et al. (2014)
Regulating	Climate regulation	DS	Armstrong et al. (2012); Thurber et al. (2014); Batker and Schmidt (2015); Le et al. (2017)
	Life cycle maintenance	SM	Taranto et al. 2012; Liquete et al. (2013)
	Biological regulation	DS	Armstrong et al. (2012)
	Waste absorption	DS/SM	Armstrong et al. (2012); Batker and Schmidt (2015); Le et al. (2017)/Secretariat of the Pacific Community (2016)
	Carbon sequestration and storage	DS/SM	Armstrong et al., (2012, 2014); Thurber et al. (2014); Le et al. (2017)/Secretariat of the Pacific Community (2016)
Cultural	Educational	DS/SM	Armstrong et al., (2012, 2014); Batker and Schmidt (2015); Le et al. (2017)/Thurber et al. (2014); Secretariat of the Pacific Community (2016)
	Scientific	DS/SM	Armstrong et al. (2014); Thurber et al. (2014); Batker and Schmidt (2015)/Secretariat of the Pacific Community (2016)
	Aesthetic	DS	Armstrong et al., (2012, 2014); Thurber et al. (2014); Batker and Schmidt (2015); Le et al. (2017)
	Source of climate data	DS	Armstrong et al., (2012, 2014)
	Cobalt crusts	SM/RGR	Le et al. (2017)/Cavalcanti et al. (2016)
Supporting	Increased carbon flux to the seafloor	DS/RGR	Thurber et al. (2014); Le et al. (2017)/this study
	Habitat for VME taxa	SM/RGR	Armstrong et al. (2012); Yesson et al. (2016); Le et al. (2017)/Morato et al. (2016); this study
	Habitat for commercial value species	DS	Armstrong et al. (2014)
	Habitat for hard-substrate benthic organisms	DS/SM/RGR	Armstrong et al. (2012)/Thurber et al. (2014); Le et al. (2017)/Perez et al. (2018); this study
	Nutrient regeneration (upwelling)	DS/RGR	Le et al. (2017)/Florindo et al. (2015); Morato et al. (2016); this study
	Habitat diversity	SM/RGR	Le et al. (2017)/this study
	Nursery habitats	DS/SM	Batker and Schmidt (2015)/Baillon et al. (2012); Secretariat of the Pacific Community (2016); Le et al. (2017)
	Hard-attachment substrate (crust formation)	SM/RGR	Le et al. (2017)/this study
	Water circulation and exchange	DS/SM	Armstrong et al. (2010)/Kvile et al. (2014)
	Nutrient cycling	DS/SM	Armstrong et al. (2012); Thurber et al. (2014); Batker and Schmidt (2015); Le et al. (2017)/Secretariat of the Pacific Community (2016)
	Higher primary production - chemosynthesis	DS	Armstrong et al. (2012); Thurber et al. (2014); Le et al. (2017)
	Higher primary production - phytoplankton	DS/SM/RGR	Le et al. (2017)/Kvile et al. (2014)/this study
	Higher biodiversity	SM/RGR	Taranto et al. (2012); Le et al. (2017)/this study
	Increased secondary production	DS/SM/RGR	Armstrong et al. (2012);Thurber et al. (2014)/Rowden et al. (2010);Taranto et al. (2012); Le et al. (2017), this study
	Three-dimensionality (habitat complexity)	SM	Kvile et al. (2014); Le et al. (2017)

Table 3
Mean, standard deviation and ranges of environmental variables pertaining to the CPRM mining blocks.

Variable	Unit	Mean	SD	min.	max.
Distance from MAR	km	2054	109	1701	2203
Surface primary productivity	mg Carbon/ m2/day	366	7	348	378
Depth	m	949	291	443	1925
Seabed slope	degrees angle	3.3	2.7	0.01	26.4
Bottom current velocity	m/s	0.06	0.03	0.02	0.14
Bottom temperature	°C	3.85	0.94	2.92	8.22
Bottom water salinity	PSU	34.52	0.15	34.26	35.05
Bottom water oxygen concentration	mL/L	4.86	0.18	4.52	5.28
Bottom water nitrate concentration	µmol/L	32.31	2.46	24.41	34.02
Bottom water phosphate concentration	µmol/L	2.06	0.16	1.52	2.16
Bottom water silicate concentration	µmol/L	47.66	5.74	37.54	59.81

functions that are necessary for all other ecosystem services to occur, and thus affect human well-being indirectly.

The ES classification for the RGR proposed in Table 2 is based on information available in scientific literature. The references in Table 2 represent the main available literature regarding each of the indicators as ecosystem services, and were selected based on their applicability to the RGR context (e.g. ES derived from seamounts, deep-sea ES, and marine and coastal ES in general; see Suppl. Mat. for detailed explanation). The "scale of application" in Table 2 represents the maximum spatial scale (above mentioned) from which it was possible to gather data to characterise the services provided by the RGR. The literature sources in which the particular ecosystem service was mentioned, which may include all the scales of application (from the most general to the most specific), are found in the "reference" column.

Characterisation of ES for a given area requires details on local ecosystem structure, processes and dynamics. It becomes clear from Table 2, that most data available applies to the regional (seamount; SM) or global scale (deep sea; DS), with scarce (if any) local data for the RGR. Data limitation for the RGR seriously hampers a precise evaluation of the ecosystem goods and services provided by the area. There is insufficient regional knowledge, and studies on the RGR ecosystem functioning are lacking, which is of serious concern in this context of compulsory and comprehensive impact assessment of e.g. mining.

Folkersen et al. (2018) identified that factors related to the economic valorisation of deep sea environments are mostly determined by how socio-economic variables (e.g tax rates, resource market values, operation costs, equipment development etc.) interact with deep-sea resources. Therefore, understanding the interests, policies and (monetary) values involved in a particular DSM mining process, can strengthen discussions on aspects of resource use and sustainability.

This overview clarifies the necessity to invest resources and increase efforts in the collection and analysis of data for the region, through targeted research cruises. Although expensive and time-consuming, research initiatives in the high seas, in combination with intelligent data sharing through geo-referenced databases, are needed to generate high-quality data. Only by better defining the ecosystem structure, processes and services on individual underwater features like the RGR, will it be possible to perform evidence-based and case-specific management of high and deep seas (Kvile et al., 2014).

6. Mining plans, resources, environment and impacts

6.1. CRC coverage and grade

While the origin of the RGR may be volcanic (Gamboa and Rabinowitz, 1984), the region contains no seismically active spreading ridges, and so the probability of seafloor massive sulfides (SMSs) presence is considered negligible (Hein et al., 2013). Although there are reports of low to medium densities of polymetallic nodules (PMN) on the abyssal plains to the south of the Alpha subregion (Kasten et al., 1998), the main mining activity on the RGR is centered around CRCs. Generally, CRC mining technology is currently considered to be less developed than PMN or SMS mining technologies (Hein, 2004). The usually steep and uneven terrain, the variability of the crusts' thickness, and the manner of "harvesting" the crusts makes CRC mining a more complex task than standard nodule or sulfide mining operations (ISA, 2007).

The area allocated to CPRM consists of 150 blocks of 20 km^2 each, all located in the western Alpha subregion (Fig. 11A). The blocks are grouped into eight clusters of between 5 and 56 blocks, arranged in a 400 × 260 km area. The majority of the blocks are situated along the apex of the western Alpha subregion, on both sides of the central graben. One small cluster of blocks is situated on the summit of the Bravo guyot (flat-topped seamount), located at the south-eastern end of the central graben.

The location where CRCs are found is a strong determinant for their composition and thus their commercial value (Hein and Morgan, 1999; Hein, 2004; Hein and Koschinsky, 2014b; Hein et al., 2016). Table 3 shows the mean, standard deviation (SD), minimum and maximum values for environmental variables retrieved from open-access databases. Although the presence of crusts is inversely proportional to the presence of sediments, crust outcrops that are found on sediment tend to have higher contents of Al and Cu, and lower Co, Mn and Ni contents (Hein, 2004; Hein et al., 2013; Secretariat of the Pacific Community, 2013; Hein and Koschinsky, 2014b).

Ferro-manganese cobalt-rich crusts (CRCs) which are formed in relative proximity to hydrothermal sites consist predominantly of base metals, like iron and manganese, while stratabound (substratum-associated) crusts farther away tend to have a higher content of (valuable) Rare Earth Elements (REEs; Hein et al., 1997, 2000; Hein and Koschinsky, 2014a, 2014b). The CPRM blocks are located between 1700 and 2200 km away from the MAR (Table 3), which is assumed to be the closest location with large-scale hydrothermal activity. Based on this, the CRCs found on the Rio Grande Rise are expected to be relatively high in REEs, but generally lower in Co and Mn.

In CRCs investigated in the Hawaiian archipelago, the contents of Co, Mn and Ni tended to decrease with depth, while Fe content tended to increase (Hein et al., 2000; Hein, 2002; Hein and Petersen, 2013; Secretariat of the Pacific Community, 2013). The depth at which the CPRM blocks are located ranges between 400 and 2000 m, with a mean depth ± SD of 949 ± 291 m, while CRCs reported around the Hawaiian archipelago are associated with underwater features that tend to start around ca. 1000 m depth (Morgan et al., 2015). It is thus expected that, because of the limited depth of the CPRM blocks (range: 400–2000 m, mean depth ± SD of 949 ± 291 m), the targeted crusts at the RGR contain relatively high amounts of Co, Ni and Mn.

Both occurrence and thickness of the crusts increase with slope angle of the underlying substrate, reflecting the angle of repose, which determines whether sediment accumulation can take place (Hein and Koschinsky, 2013, 2014a). As such, a slope angle > 15° ensures crust coverage of > 80% (Yamazaki and Sharma, 2000). Table 3 shows the mean ± SD slope angle of the CPRM blocks to be 3.3 ± 2.7 degrees, with extreme values up to 26 degrees. In fact, less than 1% of the CPRM blocks at the RGR have a slope angle > 15° (Table 3). These notably steep slopes are mostly located in the north-western part of the Alpha subregion, where a southwest-tending canyon cuts into the northern ridge of the Alpha graben. Based on the low average slope, it is thus expected that crust coverage in the vast majority of the CPRM blocks is less than 80%.

6.2. Impacts from CRC mining

To be cost-effective, deep-sea mining is to be performed on extended temporal and spatial scales (Boschen et al., 2013; Levin et al., 2016b). A typical commercial mining operation is estimated to be sustained with the exploitation of ca. 600 km^2 crust area (ISA, 2007). From such an area, ca. 1 million metric tonnes are expected to be mined annually, for a period of 15–20 years (ISA, 2007). In the case of the CRCs located on the RGR, the (valuable) metal content is lower compared to those in the Pacific (Hein, 2002; Hein and Koschinsky, 2013; Secretariat of the Pacific Community, 2013), which may lead to a larger amount mined, in order to be profitable. This is expected to cause severe impacts on benthic habitats and ecological communities, both directly and indirectly.

The most obvious and direct effect is the removal of benthic hard substrate habitat made up by the CRC itself. Due to the extremely low growth rate (1–6 mm per million years; (Hein, 2004)), the crust substrate can be considered lost for all practical purposes. The loss of CRC substrate will result in a reduction of habitat heterogeneity (Levin et al., 2016b). In response, mobile fauna will display avoidance behaviour and move away from the affected area (Schlacher et al., 2013; Hughes et al., 2015; Brown et al., 2016). However, as hard substrate is more often a habitat for sessile benthic macrofauna, these will not survive the operations and subsequently be lost (Schlacher et al., 2013; Gollner et al., 2017). The expected avoidance migration and/or large-scale mass-mortality, combined with very low rates of recolonisation and growth in deep-sea environments, will greatly reduce the benthic biodiversity in the directly affected mine site (Gollner et al., 2017). Consequently, associated benthic ecosystem functioning will be impaired for decades, and likely even centuries (Ramirez-Llodra et al., 2011; Van Dover, 2014; Levin et al., 2016b; Gollner et al., 2017).

The deep-sea environments where CRCs are located usually have very low suspended particulate matter (SPM) loads. The CRCs are naturally home to sessile, hard-substrate fauna, which generally can be classified as suspension feeders (Hessler and Jumars, 1974; Lundsten et al., 2009; Perez et al., 2018). These typical hard-substrate species tend to have a life history which is not compatible with high loads of suspended particulate matter (SPM; Sharma, 2015). Besides the area primarily affected by the crust removal, the surrounding area will certainly experience highly increased sediment loads, caused by the mining plumes (Miller et al., 2018). The areas directly downstream of the mining site will become covered by the densest material, while lighter particles may travel distances in the order of 10^2 km (MIDAS, 2015). High sedimentation rates, consisting of relatively dense material, will smother sessile fauna and invariably compromise the unique, sediment-poor crust ecosystem.

Both the breathing apparatus (gills) and food particle-collecting structures of benthic fauna are at risk of becoming clogged (Abdul Wahab et al., 2017) by a significantly increased and strongly persistent SPM concentration (ca. 250 days/year; ISA, 2007). In addition, as the low background of food particles will be diluted with large quantities of material of low or no nutritional value (Miller et al., 2018, and see website https://jpio-miningimpact.geomar.de/wp4-sediment-plume-dilution-and-dispersion), the quality of the SPM decreases dramatically. This potentially threatens organisms' energy budgets (and thus their fitness), as they may spend more energy on cleaning their filtering structures, while obtaining no net higher nutritional input.

Upon extraction, metals incorporated in the crusts will be released in unprecedented rates and (toxic) concentrations during the mining process (MIDAS, 2016).[2] Products originating from the mining, crushing and transport of the CRCs, will include dissolved (metal) ions, chelate complexes and biogenic ligands, especially in the presence of Redox-clines caused by e.g. oxygen-minimum zones (OMZ; ISA, 2007; Sharma, 2015; MIDAS, 2016). For transport to be efficient, the mined ore slurry needs to be de-watered (ISA, 2007; Sharma, 2015). The de-watering location of the so-called return water then determines the primary effects of metal contamination. Release of return water in surface waters will affect photosynthetic algae and/or pelagic animals, while return discharge near the ocean floor will carry the potential toxicants to affect deep-sea benthic communities (Hughes et al., 2015; MIDAS, 2016; Miller et al., 2018).

Ecotoxicological protocols for assessment of toxicant lethal doses prescribe both standard temperature (20 °C) and pressure (0.1 MPa = 0.987 atm). However, neither of these conditions apply to deep-sea mining locations, where temperatures are much lower (ca. 2 °C) and pressures are much higher (up to 60 MPa). Although lower temperatures generally reduce apparent lethal toxicity, higher pressures are known to greatly increase apparent toxicity (Mestre et al., 2014; MIDAS, 2016). Because metal ores are location-specific mixtures of metals and the effects of temperature and pressure are not consistent among metal ions (Mestre et al., 2014; Auguste et al., 2016), interaction effects are highly unpredictable and need thus to be assessed for individual mineral deposits (MIDAS, 2016).

Another issue with standard ecotoxicological protocols is that these are typically designed to determine the acute impacts (e.g. mortality). Typical exposure to (metal) contaminants from mining will last for years or even decades (ISA, 2007; MIDAS, 2016), and are thus of a highly chronic nature. Organisms chronically exposed to sub-lethal (i.e. order[s] of magnitude lower) concentrations may mitigate toxicity effects by effectively removing metals from their tissues using metallothionein (MT) proteins (Auguste et al., 2016). However, as is the case with the lower energy yield due to dilution of suspended matter by sediment plumes (see above), the physiology of MT protein production requires more energy to be allocated (Auguste et al., 2016). Other essential biological processes may thus be compromised by the extra energy expenditure caused by metal toxicity, even though organisms may be located far away from the principal mining locations (Sokolova et al., 2012; MIDAS, 2016). Finally, motile deep-sea organisms may detect and actively avoid metal-contaminated environments (Brown et al., 2017). As the mining-induced metal contamination represents a highly persistent disturbance, long-term migrations of organisms will invariably cause changes in biodiversity and functioning of the affected benthic ecosystems.

A secondary impact (i.e. not directly caused by the extraction process itself) of CRC mining operations are the resulting tailings. A rather common practice in land-based mining is (shallow) Submarine Tailings Disposal (STD) or Deep-Sea Tailings Placement (DSTP). In STD/DSTP, tailings are disposed at sea, often not far from shore, such that from the place of disposal the tailings will follow the natural slope of the seabed until it settles further away and at greater depth (Angel et al., 2013). One of the strongest critiques of the tailing placement practice is that all too often insufficient baseline information of the receiving system is available, thus limiting the accuracy of environmental impact assessments (EIAs) and the ability to predict impact and recovery (Ramirez-Llodra et al., 2015).

The main impacts of STD/DSTP are hypersedimentation, toxicity, turbidity and acute changes in sediment granulometry (Ramirez-Llodra et al., 2015). DSTP is invariably associated with strongly reduced diversity and ecosystem functioning, and its effects have been detected up to 20 km away from the discharge point (Hughes et al., 2015, and references therein). There is evidence that total benthic abundance returns to pre-impact values, within one to three years after cessation of tailing disposal. However, impacts on community structure are persistent and diversity remains very low for up to a decade (Hughes et al., 2015, and references therein). The inherently unstable character of such tailing slumps cause frequently recurring slope failures, which hamper community recovery by effectively re-setting the recolonisation stage. In a recent study, Mevenkamp et al. (2017) demonstrated that

[2] https://www.eu-midas.net/sites/default/files/downloads/Briefs/MIDAS_brief_ecotox_lowres.pdf.

already a low level of deposition of relatively inert (crushed minerals or sediment with low or no toxic metals) tailings, caused significant negative effects on benthic fauna diversity and functioning. Alongside an improvement of national and international legal frameworks, there is a strong and continued call for intensified communication and data sharing between all deep-sea mining stakeholders, the scientific community and mining industry in particular (Ramirez-Llodra et al., 2015; Vare et al., 2018).

Because the economically viable crust thickness is mostly in the order of cm, there will be a non-negligible amount of rocky substrate extracted during the process. ISA (2007) considers a crust-to-substrate ratio of 70: 30, meaning that 70% of the mined material will be processed, while the remaining 30% consists of the underlying rock (substrate). However, the metal content (Fe + Mn + Co + Ni) of the 70% mined crust is roughly between 30% and 40% (Hein and Koschinsky, 2014b). This means that more than 60% of the annually processed 1 million tonnes (Mt) of material needs to be either deposited on land or discharged back into the ocean. Given the obvious higher cost of transporting and storing on land, it seems likely that these tailings will be re-deposited either in the ocean or directly at the seabed. In either case, the tailings constitute very large volumes, with potentially strong impacts on the receiving ecosystem.

Finally, there may be damages to and/or losses of equipment operational in the deep sea. This may result in oil or other chemical spills, or the introduction of foreign materials into the receiving ecosystem. Industrial operations are intrinsically large-scale and crude. In the case of deep-sea mining, such operations would take place in hostile environments far beneath the ocean's surface, where damage control and/or recovery of lost (parts of) equipment is inherently difficult and time-consuming.

6.3. Climate change and cumulative impacts

Anthropogenic excess emissions of greenhouse gases (GHG) are affecting Earth's climate, by altering the global carbon cycle (Keeling et al., 1995; IPCC, 2007, 2014). The deep ocean and the ecosystems it contains, play an important role in climate regulation by absorbing vast amounts of both heat energy and atmospheric carbon dioxide (Watson et al., 2011). The most discussed and best-established consequences of climate change are the disturbance of the global climate (commonly referred to as “global warming”) and the acidification of the global surface ocean (Feely et al., 2004; Doney et al., 2009; Gattuso and Hansson, 2011). Thermohaline circulation ensures continuous transport of not only warmed, but also acidified surface waters to the deep ocean, which has been observed in the North Atlantic (Ríos et al., 2015). For the deep ocean, Levin and Le Bris (2015) and Sweetman et al. (2017) identified four main climate change impacts: (1) increase of temperature, (2) decrease of pH, (3) seawater de-oxygenation, and (4) decrease of particulate organic carbon (POC) export from the surface ocean.

Temperatures at the ocean floor currently range between 2 and 8 °C in the bathyal and between 0.01 and 4 °C for the abyssal Atlantic, Pacific and Indian oceans (Yasuhara and Danovaro, 2016; Sweetman et al., 2017). Although the highest temperature increases are expected to occur in the abyssal depths, the shallower bathyal waters are projected to experience average temperature increases of 3.5–4.5 °C by the year 2100 (Sweetman et al., 2017; Danovaro et al., 2017). Because of their shallower depth, the bottom waters over the RGR are significantly warmer than the surrounding abyssal plains of the Argentine and Brazilian basins. The increase in temperature projected to occur in the RGR bottom waters by 2100 is ca. 0.5 °C (Sweetman et al., 2017). In addition, the warming of the surface ocean enhances stratification, which will lead to decreased circulation and exchange between the upper water column and the deep ocean.

There is a spatial gradient in pH throughout the global ocean, with the North Atlantic being the most alkaline and the far North Pacific the least alkaline (Gattuso and Hansson, 2011). This gradient mainly reflects age and isolation of water masses, accumulating respiratory CO_2 over time. Acidification of the global ocean will lead to shoaling of the carbonate compensation depth (CCD), and will likely squeeze calcifying organisms, like corals, in the abyssal and lower bathyal to shallower depth zones (Kleypas et al., 2006; Doney et al., 2009; Gattuso and Hansson, 2011). Even though live corals may adapt and persist, the (dead) coral framework -providing important 3D habitat complexity- will dissolve over time in the carbonate-undersaturated waters of the future (van Woesik et al., 2013). Model predictions revealed that the downwelling of high-CO_2 surface waters will cause a pH decrease of ≥ 0.2 for more than 17% of the ocean floor below 500 m by 2100, with major pH reductions occurring over deep-sea features like seamounts (Gehlen et al., 2014, cited in Sweetman et al., 2017). The major downwelling sites lie in the North Atlantic, where surface water masses sink to greater depths and eventually travel southward into the South Atlantic as North Atlantic Deep Water (NADW; Broecker, 1991). Excess atmospheric CO_2 thus contributes to deep-ocean acidification. As the RGR lies directly in the path of the southbound, acidified NADW, it may experience ever increasing rates of deep-sea acidification already in the nearby future (Ríos et al., 2015).

Enhanced thermal stratification will reduce vertical water mixing, preventing oxygenated surface waters to reach the deep ocean (Levin and Le Bris, 2015; Sweetman et al., 2017). In addition, warmer seawater has a lower oxygen solubility. The combination of enhanced stratification and lower O_2 concentrations is projected to cause ocean deoxygenation on a global scale. In addition, sediment resuspension caused by human disturbances (e.g. bottom trawling, drilling, mining, de-watering) releases associated sources of organic matter, increasing respiration and so drive (localised) deoxygenation (Levin, 2018). So-called time-of-emergence analysis can distinguish between natural (background) variability and anthropogenically forced deoxygenation (Long et al., 2016, cited in Levin, 2018). Levin (2018) show maps in which (parts of) global ocean basins already experience climate change-driven deoxygenation, such as the Indian Ocean and parts of the tropical Pacific and Atlantic Oceans. In these maps, the RGR is projected to experience anthropogenically forced deoxygenation between 30 and 50 years from now (Levin, 2018). Waters between 100 and 1000 m depth, like those over the summits of the RGR, would be especially vulnerable to deoxygenation (Sweetman et al., 2017, and references therein). Bathyal seafloor environments in the Atlantic may experience reduction of up to 3.7% in oxygen levels by the year 2100, which may lead to habitat compression of many fish species over the RGR (Sweetman et al., 2017).

Most of the deep ocean floor is characterised by extreme food limitation, with particulate organic carbon (POC) influxes of 1–2 g C m^{-2} yr^{-1} (Watling et al., 2013). Although lower latitudes experience lower export due to high mineralisation in the upper water column, the transfer efficiency (% POC arriving at seafloor) is higher due to the mostly refractory nature of exported carbon (Henson et al., 2012, cited in Sweetman et al., 2017). Enhanced stratification (due to a warming surface ocean) will reduce downward flux of dissolved nutrients. In addition, a warmer ocean is predicted to cause shifts in phytoplankton towards smaller, slow-sinking picoplankton, which is likely to drastically reduce both export and transfer efficiency of POC to the deep ocean (Sweetman et al., 2017, and references therein). Although the South Atlantic is not projected to experience the strongest reduction in POC export of all ocean basins, flux decreases of as much as 35% could occur by the year 2100 (Sweetman et al., 2017).

Deep-sea mining may encompass prolonged activities with multiple impacts on surrounding ecosystems. Climate change effects are complex and may affect the functioning, recovery and resilience of deep ocean ecosystems over a range of scales. The convergence of anthropogenic disturbance(s) and climate change effects may in fact cause impacts which are highly non-linear in nature and therefore intrinsically difficult to predict. The very limited amount of data on processes in the deep sea, and in the deep South Atlantic in particular (Perez et al.,

2012), makes it paramount to increase the knowledge base of biodiversity and ecosystem functioning on the Rio Grande Rise.

Besides mining activities, demersal and longline fishing are also known to occur in the region of the RGR (Morato et al., 2016, and see above), representing additional human uses that may compromise deep-sea ecosystem functions. Additionally, man-made pollution was found in organisms originating from the deepest place on Earth (Taylor et al., 2016), signalling that deep-sea environments may be sinks for pollution. Just as with climate change, all other human (pollution) pressures shift environmental baselines downward, decreasing ecosystems' resilience. In a holistic, ecosystem-based management approach, such (downward) shifting baselines need to be properly included.

7. Conclusions

1. A prerequisite for moving from *exploration* to *exploitation* in a deep-sea mining (DSM) project under ISA regulations is the formulation of an effective Environmental Management Plan (EMP). In order to do this for the RGR, capturing the dynamics of its ecosystem, accurate, high-resolution and high-quality data are needed.
2. For the RGR, there is very little information on the benthic environment in the scientific literature or databases. The available information has a strong skew towards geological and geophysical research. Biological (e.g. species' life history, physiology, response to stress and disturbances), ecological (e.g. biodiversity) and environmental (e.g. elemental fluxes and cycles, biogeochemistry) data for the ocean bottom in and around the RGR are very rare. Consequently, it is very difficult to accurately determine ecosystem functions and processes, as well as any derived ecosystem services.
3. The large gaps in the knowledge of the benthic ecosystem functioning on and around the RGR, cause the full extent of the impacts of planned DSM at the RGR to be largely unknown. Being able to confidently determine the impacts on and the resilience of the RGR ecosystem under predicted mining impacts, is simply not feasible without more detailed knowledge on its structure and functioning.
4. Although very useful to create a first overview, most data from open databases are global and low-resolution in format, and only modestly represent the underlying dynamics. A strong, concerted effort is needed to collect in situ data on a regional scale. The good news is that the first expeditions are currently being undertaken, which will invariably contribute to increasing our limited knowledge on the geo-physical, geochemical and biological oceanography of the RGR, as well as serve to validate existing models.
5. From the few research cruises performed over the last decades, the RGR can be characterised as a large deep-sea area, with strong seascape heterogeneity and potentially high biodiversity. It presents habitats for both soft- and hard-substrate species, and many other associated species.
6. Deep-sea ecosystems are characterised by slow dynamics and high environmental stability. Large-scale, inherently destructive activities such as deep-sea mineral mining will exert enormous pressure on these ecosystems. As they take millions of years to grow, mining of cobalt-rich crusts (CRCs) will effectively remove the particular hard substrate permanently. Consequently, associated benthic ecosystem functioning will be impaired for decades, and likely even centuries.
7. Ecological and ecotoxicological disturbances from deep-sea mining comprise (but are not restricted to) destruction of habitat, clogging and smothering effects, toxicity of released metals, oxygen depletion by buried organic matter (OM) release and alteration of organisms' energy budgets by e.g. dilution of suspended food particles.
8. Secondary impacts like crushing and smothering, increased sediment loading, release of contaminants and underwater noise are also extremely likely to have long-lasting impacts on surrounding ecosystems.
9. Resolving regional hydrodynamics can greatly aid in determining the total area impacted by e.g. sediment plumes and dissolved toxic substances. In this way, direction and extent of the primary mining-associated disturbances (e.g. overburden slumps, increased particulate matter loadings) can be modelled.
10. In the absence of knowledge on local and/or regional biodiversity and ecosystem functioning (BEF), analogues may be used, where more information is available from similar features (seamounts), similar depth zones (deep sea) and/or similar processes (coastal benthic processes). In particular, analogues from coastal environments with knowledge and models from the (coastal) dredging industry may be utilised for the prediction of impacts of e.g. silt plumes on deep-sea processes. Similarly, there has been considerable progress in research on seamounts and the role they play in oceanic BEF. The information from seamount research may be applied to the RGR, under the assumption that it (the RGR) can be considered essentially a huge seamount system. However, the latter should be treated like an outstanding question.
11. The topographic heterogeneity found in seamounts, can harbour a high variation of species in the otherwise low-diversity, stable environments of the abyssal plains. Areas with cobalt-rich crusts are considered highly heterogeneous habitats, which potentially harbour rich and diverse benthic communities. The CRC-associated biodiversity on the RGR is expected to be high and considerably sensitive to persistent disturbances. Moreover, the high current velocities and high aragonite saturation state of the waters over the RGR constitute favourable conditions for ecosystem engineering organisms like cold-water corals. At the same time, the current regime around seamounts may pose a physical isolation mechanism to sessile fauna, causing high levels of relatively small-scale endemism. Severe disturbances like trawling or mining impacts could therefore lead to extinction of (portions of) seamount fauna on a regional level.
12. In order to implement a strategic environmental management plan (SEMP), it is important to investigate both temporal and spatial variability of ecosystem functions in the RGR deep sea ecosystems. In doing this, rather than using metrics which focus only on biodiversity (e.g. total abundance, species diversity), biological traits analysis (BTA) may be used to analyse patterns of functional ecology.
13. The effect of climate change is extremely non-trivial. Rather than an extra disturbance, climate change acts as a shifting baseline, under which the effects of other stressors may be permanently enhanced. The effect of cumulative impacts also poses a threat, as potential interactions are difficult to study and only slowly being discovered.
14. It is extremely likely that there is no such thing as "sustainable deep-sea mining". Following the central tenet in the guidelines and regulations set out by ISA, i.e. employing both the precautionary principle and best scientific practice, extensive analyses of benthic communities and processes are recommended, in order to determine management priority areas in the framework of deep-sea mining activities.

Funding and acknowledgements

This is a contribution to the topical research project "Marine ferromanganese deposits — a major resource of E- tech elements (MarineE-tech)", which is funded under FAPESP Grant number 2014/50820-7o. In addition, the following authors were funded by: FM was funded by FAPESP Grant number 2016/10091-1; MG was funded by FAPESP Grant number 2016/24677-8; PVFC was funded by FAPESP Grant number 2017/11884-8; CNS was funded by FAPESP Grant number 2016/16183-5; PMT and NMB were financed in part by the Coordenação de Aperfeiçoamento de Pessoal de Nível Superior - Brasil (CAPES) - Finance Code 001; MSM, DM, LJ, VP and FPB were funded by

FAPESP Grant number 2014/50820-7; PYGS was funded by CNPq Grant number 301089/2016-7; AT was funded by CNPq research scholarship 309697/2015-8.

We would like to thank Andrew J. Davies and Chris Yesson for kindly sharing their habitat suitability model data.

Appendix A. Supporting information

Supplementary data associated with this article can be found in the online version at doi:10.1016/j.dsr.2018.12.007.

References

Abdul Wahab, M.A., Fromont, J., Gomez, O., Fisher, R., Jones, R., 2017. Comparisons of benthic filter feeder communities before and after a large-scale capital dredging program. Mar. Pollut. Bull. 122, 176–193. https://doi.org/10.1016/j.marpolbul.2017.06.041.

Anantharaman, K., Breier, J.A., Sheik, C.S., Dick, G.J., 2013. Evidence for hydrogen oxidation and metabolic plasticity in widespread deep-sea sulfur-oxidizing bacteria. Proc. Natl. Acad. Sci. USA 110, 330–335. https://doi.org/10.1073/pnas.1215340110.

Angel, B.M., Simpson, S.L., Jarolimek, C.V., Jung, R., Waworuntu, J., Batterham, G., 2013. Trace metals associated with deep-sea tailings placement at the Batu Hijau copper–gold mine, Sumbawa, Indonesia. Mar. Pollut. Bull. 73, 306–313. https://doi.org/10.1016/j.marpolbul.2013.04.013.

Anticamara, J.A., Watson, R., Gelchu, A., Pauly, D., 2011. Global fishing effort (1950–2010): trends, gaps, and implications. Fish. Res. 107, 131–136. https://doi.org/10.1016/j.fishres.2010.10.016.

Armstrong, C.W., Foley, N., Tinch, R., van den Hove, S., 2010. Ecosystem goods and services of the deep sea. Deliv. D6.2 HERMIONE Proj. 1–68.

Armstrong, C.W., Foley, N.S., Tinch, R., van den Hove, S., 2012. Services from the deep: steps towards valuation of deep sea goods and services. Ecosyst. Serv. 2, 2–13. https://doi.org/10.1016/j.ecoser.2012.07.001.

Armstrong, C.W., Foley, N.S., Kahui, V., Grehan, A., 2014. Cold water coral reef management from an ecosystem service perspective. Mar. Policy 50, 126–134. https://doi.org/10.1016/j.marpol.2014.05.016.

Auguste, M., Mestre, N.C., Rocha, T.L., et al., 2016. Development of an ecotoxicological protocol for the deep-sea fauna using the hydrothermal vent shrimp Rimicaris exoculata. Aquat. Toxicol. 175, 277–285. https://doi.org/10.1016/j.aquatox.2016.03.024.

Baker, E.T., German, C.R., Elderfield, H., 1995. Hydrothermal plumes over spreading-center axes: global distributions and geological inferences, p. 47–71. In: Seafloor Hydrothermal Systems: Physical, Chemical, Biological, and Geological Interactions. American Geophysical Union.

Baltar, F., Lundin, D., Palovaara, J., Lekunberri, I., Reinthaler, T., Herndl, G.J., Pinhassi, J., 2016. Prokaryotic responses to ammonium and organic carbon reveal alternative CO_2 fixation pathways and importance of alkaline phosphatase in the mesopelagic North Atlantic. Front. Microbiol. 7, 1670. https://doi.org/10.3389/fmicb.2016.01670.

Barker, P.F., Carlson, R.L., 1983. Regional tectonic setting of the Southwestern Atlantic, p. 5–13. In: Initial Reports of the Deep Sea Drilling Project, 72. U.S. Government Printing Office.

Barker, P.F., Buffler, R.T., Gamboa, L.A., 1983a. A seismic reflection study of the Rio Grande Rise, p. 499–517. *In* Initial Reports of the Deep Sea Drilling Project.

Barker, P.F., Carlson, R.L., Johnson, D.A., 1983b. Tectonic evolution and subsidence history of the Rio Grande Rise. Initial Rep. Deep Sea Drill. Proj. 72, 953–976. https://doi.org/10.2973/dsdp.proc.72.151.1983.

Batker, D., Schmidt, R., 2015. Environmental and Social Benchmarking Analysis of Nautilus Minerals Inc., Solwara 1 Project.

Beaumont, N.J., Austen, M.C., Atkins, J.P., et al., 2007. Identification, definition and quantification of goods and services provided by marine biodiversity: implications for the ecosystem approach. Mar. Pollut. Bull. 54, 253–265. https://doi.org/10.1016/j.marpolbul.2006.12.003.

Blöthe, M., Wegorzewski, A., Müller, C., Simon, F., Kuhn, T., Schippers, A., 2015. Manganese-cycling microbial communities inside deep-sea manganese nodules. Environ. Sci. Technol. 49, 7692–7700. https://doi.org/10.1021/es504930v.

Boehlert, G., Genin, A., 1987a. A review of the effects of seamounts on biological processes. Geophys. Monogr. 43, 319–335. https://doi.org/10.1029/GM043p0319.

Boehlert, G.W., Genin, A., 1987b. A Review of the Effects of Seamounts on Biological Processes. Geophys. Monogr. 43, 319–334. https://doi.org/10.1029/GM043p0319.

Böhnke-Henrichs, A., Baulcomb, C., Koss, R., Hussain, S.S., de Groot, R.S., 2013. Typology and indicators of ecosystem services for marine spatial planning and management. J. Environ. Manag. 130, 135–145. https://doi.org/10.1016/j.jenvman.2013.08.027.

Boschen, R.E., Rowden, A.A., Clark, M.R., Gardner, J.P.A., 2013. Mining of deep-sea seafloor massive sulfides: a review of the deposits, their benthic communities, impacts from mining, regulatory frameworks and management strategies. Ocean Coast. Manag. 84, 54–67. https://doi.org/10.1016/j.ocecoaman.2013.07.005.

Boschker, H.T.S., Vasquez-Cardenas, D., Bolhuis, H., Moerdijk-Poortvliet, T.W.C., Moodley, L., 2014. Chemoautotrophic carbon fixation rates and active bacterial communities in intertidal marine sediments. PLoS One 9. https://doi.org/10.1371/journal.pone.0101443.

Brandini, F.P., Boltovskoy, D., Piola, A., Kocmur, S., Röttgers, R., Cesar Abreu, P., Mendes Lopes, R., 2000. Multiannual trends in fronts and distribution of nutrients and chlorophyll in the southwestern Atlantic (30–62°S). Deep Sea Res. Part I Oceanogr. Res. Pap. 47, 1015–1033. https://doi.org/10.1016/S0967-0637(99)00075-8.

Bremner, J., 2008. Species' traits and ecological functioning in marine conservation and management. J. Exp. Mar. Biol. Ecol. 366, 37–47. https://doi.org/10.1016/j.jembe.2008.07.007.

Bremner, J., Rogers, S., Frid, C., 2006. Matching biological traits to environmental conditions in marine benthic ecosystems. J. Mar. Syst. 60, 302–316. https://doi.org/10.1016/j.jmarsys.2006.02.004.

Broecker, W.S., 1991. The great ocean conveyor. Oceanography 4, 79–89. https://doi.org/10.5670/oceanog.1991.07.

Brown, A., Wright, R., Hauton, C., 2016. Evidence of behavioural avoidance of metals in coastal and abyssal sea cucumbers (Phylum Echinodermata). MIDAS Final Meeting. MIDAS.

Brown, A., Wright, R., Mevenkamp, L., Hauton, C., 2017. A comparative experimental approach to ecotoxicology in shallow-water and deep-sea holothurians suggests similar behavioural responses. Aquat. Toxicol. 191, 10–16. https://doi.org/10.1016/j.aquatox.2017.06.028.

Brown, C.J., Smith, S.J., Lawton, P., Anderson, J.T., 2011. Benthic habitat mapping: a review of progress towards improved understanding of the spatial ecology of the seafloor using acoustic techniques. Estuar. Coast. Shelf Sci. 92, 502–520. https://doi.org/10.1016/j.ecss.2011.02.007.

Bugoni, L., Mancini, P.L., Monteiro, D.S., Nascimento, L., Neves, T.S., 2008. Seabird bycatch in the Brazilian pelagic longline fishery and a review of capture rates in the southwestern Atlantic Ocean. Endanger. Species Res. 5, 137–147. https://doi.org/10.3354/esr00115.

Burnett, B.R., Nealson, K.H., 1981. Organic films and microorganisms associated with manganese nodules. Deep Sea Res. Part A Oceanogr. Res. Pap. 28, 637–645. https://doi.org/10.1016/0198-0149(81)90124-2.

Canfield, D.E., Stewart, F.J., Thamdrup, B., De Brabandere, L., Dalsgaard, T., Delong, E.F., Revsbech, N.P., Ulloa, O., 2010. A cryptic sulfur cycle in oxygen-minimum-zone waters off the Chilean coast. Science (80-.) 330, 1375–1378. https://doi.org/10.1126/science.1196889.

Casamayor, E., García-Cantizano, J., Mas, J., Pedrós-Alió, C., 2001. Primary production in estuarine oxic/anoxic interfaces: contribution of microbial dark CO_2 fixation in the Ebro River Salt Wedge Estuary. Mar. Ecol. Prog. Ser. 215, 49–56. https://doi.org/10.3354/meps215049.

Cavalcanti, J.A.D., Santos, R.V., Lacasse, C.M., Rojas, J.N.L., Nobrega, M., 2016. Potential mineral resources of phosphates and trace elements on the Rio Grande rise, South Atlantic Ocean. Nearshore Underw. Min.: Crit. Commod. Future 545–557.

Yesson, Chris, Bedford, Faye, Rogers, Alex David, Taylor, Michelle L., 2016. Global habitat suitability of deep-water Antipatharia. Pangaea.

Chung, S.-N., Lee, K., Feely, R.A., et al., 2003. Calcium carbonate budget in the Atlantic Ocean based on water column inorganic carbon chemistry. Glob. Biogeochem. Cycles 17. https://doi.org/10.1029/2002GB002001.

Clark, M.R., Schlacher, T.A., Rowden, A.A., Stocks, K.I., Consalvey, M., 2012. Science priorities for Seamounts: research links to conservation and management M. Solan [ed.]. PLoS One 7, e29232. https://doi.org/10.1371/journal.pone.0029232.

Claypool, G.E., Kaplan, I.R., 1974. The origin and distribution of methane in marine sediments. In: Kaplan, I.R. (Ed.), Natural Gases in Marine Sediments. Springer, US, pp. 99–139.

Conrad, T., Hein, J.R., Paytan, A., Clague, D.A., 2017. Formation of Fe-Mn crusts within a continental margin environment. Ore Geol. Rev. 87, 25–40. https://doi.org/10.1016/j.oregeorev.2016.09.010.

Constantino, R.R., Hackspacher, P.C., de Souza, I.A., Lima Costa, I.S., 2017. Basement structures over Rio Grande Rise from gravity inversion. J. S. Am. Earth Sci. 75, 85–91. https://doi.org/10.1016/j.jsames.2017.02.005.

Costello, M.J., Chaudhary, C., 2017. Marine biodiversity, biogeography, deep-sea gradients, and conservation. Curr. Biol. 27, R511–R527. https://doi.org/10.1016/j.cub.2017.04.060.

Cullen, J.J., 2015. Subsurface chlorophyll maximum layers: enduring enigma or mystery solved? Ann. Rev. Mar. Sci. 7, 207–239. https://doi.org/10.1146/annurev-marine-010213-135111.

Danovaro, R., Gambi, C., Dell'Anno, A., Corinaldesi, C., Fraschetti, S., Vanreusel, A., Vincx, M., Gooday, A.J., 2008. Exponential decline of deep-sea ecosystem functioning linked to benthic biodiversity loss. Curr. Biol. 18, 1–8. https://doi.org/10.1016/j.cub.2007.11.056.

Danovaro, R., Corinaldesi, C., Dell'Anno, A., Snelgrove, P.V.R., 2017. The deep-sea under global change. Curr. Biol. 27, R461–R465. https://doi.org/10.1016/j.cub.2017.02.046.

Davies, A.J., Guinotte, J.M., 2011. Global habitat suitability for framework-forming cold-water corals R.K.F. Unsworth [ed.]. PLoS One 6, e18483. https://doi.org/10.1371/journal.pone.0018483.

Davies, J.S., Stewart, H.A., Narayanaswamy, B.E., Jacobs, C., Spicer, J., Golding, N., Howell, K.L., 2015. Benthic Assemblages of the Anton Dohrn Seamount (NE Atlantic): defining Deep-Sea Biotopes to Support Habitat Mapping and Management Efforts with a Focus on Vulnerable Marine Ecosystems A. Davies [ed.]. PLoS One 10. pp. e0124815. https://doi.org/10.1371/journal.pone.0124815.

Detrick, R.S., Sclater, J.G., Thiede, J., 1977. The subsidence of aseismic ridges. Earth Planet. Sci. Lett. 34, 185–196. https://doi.org/10.1016/0012-821X(77)90003-6.

Doney, S.C., Fabry, V.J., Feely, R.A., Kleypas, J.A., 2009. Ocean acidification: the other CO_2 problem. Ann. Rev. Mar. Sci. 1, 169–192. https://doi.org/10.1146/annurev.marine.010908.163834.

Doolittle, D.F., Li, W.K.W., Wood, A.M., 2008. Wintertime abundance of picoplankton in the Atlantic sector of the Southern Ocean. Nov. Hedwig. 133, 147–160.

Duarte, C.M., Regaudie-de-Gioux, A., Arrieta, J.M., Delgado-Huertas, A., Agustí, S., 2013.

The Oligotrophic Ocean Is Heterotrophic. Ann. Rev. Mar. Sci. 5, 551–569. https://doi.org/10.1146/annurev-marine-121211-172337.
Dugdale, R.C., Goering, J.J., 1967. Uptake of new and regenerated forms of nitrogen in primary productivity. Limnol. Oceanogr. 12, 196–206.
Dunn, D.C., Van Dover, C.L., Etter, R.J., et al., 2018. A strategy for the conservation of biodiversity on mid-ocean ridges from deep-sea mining. Sci. Adv. 4, eaar4313. https://doi.org/10.1126/sciadv.aar4313.
Dyksma, S., Bischof, K., Fuchs, B.M., et al., 2016. Ubiquitous Gammaproteobacteria dominate dark carbon fixation in coastal sediments. ISME J. 10, 1–15. https://doi.org/10.1038/ISMEJ.2015.257.
Egge, J., Aksnes, D., 1992. Silicate as regulating nutrient in phytoplankton competition. Mar. Ecol. Prog. Ser. 83, 281–289. https://doi.org/10.3354/meps083281.
Ehrlich, H., 2001. Ocean manganese nodules: biogenesis and bioleaching possibilities. Miner. Biotechnol. Microb. Asp. Miner. Benef. Met. Extr. Environ. Control 239–252.
Ehrlich, H.L., 2002. Geomicrobiology. CRC Press.
Ehrlich, H.L., Ghiorse, W.C., Johnson, G.L., 1972. Distribution of microbes in manganese nodules from the Atlantic and Pacific oceans. Dev. Ind. Microbiol 13, 57–65.
Emelyanov, E.M., 2005. Calcium carbonate compensation depth (CCD). In: The Barrier Zones in the Ocean. Springer-Verlag, pp. 345–361.
Emelyanov, E.M., Trimonis, E.S., Shirshov, P.P., Barker, P.F., Carlson, R.L., 1983. Geochemical investigation of sediments from the Brazil Basin and the Rio Grande rise. Initial Rep. Deep Sea Drill. Proj. 72.
Enrich-Prast, A., Bastviken, D., Crill, P., Santoro, A.L., Signori, C.N., Sanseverino, A.M., 2014. Chemosynthesis. In: Reference Module in Earth Systems and Environmental Sciences. Elsevier.
Evain, M., Afilhado, A., Rigoti, C., et al., 2015. Deep structure of the Santos Basin-São Paulo Plateau System, SE Brazil. J. Geophys. Res. B Solid Earth 120, 5401–5431. https://doi.org/10.1002/2014JB011561.
Feely, R.A., Sabine, C.L., Lee, K., Berelson, W., Kleypas, J.A., Fabry, V.J., Millero, F., 2004. Impact of Anthropogenic CO_2 on the CaCO3 System in the Oceans. Science (80-) 305, 362–366. https://doi.org/10.1126/science.1097329.
Florindo, F., Gennari, R., Persico, D., et al., 2015. New magnetobiostratigraphic chronology and paleoceanographic changes across the Oligocene-Miocene boundary at DSDP Site 516 (Rio Grande Rise, SW Atlantic). Paleoceanography 30, 659–681. https://doi.org/10.1002/2014PA002734.
Fodor, R.V., Thiede, J., 1977. Volcanic breccia from DSDP site 357: implications for the composition and origin of the Rio Grande Rise. Initial Rep. Deep Sea Drill. Proj. 39, 537–543. https://doi.org/10.2973/dsdp.proc.39.1977.
Fodor, R.V., Husler, J.W., Kumar, N., 1977. Petrology of volcanic rocks from an aseismic rise: implications for the origin of the Rio Grande Rise, South Atlantic Ocean. Earth Planet. Sci. Lett. 35, 225–233. https://doi.org/10.1002/14356007.a28.
Folkersen, M.V., Fleming, C.M., Hasan, S., 2018. The economic value of the deep sea: a systematic review and meta-analysis. Mar. Policy 94, 71–80. https://doi.org/10.1016/j.marpol.2018.05.003.
Frid, C.L.J., Paramor, O.A.L., Brockington, S., Bremner, J., 2008. Incorporating ecological functioning into the designation and management of marine protected areas. Hydrobiologia 606, 69–79. https://doi.org/10.1007/s10750-008-9343-y.
Froelich, P.N., Klinkhammer, G.P., Bender, M.L., et al., 1979. Early oxidation of organic-matter in pelagic sediments of the eastern equatorial Atlantic - suboxic diagenesis. Geochim. Cosmochim. Acta 43, 1075–1090. https://doi.org/10.1016/0016-7037(79)90095-4.
Froneman, P.W., Laubscher, R.K., McQuaid, C.D., 2001. Size-fractionated primary production in the south Atlantic and Atlantic sectors of the Southern Ocean. J. Plankton Res. 23, 611–622. https://doi.org/10.1093/plankt/23.6.611.
Fung, Inez Y., Meyn, Stephanie K., Tegen, Ina, Doney, Scott C., John, Jasmin G., Bishop, James K.B., et al., 2000. Iron supply and demand in the upper ocean. Glob. Biogeochem. Cycles 14, 281–295. https://doi.org/10.1029/1999GB900059.
Gallagher, K., Hawkesworth, C., 1994. Mantle plumes, continental magmatism and asymmetry in the South Atlantic. Earth Planet. Sci. Lett. 123, 105–117. https://doi.org/10.1016/0012-821X(94)90261-5.
Gamboa, L.A., Buffler, R.T., Barker, P.F., 1983. Seismic Stratigraphy and Geologic History of the Rio Grande Gap and Southern Brazil Basin.
Gamboa, L.A.P., Rabinowitz, P.D., 1981. The Rio Grande fracture zone in the western South Atlantic and its tectonic implications. Earth Planet. Sci. Lett. 52, 410–418. https://doi.org/10.1016/0012-821X(81)90193-X.
Gamboa, L.A.P., Rabinowitz, P.D., 1984. The evolution of the Rio Grande Rise in the southwest Atlantic Ocean. Mar. Geol. 58, 35–58. https://doi.org/10.1016/0025-3227(84)90115-4.
Garcia, C.A.E., Sarma, Y.V.B., Mata, M.M., Garcia, V.M.T., 2004. Chlorophyll variability and eddies in the Brazil–Malvinas Confluence region. Deep Sea Res. Part II Top. Stud. Oceanogr. 51, 159–172. https://doi.org/10.1016/j.dsr2.2003.07.016.
Gardner, W.D., Biscaye, P.E., Richardson, M.J., 1997. A sediment trap experiment in the Vema Channel to evaluate the effect of horizontal particle fluxes on measured vertical fluxes. J. Mar. Res. 55, 995–1028. https://doi.org/10.1357/0022240973224139.
Gasol, J., Pinhassi, J., Alonso-Sáez, L., et al., 2008. Towards a better understanding of microbial carbon flux in the sea*. Aquat. Microb. Ecol. 53, 21–38. https://doi.org/10.3354/ame01230.
Gattuso, J.-P., Hansson, L., 2011. Ocean Acidification. Oxford University Press.
Gehlen, M., Séférian, R., Jones, D.O.B., et al., 2014. Projected pH reductions by 2100 might put deep North Atlantic biodiversity at risk. Biogeosciences 11, 6955–6967. https://doi.org/10.5194/bg-11-6955-2014.
Genin, A., Boehlert, G.W., 1985. Dynamics of temperature and chlorophyll structures above a seamount: an oceanic experiment. J. Mar. Res. 43, 907. https://doi.org/10.1357/002224085788453868.
Taranto, Gerald H., Kvile, Kristina Ø., Pitcher, Tony J., Morato, Telmo, 2012. An Ecosystem Evaluation Framework for Global Seamount Conservation and Management. PLoS ONE 7, e42950 no. 8.
Glaubitz, S., Lueders, T., Abraham, W., Jost, G., Jürgens, K., Labrenz, M., 2009. 13C-isotope analyses reveal that chemolithoautotrophic Gamma - and Epsilonproteobacteria feed a microbial food web in a pelagic redoxcline of the central Baltic Sea. Environ. Microbiol. 11, 326–337. https://doi.org/10.1111/j.1462-2920.2008.01770.x.
Gollner, S., Kaiser, S., Menzel, L., et al., 2017. Resilience of benthic deep-sea fauna to mining activities. Mar. Environ. Res. https://doi.org/10.1016/j.marenvres.2017.04.010.
Gomez-Saez, G.V., Pop Ristova, P., Sievert, S.M., Elvert, M., Hinrichs, K., Bühring, S.I., 2017. Relative importance of chemoautotrophy for primary production in a light exposed marine shallow hydrothermal system. Front. Microbiol. 8, 1–15. https://doi.org/10.3389/fmicb.2017.00702.
Gordon, A.L., 1989. Brazil-Malvinas Confluence-1984. Deep Sea Res. Part A Oceanogr. Res. Pap. 36, 359–384. https://doi.org/10.1016/0198-0149(89)90042-3.
Grigg, R.W., Malahoff, A., Chave, E.H., Landahl, J., 1987. Seamount benthic ecology and potential environmental impact from manganese crust mining in Hawai'i. Geophys. Monogr. Ser. 43, 379–390.
de Groot, R., Fisher, B., Christie, M., et al., 2010. In: Kumar, P. (Ed.), The Economics of Ecosystems and Biodiversity: Ecological and Economic Foundations. Routledge.
Haines-Young, R., Potschin, M., 2013. Consultation on CICES Version 4 , August-December 2012 Report to the European Environment Agency Revised January 2013. pp. 1–34.
Hajdu, E., Castello-Branco, C., Lopes, D.A., Sumida, P.Y.G., Perez, J.A.A., 2017. Deep-sea dives reveal an unexpected hexactinellid sponge garden on the Rio Grande Rise (SW Atlantic). A mimicking habitat? Deep Sea Res. Part II Top. Stud. Oceanogr. 146, 93–100. https://doi.org/10.1016/j.dsr2.2017.11.009.
Halbach, P., Manheim, F.T., Otten, P., 1982. Co-rich ferromanganese deposits in the marginal seamount regions of the central Pacific Basin - results of the MIDPAC '81. Erzmetall 35, 447–453.
Hansell, D., Carlson, C., Repeta, D., Schlitzer, R., 2009. Dissolved organic matter in the ocean: a controversy stimulates new insights. Oceanography 22, 202–211. https://doi.org/10.5670/oceanog.2009.109.
Harris, P.T., Whiteway, T., 2009. High seas marine protected areas: benthic environmental conservation priorities from a GIS analysis of global ocean biophysical data. Ocean Coast. Manag. 52, 22–38. https://doi.org/10.1016/j.ocecoaman.2008.09.009.
Harris, P.T., Heap, A.D., Whiteway, T., Post, A., 2008. Application of biophysical information to support Australia's representative marine protected area program. Ocean Coast. Manag. 51, 701–711. https://doi.org/10.1016/j.ocecoaman.2008.07.007.
Hein, J.R., 2004. Cobalt–rich ferromanganese crusts: Global distribution, composition, origin and research activities.
Hein, J.R., Koschinsky, A., 2013. Deep-Ocean Ferromanganese Crusts and Nodules. Treatise Geochemistry, second ed. pp. 273–291. https://doi.org/10.1016/B978-0-08-095975-7.01111-6.
Hein, J.R., Koschinsky, A., 2014b. Deep-ocean ferromanganese crusts and nodules. In: Scott, S. (Ed.), Treatise on Geochemistry. Elsevier, pp. 273–291.
Hein, J.R., Koschinsky, A., 2014a. Deep-Ocean Ferromanganese Crusts and Nodules, 2nd ed. Published by Elsevier Inc.
Hein, J.R., Morgan, C.L., 1999. Influence of substrate rocks on Fe-Mn crust composition. Deep. Res. I 46, 855–875.
Hein, J.R., Petersen, S., 2013. The geology of cobalt-rich ferromanganese crusts. In: Baker, E., Beaudoin, Y. (Eds.), Deep Sea Minerals: Cobalt-rich Ferromanganese Crusts; A Physical, Biological, Environmental, and Technical Review. Secretariat of the Pacific Community, pp. 7–14.
Hein, J.R., Koschinsky, A., Halbach, P., Manheim, F.T., Bau, M., Kang, J.-K., Lubick, N., 1997. Iron and manganese oxide mineralization in the Pacific. In: Nicholson, S., Hein, K., Buhn, J.R., Dasgupta, J.R. (Eds.), Manganese Mineralization: Geochemistry and Mineralogy of Terrestrial and Marine Deposits. The Geological Society, pp. 123–138.
Hein, J.R., Koschinsky, A., Bau, M., Manheim, F.T., Kang, J.-K., Roberts, L., 2000. Cobalt-Rich Ferromanganese crusts in the Pacific. In: Cronan, D.S. (Ed.), Handbook of Marine Mineral Deposits. CRC Press, pp. 239–279.
Hein, J.R., Mizell, K., Koschinsky, A., Conrad, T.A., 2013a. Deep-ocean mineral deposits as a source of critical metals for high- and green-technology applications: comparison with land-based resources. Ore Geol. Rev. 51, 1–14. https://doi.org/10.1016/j.oregeorev.2012.12.001.
Hein, J.R., Conrad, T., Mizell, K., Banakar, V.K., Frey, F.A., Sager, W.W., 2016. Controls on ferromanganese crust composition and reconnaissance resource potential, Ninetyeast Ridge, Indian Ocean. Deep Sea Res. Part I Oceanogr. Res. Pap. 110, 1–19. https://doi.org/10.1016/j.dsr.2015.11.006.
Hein, J.R.J.R., 2002. Cobalt-rich ferromanganese crusts: Global distribution, composition, origin and research activities.
Henson, S.A., Sanders, R., Madsen, E., 2012. Global patterns in efficiency of particulate organic carbon export and transfer to the deep ocean. Glob. Biogeochem. Cycles 26. https://doi.org/10.1029/2011GB004099.
Herbland, A., Voituriez, B., 1979. Hydrological structure analysis for estimating the primary production in the tropical Atlantic Ocean. J. Mar. Res. 37, 87–101.
Herndl, G.J., Reinthaler, T., 2013. Microbial control of the dark end of the biological pump. Nat. Geosci. 6, 718–724. https://doi.org/10.1038/ngeo1921.
Hessler, R.R., Jumars, P.A., 1974. Abyssal community analysis from replicate box cores in the central North Pacific. Deep Sea Res. Oceanogr. Abstr. 21, 185–209. https://doi.org/10.1016/0011-7471(74)90058-8.
Hoernle, K., Rohde, J., Hauff, F., Garbe-Schönberg, D., Homrighausen, S., Werner, R., Morgan, J.P., 2015. How and when plume zonation appeared during the 132 Myr evolution of the Tristan Hotspot. Nat. Commun. 6, 7799. https://doi.org/10.1038/ncomms8799.

Honeyman, B.D., Balistrieri, L.S., Murray, J.W., 1988. Oceanic trace-metal scavenging - the importance of particle concentration. Deep. Res. Part A-Oceanogr. Res. Pap. 35, 227–246.
Hughes, D.J., Shimmield, T.M., Black, K.D., Howe, J.A., 2015. Ecological impacts of large-scale disposal of mining waste in the deep sea. Sci. Rep. 5, 9985. https://doi.org/10.1038/srep09985.
Hügler, M., Sievert, S.M., 2011. Beyond the calvin cycle: autotrophic carbon fixation in the ocean. Ann. Rev. Mar. Sci. 3, 261–289. https://doi.org/10.1146/annurev-marine-120709-142712.
Huo, Y., Cheng, H., Post, A.F., Wang, C., Jiang, X., Pan, J., Wu, M., Xu, X., 2015. Ecological functions of uncultured microorganisms in the cobalt-rich ferromanganese crust of a seamount in the central Pacific are elucidated by fosmid sequencing. Acta Oceanol. Sin. 34, 92–113. https://doi.org/10.1007/s13131-015-0650-7.
IPCC, 2007. Climate Change 2007: The Physical Science Basis. Contribution of Working Group I to the Fourth Assessment Report of the Inter governmental Panel on Climate Change. Cambridge University Press.
IPCC, 2014. Climate Change 2014: Synthesis Report. Contribution of Working Groups I, II and III to the Fifth Assessment Report of the Intergovernmental Panel on Climate Change.
ISA, 2007. Polymetallic sulphides and cobalt-rich ferromanganese crusts deposits. Establishing of environmental: baselines and an associated monitoring programme during exploration.
ISA, 2011b. Draft regulations on prospecting and exploration for cobalt-rich ferro-manganese crusts in the Area*.
ISA. 2011a. Environmental Management Plan for the Clarion-Clipperton Zone. Isba/17/Ltc/7, 194, pp. 1–18.
Jiang, X.-D., Sun, X.-M., Guan, Y., Gong, J.-L., Lu, Y., Lu, R.-F., Wang, C., 2017. Biomineralisation of the ferromanganese crusts in the Western Pacific Ocean. J. Asian Earth Sci. 136, 58–67. https://doi.org/10.1016/j.jseaes.2017.01.025.
Jiménez, S., Abreu, M., Pons, M., Ortiz, M., Domingo, A., 2010. Assessing the impact of the pelagic longline fishery on albatrosses and petrels in the southwest Atlantic. Aquat. Living Resour. 23, 49–64. https://doi.org/10.1051/alr/2010002.
Johnson, D.A., 1983. Regional oceanographic setting of the Southwestern Atlantic.
Johnson, D.A., 1984. The Vema Channel: physiography, structure and sediment-current interactions. Mar. Geol. 58, 1–34.
Johnson, D.A., Ledbetter, M.T., Tappa, E., Thunell, R., 1984. Late Tertiary/Quaternary magnetostratigraphy and biostratigraphy of Vema Channel sediments. Mar. Geol. 58, 89–100. https://doi.org/10.1016/0025-3227(84)90117-8.
Jones, G.A., 1984. Advective transport of clay minerals in the region of the Rio Grande Rise. Mar. Geol. 58, 187–212.
Jørgensen, B.B., Fossing, H., Wirsen, C.O., Jannasch, H.W., 1991. Sulfide oxidation in the anoxic Black Sea chemocline. Deep Sea Res. Part A Oceanogr. Res. Pap. 38, S1083–S1103. https://doi.org/10.1016/S0198-0149(10)80025-1.
Kasten, S., Glasby, G., Schulz, H., Friedrich, G., Andreev, S., 1998. Rare earth elements in manganese nodules from the South Atlantic Ocean as indicators of oceanic bottom water flow. Mar. Geol. 146, 33–52. https://doi.org/10.1016/S0025-3227(97)00128-X.
Keeling, C.D., Whorf, T.P., Wahlen, M., van der Plichtt, J., 1995. Interannual extremes in the rate of rise of atmospheric carbon dioxide since 1980. Nature 375, 666.
Kim, G.Y., Richardson, M.D., Bibee, D.L., Kim, D.C., Wilkens, R.H., Shin, S.R., Song, S.T., 2004. Sediment types determination using acoustic techniques in the Northeastern Gulf of Mexico. Geosci. J. 8, 95–103.
Kleypas, J., Feely, R., Fabry, V., Langdon, C., Sabine, C., Robbins, L., 2006. Impacts of Ocean acidification on coral reefs and other marine calcifiers: a guide for future research. Atmos. Res. 18, 88. (doi:). 〈www.ucar.edu/communications/Final_acidification.pdf〉.
Koltermann, K.P., Gouretski, V., Jancke, K., 2011. In: Ocean, M., Sparrow, P., Chapman, Gould, J. (Eds.), Hydrographic Atlas of the World Ocean Circulation Experiment (WOCE) Volume 3: Atlantic. Atlas World Ocean Circ. Exp, Hydrogr.
Konhauser, K.O., 2009. Introduction to geomicrobiology, John Wiley and Sons Inc.,
Konneke, M., Bernhard, A.E., de la Torre, J.R., Walker, C.B., Waterbury, J.B., Stahl, D.A., 2005. Isolation of an autotrophic ammonia-oxidizing marine archaeon. Nature 437, 543–546.
Kumar, N., 1979. Origin of “paired” aseismic rises: Ceará and Sierra Leone rises in the equatorial, and the Rio Grande Rise and Walvis Ridge in the South Atlantic. Mar. Geol. 30, 175–191. https://doi.org/10.1016/0025-3227(79)90014-8.
Kvile, K.O., Taranto, G.H., Pitcher, T.J., Morato, T., 2014. A global assessment of seamount ecosystems knowledge using an ecosystem evaluation framework. Biol. Conserv. 173, 108–120. https://doi.org/10.1016/j.biocon.2013.10.002.
Le, J.T., Levin, L.A., Carson, R.T., 2017. Incorporating ecosystem services into environmental management of deep-seabed mining. Deep. Res. Part II Top. Stud. Oceanogr. 137, 486–503. https://doi.org/10.1016/j.dsr2.2016.08.007.
Levin, L.A., 2018. Manifestation, drivers, and emergence of open ocean deoxygenation. Ann. Rev. Mar. Sci. 10, 229–260. https://doi.org/10.1146/annurev-marine-121916-063359.
Levin, L.A., Le Bris, N., 2015. The deep ocean under climate change. Science (80-.) 350, 766–768. https://doi.org/10.1126/science.aad0126.
Levin, L.A., Baco, A.R., Bowden, D.A., et al., 2016a. Hydrothermal vents and methane seeps: rethinking the sphere of influence. Front. Mar. Sci. 3, 72. https://doi.org/10.3389/fmars.2016.00072.
Levin, L.A., Mengerink, K., Gjerde, K.M., et al., 2016b. Defining “serious harm” to the marine environment in the context of deep-seabed mining. Mar. Policy 74, 245–259. https://doi.org/10.1016/j.marpol.2016.09.032.
Leyden, R., Ludwig, W.J., Ewing, M., 1971. Structure of continental margin off Punta del Este, Uruguay, and Rio de Janeiro, Brazil. Am. Assoc. Pet. Geol. Bull. 55, 2161–2173.
Liao, L., Xu, X.W., Jiang, X.W., Wang, C.S., Zhang, D.S., Ni, J.Y., Wu, M., 2011. Microbial diversity in deep-sea sediment from the cobalt-rich crust deposit region in the Pacific Ocean. FEMS Microbiol. Ecol. 78, 565–585. https://doi.org/10.1111/j.1574-6941.2011.01186.x.
Liquete, C., Piroddi, C., Drakou, E.G., Gurney, L., Katsanevakis, S., Charef, A., Egoh, B., 2013. Current status and future prospects for the assessment of marine and coastal ecosystem services: a Systematic Review. PLoS One 8. https://doi.org/10.1371/journal.pone.0067737.
Lisitzin, A.P., 1977. Terrigenous sedimentation, climatic zonality and correlation of terrigenous and biogenic sedimentation in the oceans. Lithol. Miner. Depos. 6, 3–22 (in Russ.).
Lodge, M., Johnson, D., Le Gurun, G., Wengler, M., Weaver, P., Gunn, V., 2014. Seabed mining: international Seabed Authority environmental management plan for the Clarion-Clipperton Zone. A partnership approach. Mar. Policy 49, 66–72. https://doi.org/10.1016/j.marpol.2014.04.006.
Long, M.C., Deutsch, C., Ito, T., 2016. Finding forced trends in oceanic oxygen. Glob. Biogeochem. Cycles 30, 381–397. https://doi.org/10.1002/2015GB005310.
Longhurst, A., Sathyendranath, S., Platt, T., Caverhill, C., 1995. An estimate of global primary production in the ocean from satellite radiometer data. J. Plankton Res. 17, 1245–1271. https://doi.org/10.1093/plankt/17.6.1245.
Longhurst, A.R., 2007. Ecological Geography of the Sea, 2nd ed. Academic Press.
Loreau, M., 2008. Biodiversity and ecosystem functioning: the mystery of the deep sea. Curr. Biol. 18, R126–R128. https://doi.org/10.1016/j.cub.2007.11.060.
Lundsten, L., Barry, J.P., Cailliet, G.M., Clague, D.A., DeVogelaere, A.P., Geller, J.B., 2009. Benthic invertebrate communities on three seamounts off southern and central California, USA. Mar. Ecol. Prog. Ser. 374, 23–32.
Lupton, J.E., Craig, H., 1981. A major Helium-3 source at 15.degree.S on the East Pacific Rise. Science 214, 13–18 (80-.).
Maes, J., Egoh, B., Willemen, L., et al., 2012. Mapping ecosystem services for policy support and decision making in the European Union. Ecosyst. Serv. 1, 31–39. https://doi.org/10.1016/j.ecoser.2012.06.004.
de Mahiques, M.M., Hanebuth, T.J.J., Nagai, R.H., et al., 2017. Inorganic and organic geochemical fingerprinting of sediment sources and ocean circulation on a complex continental margin (São Paulo Bight, Brazil). Ocean Sci. Discuss. 13, 1–30. https://doi.org/10.5194/os-13-209-2017.
Maldonado, M., Carmona, M.C., Velásquez, Z., Puig, A., Cruzado, A., López, A., Young, C.M., 2005. Siliceous sponges as a silicon sink: an overlooked aspect of benthopelagic coupling in the marine silicon cycle. Limnol. Oceanogr. 50, 799–809. https://doi.org/10.4319/lo.2005.50.3.0799.
Manganelli, M., Malfatti, F., Samo, T.J., Mitchell, B.G., Wang, H., Azam, F., 2009. Major role of microbes in carbon fluxes during Austral winter in the Southern Drake Passage F. Rodriguez-Valera [ed.]. PLoS One 4, e6941. https://doi.org/10.1371/journal.pone.0006941.
Marañón, E., Behrenfeld, M.J., González, N., Mouriño, B., Zubkov, M.V., 2003. High variability of primary production in oligotrophic waters of the Atlantic Ocean: uncoupling from phytoplankton biomass and size structure. Mar. Ecol. Prog. Ser. 257, 1–11. https://doi.org/10.3354/meps257001.
Marcovaldi, M.Â., Sales, G., Thomé, J.C.A., Dias Da Silva, A.C.C., Gallo, B.M.G., Lima, E.H.S.M., Lima, E.P., Bellini, C., 2006. Sea turtles and fishery interactions in Brazil: identifying and mitigating potential conflicts. Mar. Turt. Newsl. 112, 4–8.
Mestre, N.C., Calado, R., Soares, A.M.V.M., 2014. Exploitation of deep-sea resources: the urgent need to understand the role of high pressure in the toxicity of chemical pollutants to deep-sea organisms. Environ. Pollut. 185, 369–371. https://doi.org/10.1016/j.envpol.2013.10.021.
Mevenkamp, L., Stratmann, T., Guilini, K., Moodley, L., van Oevelen, D., Vanreusel, A., Westerlund, S., Sweetman, A.K., 2017. Impaired short-term functioning of a benthic community from a deep Norwegian Fjord following deposition of mine tailings and sediments. Front. Mar. Sci. 4. https://doi.org/10.3389/fmars.2017.00169.
Rex, Michael A., Etter, Ron J., Morris, Jeremy S., Crouse, Jenifer, McClain, Craig R., Johnson, Nicholas A., Stuart, Carol T., Deming, Jody W., Thies, Rebecca, Avery, Renee, 2006. Global bathymetric patterns of standing stock and body size in the deep-sea benthos. Marine Ecol. Prog. Ser. 1–8.
MIDAS, 2015. Plumes from deep-sea mining. 〈https://www.eu-midas.net/sites/default/files/downloads/Briefs/MIDAS_plumes_brief_lowres.pdf〉.
MIDAS, 2016. Toxic impacts of Deep-Sea mining. 〈https://www.eu-midas.net/sites/default/files/downloads/Briefs/MIDAS_brief_ecotox_lowres.pdf〉.
Millennium Ecosystem Assessment, 2005. Ecosystems and Human Well-being: Synthesis.
Miller, K.A., Thompson, K.F., Johnston, P., Santillo, D., 2018. An overview of seabed mining including the current state of development, environmental impacts, and knowledge gaps. Front. Mar. Sci. 4. https://doi.org/10.3389/fmars.2017.00418.
Miyata, N., Maruo, K., Tani, Y., Tsuno, H., Seyama, H., Soma, M., Iwahori, K., 2006. Production of biogenic manganese oxides by anamorphic ascomycete fungi isolated from streambed pebbles. Geomicrobiol. J. 23, 63–73. https://doi.org/10.1080/01490450500533809.
Mohriak, W., Rosendahl, B.R., Turner, J.P., Valente, S.C., 2002. Crustal architecture of South Atlantic margins. Geol. Soc. Am. - Spec. Pap. 362, 159–202.
Mohriak, W., Nemcok, M., Enciso, G., 2008. South Atlantic divergent margin evolution: rift-border uplift and salt tectonics in the basins of SE Brazil. Geol. Soc. Lond. Spec. Publ. 294, 365–398. https://doi.org/10.1144/SP294.19.
Mohriak, W.U., Nobrega, M., Odegard, M.E., Gomes, B.S., Dickson, W.G., 2010. Geological and geophysical interpretation of the Rio Grande Rise, south-eastern Brazilian margin: extensional tectonics and rifting of continental and oceanic crusts. Pet. Geosci. 16, 231–245. https://doi.org/10.1144/1354-079309-910.
Morato, T., Hoyle, S.D., Allain, V., Nicol, S.J., 2010. Seamounts are hotspots of pelagic biodiversity in the open ocean. Proc. Natl. Acad. Sci. USA 107, 9707–9711. https://doi.org/10.1073/pnas.0910290107.
Morato, T., Cleary, J., Taranto, G.H., Vandeperre, F., Pham, C.K., Dunn, D.C., Colaço, A.,

Halpin, P.N., 2015. Data Report: Towards development of a Strategic Environmental Management Plan for deep seabed mineral exploitation in the Atlantic basin.
Morato, Telmo, Cleary, Jesse, Taranto, Gerald H., Vandeperre, Frederic, Pham, Christopher K., Dunn, Daniel C., Colaco, Ana, Halpin, Patrick N., 2016. Data Report: Towards development of a Strategic Environmental Management Plan for deep seabed mineral exploitation in the Atlantic basin, Tech. Report. Instituto do Mar (IMAR); Marine Geospatial Ecology Lab (MGEL).
Morgan, N.B., Cairns, S., Reiswig, H., Baco, A.R., 2015. Benthic megafaunal community structure of cobalt-rich manganese crusts on Necker Ridge. Deep. Res. Part I Oceanogr. Res. Pap. 104, 92–105. https://doi.org/10.1016/j.dsr.2015.07.003.
Mutter, J.C., Talwani, M., Stoffa, P.L., 1982. Origin of seaward-dipping reflectors in oceanic crust off the Norwegian margin by "subaerial sea-floor spreading". Geology 10, 353–357. https://doi.org/10.1130/0091-7613(1982)10<353:OOSRIO>2.0.CO;2.
Nitahara, S., Kato, S., Urabe, T., Usui, A., Yamagishi, A., 2011. Molecular characterization of the microbial community in hydrogenetic ferromanganese crusts of the Takuyo-Daigo Seamount, northwest Pacific. FEMS Microbiol. Lett. 321, 121–129. https://doi.org/10.1111/j.1574-6968.2011.02323.x.
Nitahara, S., Kato, S., Usui, A., Urabe, T., Suzuki, K., Yamagishi, A., 2017. Archaeal and bacterial communities in deep-sea hydrogenetic ferromanganese crusts on old seamounts of the northwestern Pacific. PLoS One 12, e0173071. https://doi.org/10.1371/journal.pone.0173071.
O'Connor, J.M., Duncan, R.A., 1990. Evolution of the Walvis Ridge-Rio Grande rise hot spot system: implications for African and South American plate motions over plumes. J. Geophys. Res. 95, 17475. https://doi.org/10.1029/JB095iB11p17475.
Orcutt, B.N., Sylvan, J.B., Knab, N.J., Edwards, K.J., 2011. Microbial ecology of the Dark Ocean above, at, and below the seafloor. Microbiol. Mol. Biol. Rev. 75, 361–422. https://doi.org/10.1128/MMBR.00039-10.
Orcutt, B.N., Sylvan, J.B., Rogers, D.R., Delaney, J., Lee, R.W., Girguis, P.R., 2015. Carbon fixation by basalt-hosted microbial communities. Front. Microbiol. 6, 1–14. https://doi.org/10.3389/fmicb.2015.00904.
Partensky, F., Hess, W.R., Vaulot, D., 1999. Prochlorococcus, a marine photosynthetic prokaryote of global significance. Microbiol. Mol. Biol. Rev. 63, 106–127.
Paton, D.A., Pindell, J., McDermott, K., Bellingham, P., Horn, B., 2017. Evolution of seaward-dipping reflectors at the onset of oceanic crust formation at volcanic passive margins: insights from the South Atlantic. Geology 45, 439–442. https://doi.org/10.1130/G38706.1.
Perez, J., dos Santos Alves, E., Clark, M., Bergstad, O.A., Gebruk, A., Azevedo Cardoso, I., Rogacheva, A., 2012. Patterns of life on the Southern Mid-Atlantic Ridge: compiling what is known and addressing future research. Oceanography 25, 16–31. https://doi.org/10.5670/oceanog.2012.102.
Perez, J.A.A., Kitazato, H., Sumida, P.Y.G., Sant'Ana, R., Mastella, A.M., 2018. Benthopelagic megafauna assemblages on deep habitats of the Rio Grande Rise (SW Atlantic). Deep Sea Res. Part I Oceanogr. Res. Pap. 134, 1–11. https://doi.org/10.1016/j.dsr.2018.03.001.
Peterson, R.G., Stramma, L., 1991. Upper-level circulation in the South Atlantic Ocean. Prog. Oceanogr. 26, 1–73. https://doi.org/10.1016/0079-6611(91)90006-8.
Pushcharovsky, Y.M., 2013. Microcontinents in the Atlantic ocean. Geotectonics 47, 241–250. https://doi.org/10.1134/S0016852113040067.
Ramirez-Llodra, E., Brandt, A., Danovaro, R., et al., 2010. Deep, diverse and definitely different: unique attributes of the world's largest ecosystem. Biogeosciences 7, 2851–2899. https://doi.org/10.5194/bg-7-2851-2010.
Ramirez-Llodra, E., Tyler, P.A., Baker, M.C., et al., 2011. Man and the Last Great Wilderness: Human Impact on the Deep Sea P. Roopnarine [ed.]. PLoS One 6. pp. e22588. https://doi.org/10.1371/journal.pone.0022588.
Ramirez-Llodra, E., Trannum, H.C., Evenset, A., et al., 2015. Submarine and deep-sea mine tailing placements: a review of current practices, environmental issues, natural analogs and knowledge gaps in Norway and internationally. Mar. Pollut. Bull. 97, 13–35. https://doi.org/10.1016/j.marpolbul.2015.05.062.
Reid, J.L., Nowlin, W.D., Patzert, W.C., 1977. On the characteristics and circulation of the Southwestern Atlantic Ocean. J. Phys. Oceanogr. 7, 62–91. https://doi.org/10.1175/1520-0485(1977)007<0062:OTCACO>2.0.CO;2.
Reid, T.A., Ronconi, R.A., Cuthbert, R.J., Ryan, P.G., 2014. The summer foraging ranges of adult spectacled petrels Procellaria conspicillata. Antarct. Sci. 26, 23–32. https://doi.org/10.1017/S0954102013000266.
Reinthaler, T., van Aken, H.M., Herndl, G.J., 2010. Major contribution of autotrophy to microbial carbon cycling in the deep North Atlantic's interior. Deep Sea Res. Part II Top. Stud. Oceanogr. 57, 1572–1580. https://doi.org/10.1016/j.dsr2.2010.02.023.
Richardson, M.D., Briggs, K.B., 1993. On the use of acoustic impedance values to determine sediment properties. Proc. Inst. Acoust. 15.
Richer de Forges, B., Koslow, J.A., Poore, G.C.B., 2000. Diversity and endemism of the benthic seamount fauna in the southwest Pacific. Nature 405, 944–947. https://doi.org/10.1038/35016066.
Rijkenberg, M.J.A., Middag, R., Laan, P., Gerringa, L.J.A., Aken, H.M. Van, Schoemann, V., Jong, J.T.M. De, Baar, H.J.W. De, 2014. The distribution of dissolved iron in the West Atlantic Ocean. PLoS One 9, 1–14. https://doi.org/10.1371/journal.pone.0101323.
Ríos, A.F., Resplandy, L., García-Ibáñez, M.I., et al., 2015. Decadal acidification in the water masses of the Atlantic Ocean. Proc. Natl. Acad. Sci. USA 112, 9950–9955. https://doi.org/10.1073/pnas.1504613112.
Roden, G.I., 1987. Effect of seamounts and seamount chains on ocean circulation and thermohaline structure. In: Seamounts, Islands, and Atolls. American Geophysical Union (AGU), pp. 335–354.
Rohde, J.K., van den Bogaard, P., Hoernle, K., Hauff, F., Werner, R., 2013. Evidence for an age progression along the Tristan-Gough volcanic track from new 40Ar/39Ar ages on phenocryst phases. Tectonophysics 604, 60–71.
Rosenbaum Helen, G.F., 2015. A critique of the nautilus minerals environmental and social benchmarking analysis of the solwara 1 project. Deep Sea Min. Campaign 16.
Rowden, A.A., Dower, J.F., Schlacher, T.A., Consalvey, M., Clark, M.R., 2010. Paradigms in seamount ecology: fact, fiction and future. Mar. Ecol. 31, 226–241. https://doi.org/10.1111/j.1439-0485.2010.00400.x.
Schlacher, T.A., Rowden, A.A., Dower, J.F., Consalvey, M., 2010. Seamount science scales undersea mountains: new research and outlook. Mar. Ecol. 31, 1–13. https://doi.org/10.1111/j.1439-0485.2010.00396.x.
Schlacher, T.A., Baco, A.R., Rowden, A.A., O'Hara, T.D., Clark, M.R., Kelley, C., Dower, J.F., 2013. Seamount benthos in a cobalt-rich crust region of the central Pacific: conservation challenges for future seabed mining D. Richardson [ed.]. Divers. Distrib. 20, 491–502. https://doi.org/10.1111/ddi.12142.
Schmid, C., Siedler, G., Zenk, W., 2000. Dynamics of Intermediate Water Circulation in the Subtropical South Atlantic. J. Phys. Oceanogr. 30, 3191–3211. https://doi.org/10.1175/1520-0485(2000)030<3191:WCI>2.0.CO;2.
Seascape, 2014. Review of Implementation of the Environmental Management Plan for the Clarion-Clipperton Zone - Report to the International Seabed Authority.
Secretariat of the Pacific Community, 2013. Deep Sea Minerals: Cobalt-rich Ferromanganese Crusts, a physical, biological, environmental, and technical review.
Secretariat of the Pacific Community, 2016. An Assessment of the Costs and Benefits of Mining Deep- sea Minerals in the Pacific Island Region. Tech. report. Secretariat of the Pacific Community, Suva, Fiji.
Sharma, R., 2015. Environmental issues of deep-sea mining. Procedia Earth Planet. Sci. 11, 204–211. https://doi.org/10.1016/j.proeps.2015.06.026.
Shiraishi, F., Mitsunobu, S., Suzuki, K., Hoshino, T., Morono, Y., Inagaki, F., 2016. Dense microbial community on a ferromanganese nodule from the ultra-oligotrophic South Pacific Gyre: implications for biogeochemical cycles. Earth Planet. Sci. Lett. 447, 10–20. https://doi.org/10.1016/j.epsl.2016.04.021.
Shulse, C.N., Maillot, B., Smith, C.R., Church, M.J., 2017. Polymetallic nodules, sediments, and deep waters in the equatorial North Pacific exhibit highly diverse and distinct bacterial, archaeal, and microeukaryotic communities. Microbiologyopen 6, e00428–e00444. https://doi.org/10.1002/mbo3.428.
Signori, C.N., 2014. Chemosynthesis and bacterial production in marine ecosystems: quantification, importance and regulatory factors. Federal University of Rio de Janeiro.
Smith, C.R., Deleo, F., Bernardino, A.F., Sweetman, A.K., Martínez Arbizu, P., 2008b. Abyssal food limitation, ecosystem structure and climate change. Trends Ecol. Evol. 23, 518–528. https://doi.org/10.1016/j.tree.2008.05.002.
Smith, C.R.C.R., Gaines, S., Friedlander, A., 2008a. and others. Preservation Reference Areas for Nodule Mining in the Clarion-Clipperton Zone: Rationale and Recommendations to the International Seabed Authority. 12.
Sokolova, I.M., Frederich, M., Bagwe, R., Lannig, G., Sukhotin, A.A., 2012. Energy homeostasis as an integrative tool for assessing limits of environmental stress tolerance in aquatic invertebrates. Mar. Environ. Res. 79, 1–15. https://doi.org/10.1016/j.marenvres.2012.04.003.
Speer, K., Zenk, W., Siedler, G., Pätzold, J., Heidland, C., 1992. First resolution of flow through the Hunter Channel in the South Atlantic. Earth Planet. Sci. Lett. 113, 287–292. https://doi.org/10.1016/0012-821X(92)90226-L.
Stramma, L., 2001. Current systems in the Atlantic Ocean. In: Encyclopedia of Ocean Sciences. Academic Press, pp. 718–727.
Swan, B.K., Martinez-Garcia, M., Preston, C.M., et al., 2011. Potential for chemolithoautotrophy among ubiquitous bacteria lineages in the Dark Ocean. Science (80-.) 333, 1296–1300. https://doi.org/10.1126/science.1203690.
Sweetman, A.K., Thurber, A.R., Smith, C.R., et al., 2017. Major impacts of climate change on deep-sea benthic ecosystems. Elem. Sci. Anthr. 5, 4. https://doi.org/10.1525/elementa.203.
Takahashi, T., Broecker, W.S., Bainbridge, A.E., 2006. The Alkalinity and Total Carbon Dioxide Concentration in the World Oceans, L.D.G.O. C. Scientific Committee on Problems of the Environment (SCOPE).
Takahashi, T., Sutherland, S.C., Chipman, D.W., Goddard, J.G., Ho, C., Newberger, T., Sweeney, C., Munro, D.R., 2014. Climatological distributions of pH, pCO_2, total CO_2, alkalinity, and CaCO3 saturation in the global surface ocean, and temporal changes at selected locations. Mar. Chem. 164, 95–125. https://doi.org/10.1016/j.marchem.2014.06.004.
Taylor, M.L., Gwinnett, C., Robinson, L.F., Woodall, L.C., 2016. Plastic microfibre ingestion by deep-sea organisms. Sci. Rep. 6, 33997. https://doi.org/10.1038/srep33997.
Tebo, B.M., Bargar, J.R., Clement, B.G., Dick, G.J., Murray, K.J., Parker, D., Verity, R., Webb, S.M., 2004. Biogenic manganese oxides: properties and mechanisms of formation. Annu. Rev. Earth Planet. Sci. 32, 287–328. https://doi.org/10.1146/annurev.earth.32.101802.120213.
Thurber, A.R.R., Sweetman, A.K., Narayanaswamy, B.E., Jones, D.O.B., Ingels, J., Hansman, R.L., 2014. Ecosystem function and services provided by the deep sea. Biogeosciences 11, 3941–3963. https://doi.org/10.5194/bg-11-3941-2014.
Tittensor, D.P., Baco, A.R., Brewin, P.E., et al., 2009. Predicting global habitat suitability for stony corals on seamounts. J. Biogeogr. 36, 1111–1128. https://doi.org/10.1111/j.1365-2699.2008.02062.x.
Tully, B., Heidelberg, J., 2013. Microbial communities associated with ferromanganese nodules and the surrounding sediments. Front. Microbiol. 4, 161. https://doi.org/10.3389/fmicb.2013.00161.
Tuttle, J.H., Jannasch, H.W., 1979. Microbial dark assimilation of CO_2 in the Cariaco Trench1. Limnol. Oceanogr. 24, 746–753. https://doi.org/10.4319/lo.1979.24.4.0746.
Ulloa, O., Canfield, D.E., DeLong, E.F., Letelier, R.M., Stewart, F.J., 2012. Microbial oceanography of anoxic oxygen minimum zones. Proc. Natl. Acad. Sci. USA 109, 15996–16003. https://doi.org/10.1073/pnas.1205009109.

Ussami, N., Chaves, C.A.M., Marques, L.S., Ernesto, M., 2012. Origin of the Rio Grande Rise - Walvis Ridge reviewed integrating palaeogeographic reconstruction, isotope geochemistry and flexural modelling. In: Mohriak, W.U., Danforth, A., Post, P.J., Brown, D.E., Tari, G.C., Nemcok, M., Sinha, S.T. (Eds.), Conjugate Divergent Margins. The Geological Society, pp. 129–146.

Van Dover, C.L., 2014. Impacts of anthropogenic disturbances at deep-sea hydrothermal vent ecosystems: a review. Mar. Environ. Res. https://doi.org/10.1016/j.marenvres.2014.03.008.

van Haren, H., Hanz, U., de Stigter, H., Mienis, F., Duineveld, G., 2017. Internal wave turbulence at a biologically rich Mid-Atlantic seamount F.G. Schmitt [ed.]. PLoS One 12, e0189720. https://doi.org/10.1371/journal.pone.0189720.

van Woesik, R., van Woesik, K., van Woesik, L., van Woesik, S., 2013. Effects of ocean acidification on the dissolution rates of reef-coral skeletons. PeerJ 1, e208. https://doi.org/10.7717/peerj.208.

Vare, L.L., Baker, M.C., Howe, J.A., et al., 2018. Scientific considerations for the assessment and management of mine tailings disposal in the Deep Sea. Front. Mar. Sci. 5. https://doi.org/10.3389/fmars.2018.00017.

Vilas, J.C., Arístegui, J., Kiriakoulakis, K., Wolff, G.A., Espino, M., Polo, I., Montero, M.F., Mendonça, A., 2009. Seamounts and organic matter—Is there an effect? The case of Sedlo and Seine Seamounts: part 1. Distributions of dissolved and particulate organic matter. Deep Sea Res. Part II Top. Stud. Oceanogr. 56, 2618–2630. https://doi.org/10.1016/j.dsr2.2008.12.023.

Walker, C.B., de la Torre, J.R., Klotz, M.G., et al., 2010. Nitrosopumilus maritimus genome reveals unique mechanisms for nitrification and autotrophy in globally distributed marine crenarchaea. Proc. Natl. Acad. Sci. USA 107, 8818–8823. https://doi.org/10.1073/pnas.0913533107.

Wang, X., Müller, W.E.G., 2009. Marine biominerals: perspectives and challenges for polymetallic nodules and crusts. Trends Biotechnol. 27, 375–383. https://doi.org/10.1016/j.tibtech.2009.03.004.

Wang, X., Peine, F., Schmidt, A., Schröder, H.C., Wiens, M., Schlossmacher, U., Müller, W.E.G., 2011. Concept of biogenic ferromanganese crust formation: coccoliths as bioseeds in crusts from central Atlantic Ocean (Senghor seamount/Cape Verde). Nat. Prod. Commun. 6, 679–688.

Wang, X.H., Gan, L., Müller, W.E.G., 2009. Contribution of biomineralization during growth of polymetallic nodules and ferromanganese crusts from the Pacific Ocean. Front. Mater. Sci. China 3, 109–123. https://doi.org/10.1007/s11706-009-0033-0.

Watling, L., Guinotte, J., Clark, M.R., Smith, C.R., 2013. A proposed biogeography of the deep ocean floor. Prog. Oceanogr. 111, 91–112. https://doi.org/10.1016/j.pocean.2012.11.003.

Watson, A.J., Metzl, N., Schuster, U., 2011. Monitoring and interpreting the ocean uptake of atmospheric CO_2. Philos. Trans. R. Soc. A Math. Phys. Eng. Sci. 369, 1997 (LP-2008).

Wedding, L.M., Friedlander, A.M., Kittinger, J.N., Watling, L., Gaines, S.D., Bennett, M., Hardy, S.M., Smith, C.R., 2013. From principles to practice: a spatial approach to systematic conservation planning in the deep sea. Proc. R. Soc. B Biol. Sci. 280, 20131684–20131694. https://doi.org/10.1098/rspb.2013.1684.

Wedding, L.M., Reiter, S.M., Smith, C.R., et al., 2015. Managing mining of the deep seabed. Science (80-.) 349, 144–145. https://doi.org/10.1126/science.aac6647.

White, M., Bashmachnikov, I., Aristegui, J., Martins, A., 2007. Physical processes and seamount productivity, p. 65–84. In: T.J. Pitcher, T. Morato, P.J.B. Hart, M.R. Clark, N. Haggan, and R.S. Santos [eds.], Seamounts: Ecology, Fisheries and Conservation. Wiley Blackwell.

Wilson, R.R., Kaufmann, R.S., 1987a. Seamount Biota and Biogeography. American Geophysical Union, Seamounts, Islands and Atolls, pp. 355–377.

Wilson, R.R., Kaufmann, R.S., 1987b. Seamount biota and biogeography. Geophys. Monogr. Ser. 43, 355–377. https://doi.org/10.1029/GM043p0355.

Worm, B., Barbier, E.B., Beaumont, N., et al., 2006. Impacts of biodiversity loss on Ocean ecosystem services. Science (80-) 314, 787–790. https://doi.org/10.1126/science.1132294.

Wright, J.J., Konwar, K.M., Hallam, S.J., 2012. Microbial ecology of expanding oxygen minimum zones. Nat. Rev. Microbiol. 10, 381–394. https://doi.org/10.1038/nrmicro2778.

Wu, Y.H., Liao, L., Wang, C.S., Ma, W.L., Meng, F.X., Wu, M., Xu, X.W., 2013. A comparison of microbial communities in deep-sea polymetallic nodules and the surrounding sediments in the Pacific Ocean. Deep. Res. Part I Oceanogr. Res. Pap. 79, 40–49. https://doi.org/10.1016/j.dsr.2013.05.004.

Yamazaki, T., Sharma, R., 2000. Morphological features of Co-rich manganese deposits and their relation to seabed slopes. Mar. Georesources Geotechnol. 18, 43–76. https://doi.org/10.1080/10641190009353782.

Yasuhara, M., Danovaro, R., 2016. Temperature impacts on deep-sea biodiversity. Biol. Rev. 91, 275–287. https://doi.org/10.1111/brv.12169.

Yesson, C., Taylor, M.L., Tittensor, D.P., et al., 2012. Global habitat suitability of cold-water octocorals. J. Biogeogr. 39, 1278–1292. https://doi.org/10.1111/j.1365-2699.2011.02681.x.

Yesson, C., Bedford, F., Rogers, A.D., Taylor, M.L., 2017. The global distribution of deep-water Antipatharia habitat. Deep Sea Res. Part II Top. Stud. Oceanogr. 145, 79–86. https://doi.org/10.1016/j.dsr2.2015.12.004.

Zhang, D.-C., Liu, Y.-X., Li, X.-Z., 2015. Characterization of bacterial diversity associated with deep sea ferromanganese nodules from the South China Sea. J. Microbiol. 53, 598–605. https://doi.org/10.1007/s12275-015-5217-y.

Zubkov, M.V., Sleigh, M.A., Tarran, G.A., Burkill, P.H., Leakey, R.J., 1998. Picoplanktonic community structure on an Atlantic transect from 50°N to 50°S. Deep Sea Res. Part I Oceanogr. Res. Pap. 45, 1339–1355. https://doi.org/10.1016/S0967-0637(98)00015-6.

Zubkov, M.V., Sleigh, M.A., Burkill, P.H., Leakey, R.J.G., 2000. Picoplankton community structure on the Atlantic Meridional Transect: a comparison between seasons. Prog. Oceanogr. 45, 369–386. https://doi.org/10.1016/S0079-6611(00)00008-2.